

**JAERI-Tech
2005-013**



JP0550124



**LOW TEMPERATURE TRITIUM RELEASE EXPERIMENT
FROM LITHIUM TITANETE BREEDER MATERIAL**

March 2005

**Kunihiko TSUCHIYA, Hiroshi KAWAMURA,
Masaru NAKAMICHI and Hisashi SAGAWA**

**日本原子力研究所
Japan Atomic Energy Research Institute**

本レポートは、日本原子力研究所が不定期に公刊している研究報告書です。

入手の間合わせは、日本原子力研究所研究情報部研究情報課（〒319-1195 茨城県那珂郡東海村）あて、お申し越しください。なお、このほかに財団法人原子力弘済会資料センター（〒319-1195 茨城県那珂郡東海村日本原子力研究所内）で複写による実費頒布をおこなっております。

This report is issued irregularly.

Inquiries about availability of the reports should be addressed to Research Information Division, Department of Intellectual Resources, Japan Atomic Energy Research Institute, Tokai-mura, Naka-gun, Ibaraki-ken 〒319-1195, Japan.

©Japan Atomic Energy Research Institute, 2005

編集兼発行 日本原子力研究所

Low Temperature Tritium Release Experiment from Lithium Titanate Breeder Material

Kunihiko TSUCHIYA, Hiroshi KAWAMURA⁺¹,
Masaru NAKAMICHI[※] and Hisashi SAGAWA⁺²

Department of Fusion Engineering Research
(Oarai Site)
Naka Fusion Research Establishment
Japan Atomic Energy Research Institute
Oarai-machi, Higashiibaraki-gun, Ibaraki-ken

(Received January 27, 2005)

Engineering data of neutron irradiation performance are needed to design a fusion blanket. Of the engineering data, tritium release characteristic is one of the most important data. Therefore, tritium release experiments of the tritium breeding materials were carried out to evaluate the effects of various parameters, i.e. sweep-gas flow rate, irradiation temperature, hydrogen content in sweep gas and so on, on tritium release. Lithium titanate (Li_2TiO_3) is a candidate tritium breeding material for the blanket design of International Thermonuclear Experimental Reactor (ITER). As for the shape of the breeder material, a small spherical form is preferred to enhance tritium release from the breeder and to reduce the induced thermal stress in the breeder. Li_2TiO_3 pebbles with a diameter of 1mm and a total weight of ~134g have been fabricated, and a pebble-pac assembly of the Li_2TiO_3 pebbles was irradiated in the Japan Materials Testing Reactor (JMTR), for 3 cycles (about 75 days). The tritium generated in breeder, and released from the breeder was swept downstream by the sweep gas for on-line analysis of tritium content. The total concentration and gaseous concentration of tritium released from the Li_2TiO_3 pebbles were measured, and HT/(HT+HTO) ratio was evaluated. The sweep-gas flow rate was changed from 10 to 1,000 cm^3/min , and hydrogen concentration in the sweep gas was changed from 100 to 10,000 ppm. The irradiation temperature of the outer region of the pebble-pac assembly was held below 450°C.

The results showed that tritium release from the Li_2TiO_3 pebbles was started between 100 and 140°C and that the amount of released tritium increased with increasing the irradiation temperature. The sweep-gas flow rate did not have an effect on tritium release from the Li_2TiO_3 pebble bed in the steady state. On the other hand, the hydrogen content in the sweep gas had an effect on the tritium release from the Li_2TiO_3 pebble bed.

Keywords: ITER, Fusion Blanket, Tritium Release Experiments, Lithium Titanate (Li_2TiO_3) Pebbles, JMTR

This report is based on the final report of the ITER Engineering Design Activities (EDA).

+1: Preparations Office for JAERI-JNC Integration (Serve concurrently in Department of Fusion Engineering Research)

+2: Department of Research Reactor, Tokai Research Establishment

※: On loan to Secretariat of Nuclear Safety Commission of Japan

チタン酸リチウム増殖材料からの低温トリチウム放出試験

日本原子力研究所那珂研究所核融合工学部

土谷 邦彦・河村 弘⁺¹・中道 勝[※]・佐川 尚司⁺²

(2005 年 1 月 27 日受理)

核融合炉ブランケットを設計するためには、微小球を用いたブランケット構造体の中性子照射試験に関する工学的データが必要不可欠である。工学的データの内、トリチウム放出特性は、最も重要なデータの1つである。このため、トリチウム増殖材のトリチウム放出試験を行い、トリチウム放出特性に対するスイープガス流量、照射温度、スイープガス中の水素添加量等の効果について調べた。リチウムタイタネイト (Li_2TiO_3) は国際熱核融合炉 (ITER) のトリチウム増殖材候補材料である。トリチウム増殖材の形状として、トリチウム放出の促進および熱応力の低減の観点から微小球が選定された。直径 1mm の Li_2TiO_3 微小球を約 134g 照射試験体に充填し、その微小球充填体を材料試験炉 (JMTR) で 3 サイクル (約 75 日) 照射した。 Li_2TiO_3 微小球中に生成し、放出したトリチウムは、スイープガスにより回収し、オンラインでトリチウム量を測定した。 Li_2TiO_3 微小球からの全トリチウム濃度及びガス成分トリチウム濃度を計測し、 $\text{HT}/(\text{HT}+\text{HTO})$ 比を評価した。試験条件は、スイープガス流量を 10 ~ 1,000 cm^3/min 、水素添加量を 100 ~ 10,000 ppm、 Li_2TiO_3 微小球充填部の外側照射温度を 450°C 以下とした。

この結果、100 ~ 140°C で Li_2TiO_3 微小球から生成トリチウムの放出が始まり、照射温度の上昇とともにトリチウム放出量が増加した。定常状態では、スイープガス流量はトリチウム放出に影響を及ぼさないこと、一方、スイープガス中の水素添加量はトリチウム放出に影響を及ぼすことが分かった。

本報告書は、ITER 工学設計報告書に補筆を行ったものである。

那珂研究所 (大洗駐在) : 〒311-1394 茨城県東茨城郡大洗町成田町新堀 3607

+1: 原研・機構統合準備室 (核融合工学部兼務)

+2: 東海研究所研究炉部

※: 内閣府原子力安全委員会事務局に出向中

Contents

1. Introduction	1
2. Task Description	1
3. Preparation of Li_2TiO_3 Pebbles	3
3.1 Fabrication Procedures	3
3.2 Fabrication of Li_2TiO_3 Powder	3
3.3 Granulation Process	4
3.4 Calcination and Sintering Processes	4
3.5 Characterization of Li_2TiO_3 Pebbles	4
4. In-situ Irradiation Tests	5
4.1 Fabrication of Irradiation Capsule	5
4.2 Irradiation Facility for In-situ Irradiation Test	7
4.3 Results of Irradiation Test in the JMTR 121st Cycle	8
4.3.1 Outline of the First Irradiation Test	8
4.3.2 Temperature Distribution	9
4.3.3 Tritium Release at Reactor Power-up	9
4.3.4 Effect of Hydrogen Content on Tritium Release	10
4.3.5 Effect of Sweep-gas Flow Rate on Tritium Release	10
4.3.6 Effect of Irradiation Temperature on Tritium Release	11
4.3.7 Effect of Moisture Concentration of Capsule Outlet on Tritium Release	11
4.3.8 Tritium Release at Reactor Shutdown	12
4.3.9 Memory Effect of Tritium in Sweep Gas Line	12
4.4 Results of Irradiation Test in the JMTR 122nd Cycle	12
4.4.1 Outline of the Second Irradiation Test	12
4.4.2 Tritium Release at Reactor Power-up	13
4.4.3 Effect of Irradiation Temperature on Tritium Release	13
4.4.4 Tritium Release at Reactor Shutdown	14
4.5 Results of Irradiation Test in the JMTR 123rd Cycle	14
4.5.1 Outline of the Third Irradiation Test	14
4.5.2 Tritium Release at Reactor Power-up	14
4.5.3 Effect of Sweep-gas Flow Rate on Tritium Release	15
4.5.4 Effect of Hydrogen Content on Tritium Release	15
4.5.5 Tritium Release at Reactor Shutdown	15
5. Discussion	15
6. Conclusions	17
Acknowledgments	18
References	18

目 次

1. 序 論	1
2. タスク内容	1
3. Li_2TiO_3 微小球の準備	3
3.1 製造方法	3
3.2 Li_2TiO_3 粉末の製作	3
3.3 造粒プロセス	4
3.4 仮焼及び焼結プロセス	4
3.5 Li_2TiO_3 微小球の特性評価	4
4. その場照射試験	5
4.1 照射試験体の製作	5
4.2 その場照射試験のための照射試験設備	7
4.3 JMTR 第 121 サイクルの照射試験結果	8
4.3.1 第 1 回目の照射試験概要	8
4.3.2 温度分布	9
4.3.3 原子炉起動時のトリチウム放出	9
4.3.4 トリチウム放出に対する水素添加量の影響	10
4.3.5 トリチウム放出に対するスweepガス流量の影響	10
4.3.6 トリチウム放出に対する照射温度の影響	11
4.3.7 トリチウム放出に対するキャプセル出口水分濃度の影響	11
4.3.8 原子炉停止時のトリチウム放出	12
4.3.9 スweepガスラインのトリチウムメモリー効果	12
4.4 JMTR 第 122 サイクルの照射試験結果	12
4.4.1 第 2 回目の照射試験概要	12
4.4.2 原子炉起動時のトリチウム放出	13
4.4.3 トリチウム放出に対する照射温度の影響	13
4.4.4 原子炉停止時のトリチウム放出	14
4.5 JMTR 第 123 サイクルの照射試験結果	14
4.5.1 第 3 回目の照射試験概要	14
4.5.2 原子炉起動時のトリチウム放出	14
4.5.3 トリチウム放出に対するスweepガス流量の影響	15
4.5.4 トリチウム放出に対する水素添加量の影響	15
4.5.5 原子炉停止時のトリチウム放出	15
5. 考 察	15
6. 結 論	17
謝 辞	18
参考文献	18

1. Introduction

Engineering data of neutron irradiation performance are needed to design the fusion blanket. However, knowledge about the performance of solid lithium-based ceramics as tritium breeding materials for fusion reactors is limited at present. Tritium is bred in the blanket surrounding the reactor, and is collected, and injected into the plasma chamber as fuel.

In the development of tritium breeding blankets for fusion reactors, lithium-containing ceramics such as Li_2O , Li_2TiO_3 , Li_2ZrO_3 , LiAlO_2 and Li_4SiO_4 were recently recognized as promising tritium breeding materials [1-2]. Particularly, Li_2TiO_3 has attracted the attention of many researchers from a point of easy tritium release at low temperature and chemical stability [3-5]. Application of small lithium-based ceramic pebble was proposed in the fusion blanket design in order to reduce thermal stress and so on [6-9].

Li_2TiO_3 pebbles with a diameter of 1mm and a total weight of ~134g were fabricated, and a pebble-pac assembly of the Li_2TiO_3 pebbles was irradiated in the Japan Materials Testing Reactor (JMTR), for 3 cycles (about 75 days). The tritium generated in ceramic, and released from the ceramic was swept downstream by the sweep gas for on-line analysis of tritium content. The total concentration and gaseous concentration of tritium released from the Li_2TiO_3 pebbles were measured, and $\text{HT}/(\text{HT}+\text{HTO})$ ratio was evaluated. The sweep-gas flow rate was changed from 10 to 1,000 cm^3/min , and hydrogen content in the sweep gas was changed from 100 to 10,000ppm. The irradiation temperature of the outer region of the Li_2TiO_3 pebbles was held below 450°C.

In-situ tritium release experiments of Li_2TiO_3 pebble bed were carried out to evaluate the effects of various parameters, i.e. sweep-gas flow rate, irradiation temperature, hydrogen content in sweep gas, etc., on tritium release. Some papers and reports were published so far on analyzed results of these in-situ experiments [10-13].

2. Task Description

In-situ tritium release data at low temperature from lithium titanate are important for the design of the ITER breeding blanket. An in-situ tritium release test is being carried out under steady neutron irradiation in the Japan Materials Testing Reactor (JMTR). The JMTR irradiation facility for in-situ irradiation test is shown in Fig.2-1. Main parameters of the experiment are the following:

1) Irradiation Conditions

- Reactor	: JMTR
- Irradiation position	: K-2
- Irradiation time	: 3 cycles in JMTR
- JMTR cycle	: ~25 days
- Neutron flux	
• Thermal neutron ($E < 0.683\text{eV}$)	: $\sim 2 \times 10^{17} \text{ n/m}^2/\text{s}$
• Fast neutron ($E > 1.0 \text{ MeV}$)	: $\sim 8 \times 10^{15} \text{ n/m}^2/\text{s}$
- Tritium generation rate	: $\sim 7.4 \times 10^{10} \text{ Bq/day}$ ($\sim 2 \text{ Ci/day}$)
- Breeder region irradiation temperature	: $250 - 400^\circ\text{C}$
- Average volumetric heating rate	: $\sim 5 \text{ MW/m}^3$
- Sweep gas	: Pure He or He+H ₂
- Gas flow rate	: $(10 - 1,000) \times 10^{-6} \text{ m}^3/\text{min}$ ($10 - 1,000 \text{ cm}^3/\text{min}$)
- Hydrogen content in sweep gas	: $100 - 10,000 \text{ ppm}$
- Moisture content in sweep gas	: $< 10 \text{ ppm}$

2) Irradiation Capsule

- Design	: See Fig.2-2
- Breeder material	: Li ₂ TiO ₃
- Breeder material region	: $\phi 20 \times 260 \text{ mm}$
- Weight of breeder material	: $\sim 134 \text{ g}$
- Packing fraction of breeder material	: $\sim 62\%$
- Main structure material	: SS316
- Breeder material	
• Shape	: Pebble ($\sim \phi 1 \text{ mm}$)
• Density	: $80.1 \% \text{ T.D.}$
• ⁶ Li enrichment	: Natural
• Average grain size	: $\sim 3 \mu\text{m}$
- Instrumentation	
• Multi-paired thermocouple*	: 11
(Three vertically hot junction per one multi-paired thermocouple)	
• Five self-powered neutron detectors with Rh-emitter (Rh-SPND)	

*By instrumenting one multi-paired thermocouple, it is able to measure irradiation temperatures at three places of the tritium breeder zone, vertically.

3. Preparation of Li_2TiO_3 Pebbles

3.1 Fabrication Procedures

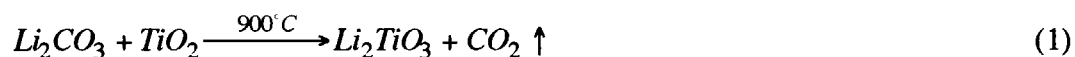
Li_2TiO_3 has attracted the attention of many researchers from a point of easy tritium release at low temperature and chemical stability. The application of small Li_2TiO_3 pebble was proposed in ITER breeding blanket design in order to reduce thermal stress and so on. The rotating granulation method is advantageous for fabricating small Li_2TiO_3 pebbles.

Fabrication of Li_2TiO_3 pebbles was carried out by the rotating granulation method and characteristics of Li_2TiO_3 pebbles were examined.

The fabrication flow of Li_2TiO_3 pebbles for the rotating-granulation/sintering method is shown in Fig.3-1. This procedure includes a fabrication process of Li_2TiO_3 powder, a granulation process to grow the nuclei to pebbles of the desired diameter, and a calcination and a sintering processes.

3.2 Fabrication of Li_2TiO_3 Powder

Li_2CO_3 and TiO_2 powders, which are starting material, were prepared with purities of 99.99% and 99.98%, respectively. Results of chemical analysis of Li_2CO_3 and TiO_2 powders are shown in Table 3-1. The Li_2CO_3 powder was manufactured by HONJO-SOREX CO. LTD. Main impurities of Li_2CO_3 powder were as follows: Na, 1; Ca, 1; Cr, 47.2; Fe, 1; K, 1, (in wt. ppm). The TiO_2 powder was manufactured by FUJI TITANIUM CO. LTD. The Li_2TiO_3 powder was prepared by a solid-solid reaction. The reaction for the production of Li_2TiO_3 powder is shown in Eq.(1).



Mixed powder of Li_2CO_3 and TiO_2 was pulverized and reacted in air at 900°C for 8 h in a Pt crucible. After the reaction, the produced Li_2TiO_3 powder was pulverized, and impurities in the Li_2TiO_3 powder and crystal structure of this powder were measured by X-ray diffractometry (XRD).

3.3 Granulation Process

This is a process of preparing nuclei of pebbles by mixing the Li_2TiO_3 powder and a binder. Polyvinyl butyral (#800) and ethyl alcohol were used as binders, based on industrial experience. The Li_2TiO_3 powder was put in the container of a rotating-granulation apparatus, and then the binder mixed polyvinyl butyral, toluene and ethyl alcohol added in rotating the blade. The granulated pebbles, i.e. green pebbles, were sieved by the classifier. The size of green pebbles was in the range of $\phi 0.85\text{--}1.18\text{mm}$. The green pebbles were dried in air at about 110°C for 1h.

3.4 Calcination and Sintering Processes

In the calcination process, the binder was removed from the green pebbles. The green pebbles were calcinated in air at 550°C for 3h. Weight of green pebbles before/after calcination was measured and weight loss by calcination was about 10%.

In the sintering process, the density of Li_2TiO_3 pebbles was improved by annealing at high temperature, and then sintering tests were conducted in air under various temperatures. Density of the sintered Li_2TiO_3 pebbles was measured by mercury porosimetry, and dependence of the sintered density on the sintering temperature was examined.

3.5 Characterization of Li_2TiO_3 Pebbles

Li_2CO_3 and TiO_2 powders were pulverized and reacted in air at 900°C for 8 h in a Pt crucible. After the reaction, impurities in the Li_2TiO_3 powder and crystal structure of this powder were measured by X-ray diffractometry (XRD). Impurity levels of the Li_2TiO_3 powder were measured by an atomic emission spectrometry with inductively coupled plasma (ICP-AES) and the results are shown in Table 3-2. Silicon (Si), iron (Fe), Sodium (Na) and chromium (Cr) were the highest impurities detected in the Li_2TiO_3 powder. The X-ray diffraction pattern of Li_2TiO_3 powder is shown in Fig.3-2, and Li_2TiO_3 was the main component detected.

Sintering tests were conducted in air in a sintering temperature range from 1200 to 1300°C for 0.5-1.0 h. In the preliminary fabrication test, Li_2TiO_3 pebble density was 78.2, 82.9 and 87.2%T.D. at sintering temperatures of 1200 , 1260 and 1300°C for 0.5 h, respectively. From the results of sintering tests, the sintering condition was decided as $1260^\circ\text{C} \times 0.5$ h in air.

Characteristics of Li_2TiO_3 pebbles fabricated in the above condition are tabulated in Table 3-3. The main features are discussed below.

Photographs of Li_2TiO_3 pebbles fabricated by rotating granulation method are shown in

Fig.3-3. Distribution of diameter of the Li_2TiO_3 pebbles is shown in Fig.3-4. Average diameter of the Li_2TiO_3 pebbles was about 1.0 mm. Sphericity of Li_2TiO_3 pebbles was measured by a photographic analysis method, and the degree of sphericity, which is defined as the maximum diameter divided by minimum diameters, was as high as 1.05 to 1.2. SEM photographs of cross sections of Li_2TiO_3 pebbles are shown in Fig.3-5. The grain size was measured using the photograph of the cross section of Li_2TiO_3 pebbles. Distribution of grain size of Li_2TiO_3 pebbles is shown in Fig.3-6. The average grain size of Li_2TiO_3 pebbles was about $3\mu\text{m}$. Result of pore size distribution of Li_2TiO_3 pebbles measured by a mercury porosimetry is shown in Fig.3-7. The pore size of Li_2TiO_3 pebbles was less than $3\mu\text{m}$. The density was 80.1%T.D. at a mercury intrusion pore size $\geq 10\mu\text{m}$.

Impurity levels of the Li_2TiO_3 pebbles were measured by ICP-AES analysis and the results are shown in Table 3-2. Silicon (Si), iron (Fe), sodium (Na) and chromium (Cr) were the highest impurities detected in Li_2TiO_3 pebbles fabricated by this method.

To evaluate the strength of Li_2TiO_3 pebbles fabricated by this method, the crushing strength was measured by a compression strength test. Crushing load ranged from 22 to 30N.

The X-ray diffraction pattern of Li_2TiO_3 pebbles is shown in Fig.3-8. The XRD analysis of Li_2TiO_3 pebbles was undertaken after packing the pebbles in a polyethylene sheet. Li_2TiO_3 was the main component detected, and the crystalline structure of the Li_2TiO_3 pebbles was not changed by the sintering.

4. In-Situ Irradiation Tests

4.1 Fabrication of Irradiation Capsule

The vertical cross-section of irradiation capsule which was used in the irradiation test is shown in Fig.4-1. This outer diameter of capsule is 65 mm which is the maximum available size in the JMTR. In the capsule, thermocouples and self-powered neutron detectors (SPNDs), mentioned below, to measure the temperature and thermal neutron flux, and electrical heaters to control the irradiation temperature of the tritium breeding material are installed. The vertical cross-section and photograph of an inner capsule in the capsule are shown in Fig.4-2 and Fig.4-3, respectively. The inner capsule is made of SS316L, and the dimensions of Li_2TiO_3 pebble container and inner container are $23\text{mm}^{\text{OD}} \times 20\text{mm}^{\text{ID}} \times 260\text{mm}^{\text{L}}$ and $48\text{mm}^{\text{OD}} \times 43\text{mm}^{\text{ID}} \times 455\text{mm}^{\text{L}}$, respectively. Beryllium (Be) pebbles are loaded in the inner capsule as a thermal transfer medium. Detail specifications of the Li_2TiO_3 pebble region and the Be pebble region is shown in Table 4-1.

In this inner capsule, two kinds of instruments, i.e. thermocouples (T/Cs) and SPNDs are used. Arrangements of the multi-paired thermocouples and SPNDs at A, B and C sections are shown in Fig.4-4. The vertical positions of the A, B and C sections in Fig.4-4 are 65, 130 and 195mm from the vertical top end of Li_2TiO_3 pebble region, respectively. At the A section, there are 11 T/Cs and one SPND; at the B section 11 T/Cs and 3 SPNDs; at the C section 11 T/Cs and one SPND. Conceptual structure of the thermocouple and the SPND is shown in Fig.4-5 and Fig.4-6, respectively. As for the thermocouples, the multi-paired thermocouples with three hot junctions were used. It is because a lot of thermocouples are necessary from a viewpoint of exact measurement on irradiation temperature distribution, while the numbers of instrument cables through the upper plug of inner capsule are limited due to the difficulty in micro-brazing. The outer diameter of multi-paired thermocouple is 1.8mm, and three small thermocouples are bundled in one multi-paired thermocouple. The outer diameter of the small thermocouple is 0.5mm. The vertical positions of hot junctions of each small thermocouple are 65, 130 and 195mm from the vertical top end of the Li_2TiO_3 pebble region. For example, the irradiation temperature distribution of Li_2TiO_3 pebble region at B section can be measured by the use of #13-#17. The thermocouples of #14, #15 and #16 are instrumented in a steady packing region. The emitter of SPND is Rh, and the outer diameter of the collector and the cable are 2 and 1.5 mm, respectively. In addition, control of the irradiation temperature in the Li_2TiO_3 pebble region was conducted by a micro-heater instrumented at the outside of the container of Be pebbles. The capacity of heater was maximum 2kW. This capsule was irradiated at the irradiation hole K-2 in JMTR. The core configuration of JMTR is shown in Fig.4-7. This irradiation hole is located at the outside of γ -ray shielding plate made of Zr. This hole is the most convenient for conducting an irradiation test of tritium breeder α -heated by ${}^6\text{Li}(n, \alpha)$ reaction, by minimizing the effect of γ -heating of structural materials like stainless steel. The γ -heating rate of K-2 hole is 0.25W/g. By nuclear calculation with SRAC or MCNP codes, α -heat and γ -heat are shown as follows.

(1) Result by SRAC code

α -heat : 0.31 kW (mean), 0.41 kW (max.)

γ -heat : 8.9 kW

(2) Result by MCNP code

α -heat : 0.31 kW (mean), 0.41 kW (max.)

γ -heat : 8.9 kW

The result of thermal calculation with GENGTC code is shown in Fig.4-8. The centerline temperature of Li_2TiO_3 pebble region is about 310°C without heater at JMTR 50

MW operation.

4.2 Irradiation Facility for In-situ Irradiation Test

The system mainly consists of four subsystems: a sweep gas supply subsystem, a tritium measuring subsystem, a tritium recovery subsystem and a clean-up subsystem of a glove box. The block diagram of these subsystems is shown in Fig.4-9, and the main design conditions are listed in Table 4-2. The schematic flow diagram of the sweep gas system is shown in Fig.4-10.

The results of design study shows that the sweep gas system was sufficient to support the in-pile functional test. It was possible to change broadly the sweep-gas flow rate, hydrogen addition and other parameters by controlling the sweep gas supply subsystem. In the tritium measuring subsystem, accurate measurement can be done without being concerned about the increase of background by installing two ceramic electrolytic cells in series. In the tritium recovery subsystem, the amount of exhaust tritium will be smaller than 1×10^{10} Bq/y. If an accident such as piping rupture occurs, the exposure will be minimized by the clean up subsystem.

a) Sweep Gas Supply Subsystem

The sweep gas supply subsystem is for providing the sweep gas to the blanket mock-up. The sweep-gas flow rate can be changed from 10 to 1,000 cm³/min. Hydrogen, oxygen and moisture can be added in the sweep gas here. The hydrogen content in the sweep gas can be changed from 10 to 10,000 ppm, the oxygen content from 10 to 1,000 ppm and the moisture concentration from 10 to 1,000 ppm by mass flow controller.

b) Tritium Measuring Subsystem

In this subsystem, the total tritium concentration, the tritium concentration of gaseous species and the water species/gaseous species ratio of tritium released from the capsule can be measured on-line. The sweep gas introduced into this subsystem from the blanket mock-up is divided into two lines. One is a line for measuring the elapsed change of the total tritium concentration. In this line, the tritium in the sweep gas is transformed into tritium gaseous species by a ceramic electrolytic cell, and the tritium concentration is measured by an ionization chamber. Two ceramic electrolytic cells are installed into this line so that the water species is perfectly transformed to the gaseous species, and the increase of background by the adsorption of tritiated water species on the ionization chamber is prevented.

The other is a line to measure the elapsed change of tritium gaseous species. After tritiated water species in the sweep gas is removed by a molecular sieve bed, tritium gaseous

species is also measured by another ionization chamber. The size of the molecular sieve bed has been determined carefully so that the time lag between above two lines dose not occur. The water species/gaseous species ratio of released tritium can be obtained from the measurement results of the two ionization chambers.

c) Tritium Recovery Subsystem

In the tritium recovery subsystem, the tritium in the sweep gas is transformed into water species by an oxidation bed with Pd-catalyst and is recovered by a molecular sieve bed. The reason why the molecular sieve bed was used to recover the tritium is that it is easier to store it without apprehension of tritium permeation. One molecular sieve bed has a sufficient ability of recovering $3.7 \times 10^{13} \text{Bq}$, which corresponds to JMTR operation period for one year. Two sets of the oxidation bed and the molecular sieve bed are installed in series, because the tritium exhaust from the stack is restricted to $1 \times 10^{10} \text{Bq/y}$.

d) Clean-Up Subsystem of Glove Box

The tritium measuring subsystem and the tritium recovery subsystem are set up in a glove box. The total leak rate from the valves and the connections between pipes and apparatuses is suppressed less than $5 \times 10^{-7} \text{Pa} \cdot \text{m}^3/\text{s}$ so that the internal exposure is suppressed less than 1mSv/week. However, the clean-up subsystem of the glove box is set up to prepare for the worst. The maximum tritium release rate from the blanket mock-up is defined to be $1.8 \times 10^{11} \text{Bq/d}$ as mentioned above. When tritium of $1.8 \times 10^{11} \text{Bq}$, corresponding to released amount in one day, is assumed to spread out in the glove box for an instant, this subsystem has ability of reducing the tritium concentration in the glove box to $7.0 \times 10^{-1} \text{Bq/cm}^3$ which is determined by Law Concerning Prevention from Radiation Hazards due to Radio-Isotopes, etc.

4.3 Results of Irradiation Test in the JMTR 121st Cycle

4.3.1 Outline of the First Irradiation Test

Li_2TiO_3 pebbles with a diameter of 1mm and a total weight of about 134g were fabricated and packed in the irradiation capsule. The tritium was generated in Li_2TiO_3 by neutron irradiation and released from Li_2TiO_3 . The generated tritium was swept by the sweep gas. And total tritium concentration (HT+HTO) and gaseous tritium concentration (HT) were measured separately, and HT/(HT+HTO) ratio was evaluated. The first irradiation test of Li_2TiO_3 with JMTR was conducted from Jan. 19th to Feb. 13th, 1998 at the 50MW full power.

The outline of experimental conditions for the first irradiation test is shown in Fig.4-11.

Specially, the first irradiation test was focused on the evaluation of low temperature irradiation behavior of Li_2TiO_3 . Therefore, the center temperature of Li_2TiO_3 pebble region was 280°C basically without using the heater, and was increased to 350°C by using a heater installed in the irradiation capsule. And the flow rate of sweep gas was constant at $200\text{cm}^3/\text{min}$ basically and changed up to $500\text{cm}^3/\text{min}$ partly. And the hydrogen concentration in sweep gas was also constant at 1,000ppm basically and changed up to 10,000ppm partly. Additionally, it seems that the test module for ITER irradiation test does not have a heating device for preheating the tritium breeder region in test module before neutron irradiation in ITER. Therefore, the tritium breeding region in the irradiation capsule for this JMTR irradiation test was not heated before the JMTR operation. However, during capsule fabrication, moisture in the irradiation capsule was carefully controlled. From these points, the effects of moisture concentration at the capsule outlet on the tritium release behavior in the Li_2TiO_3 pebble region were investigated in this irradiation test. Outline of main experiments of the first irradiation test is shown in Fig.4-12. A series of measurements revealed the effects of hydrogen content in sweep gas, sweep-gas flow rate, irradiation temperature and other conditions on tritium release from Li_2TiO_3 pebble bed.

4.3.2 Temperature Distribution

The axial temperature distribution in the inner capsule at 50MW is shown in Fig.4-13. The temperature was measured by the multi-paired thermocouples with three hot junctions. The axial temperature distribution was approximately uniform over the Li_2TiO_3 pebble region (270mm). The radial temperature distribution in the inner capsule at 50MW is shown in Fig.4-14. When the heater was off, the temperatures over the upper, middle and lower sides were not uniform. However, by heating with the two heaters, temperatures among all sides became radially uniform. In the case of using the heater, the center temperature of Li_2TiO_3 pebble region was about 340°C , and the edge temperature of Li_2TiO_3 container was about 220°C . The three dimensional temperature distributions calculated by TRAMP code both at heater-off and at heater-on are shown in Fig.4-15 and Fig.4-16, respectively. The calculation clearly shows the volumetric temperature distribution.

4.3.3 Tritium Release at Reactor Power-up

Figure 4-17 shows the release rate of total tritium (HT+HTO) and gaseous tritium (HT), the ratio of HT/(HT+HTO), the moisture concentration at the capsule outlet and the center temperature measured by thermocouple #15 under reactor power-up. The sweep gas flow rate

and the hydrogen content in sweep gas were $200\text{cm}^3/\text{min}$ and $1,000\text{ppmH}_2$, respectively. When the reactor power became 10MW, the center temperature of thermocouple #15 became 100°C . And the tritium release from Li_2TiO_3 pebbles started at 10MW. Then, the release rate of total tritium increased with increasing the irradiation temperature of Li_2TiO_3 pebble region. When the reactor power became 30MW, the center temperature measured by thermocouple #15 was 194°C and the moisture concentration of capsule outlet was 40ppm. At this time, the ratio of $\text{HT}/(\text{HT}+\text{HTO})$ was only 7%. When the reactor power became 50MW, the ratio of $\text{HT}/(\text{HT}+\text{HTO})$ increased to 30%. The ratio of $\text{HT}/(\text{HT}+\text{HTO})$ increased with decreasing the moisture concentration. Finally, on Jan. 23rd, the ratio of $\text{HT}/(\text{HT}+\text{HTO})$ became about 92% at a moisture concentration of about 2ppm.

4.3.4 Effect of Hydrogen Content on Tritium Release

Two kinds of experiments were conducted in order to evaluate the effect of hydrogen content in the sweep gas on tritium release from Li_2TiO_3 . One experiment is for evaluating tritium release behavior when the hydrogen content increased from 1,000 to 10,000ppm. The other is for evaluating the behavior when the hydrogen content decreased from 10,000 to 1,000ppm. Experimental results in the case of increasing the hydrogen content are shown in Fig.4-18. When the hydrogen content was changed from 1,000 to 10,000ppm, tritium release rate increased. After about 5h from the time of changing the hydrogen content, the tritium release rate increased by about twice than that when the hydrogen content was 1,000ppm, and became constant. The experimental results in the case of decreasing the hydrogen content are shown in Fig.4-19. When the hydrogen content was changed from 10,000 to 1,000ppm, tritium release rate decreased. After about 10h from the time of changing the hydrogen content, the tritium release rate decreased to about 75% of that before changing the hydrogen content, and became constant.

4.3.5 Effect of Sweep-gas Flow Rate on Tritium Release

The experiment was conducted twice in order to evaluate the effect of sweep-gas flow rate on tritium release from Li_2TiO_3 . The first experiment is for evaluating tritium release behavior when the sweep-gas flow rate changed from 200 to $500\text{cm}^3/\text{min}$ and from 500 to $200\text{cm}^3/\text{min}$. The second is for re-evaluating the behavior when the flow rate increased from 200 to $500\text{cm}^3/\text{min}$. Results of the first experiment are shown in Fig.4-20. When the flow rate was changed from 200 to $500\text{cm}^3/\text{min}$, the tritium release rate increased in a moment by about twice of that before changing the flow rate. However, after about 5h from the time of changing

the flow rate, the tritium release rate returned to that before changing the flow rate. And then, after keeping the condition of about 30 h at 500cm³/min continuously, the sweep-gas flow rate was changed from 500 to 200cm³/min. The tritium release rate decreased in a moment by about one half of that before changing the flow rate. However, after about 5h from the time of changing the flow rate, tritium release rate returned to that before changing the flow rate.

Results of the second experiment are shown in Fig.4-21. When the sweep-gas flow rate was changed from 200 to 500cm³/min, tritium release rate increased in a moment by about twice of that before changing the flow rate. However, after about 20h from the time of changing the flow rate, tritium release rate returned to that before changing the flow rate. It seems that the reason why the period necessary to return to tritium release rate before changing the flow rate became longer, is the increase of the tritium inventory in Li₂TiO₃ for the second experiment compared with that for the first experiment by these low temperature irradiation.

4.3.6 Effect of Irradiation Temperature on Tritium Release

This experiment was conducted for evaluating the effect of irradiation temperature on tritium release from Li₂TiO₃. The sweep-gas flow rate was 500cm³/min, and the hydrogen content in the sweep gas was 1,000ppm. Experimental results are shown in Fig.4-22 for case that the center temperature in the Li₂TiO₃ pebble region measured by thermocouple #15 was changed step-wise from 280 to 350°C. When the center temperatures were about 280 and 350°C, the temperatures at the outside edge (container) of the Li₂TiO₃ pebble region were about 160 and 220°C, respectively. The tritium release rate increased to about 20 times than that before changing the temperature. The ratio of HT/(HT+HTO) decreased from 92 to 87%. It seems that the reason is increase in release of HTO adsorbed at Li₂TiO₃ surface by the temperature increase.

4.3.7 Effect of Moisture Concentration of Capsule Outlet on Tritium Release

This experiment was conducted for evaluating the effect of moisture concentration at the capsule outlet on tritium release from Li₂TiO₃. The sweep-gas flow rate was 200cm³/min, and the moisture concentration in the sweep gas was about 1,000ppm. The center temperature in the Li₂TiO₃ pebble region measured by thermocouple #15 was about 275°C, when the reactor power reached just 50MW. This temperature was increasing gradually by a little increase of neutron flux and became 280°C on Feb. 10th. Additionally, the moisture concentration of capsule outlet was about 100ppm, when the reactor power reached just

50MW. However, the moisture concentration became lower than approximately 5ppm on Feb. 10. The experimental results are shown in Fig.4-23. The ratio of HT/(HT+HTO) was about 30% for 100ppm moisture. And the ratio of HT/(HT+HTO) increased with decreasing the moisture concentration at the capsule outlet, and became about 92% on Feb. 10. It seems that the reason of increase in the ratio of HT/(HT+HTO) is the decrease of H₂O adsorbed at the Li₂TiO₃ surface.

4.3.8 Tritium Release at Reactor Shutdown

The data were obtained at a reactor shutdown. This experiment is for evaluating the effect of neutron flux on tritium release from Li₂TiO₃. The sweep-gas flow rate was 200cm³/min, and the hydrogen content in the sweep gas was 1,000ppm. The heater was turned off before 60 min of the reactor shutdown. Therefore, the center temperature measured by thermocouple #15 changed from about 350 to 300°C. The experimental results are shown in Fig.4-24. The ratio of HT/(HT+HTO) increased with decreasing the neutron flux and irradiation temperature.

4.3.9 Memory Effect of Tritium in Sweep Gas Line

A memory effect of tritium in the sweep gas line after the capsule outlet was observed. Tritium concentrations in the sweep line measured after 3 days from a reactor shutdown are shown in Fig.4-25. The sweep-gas flow rate was 500cm³/min, and the hydrogen content in the sweep gas was 1,000ppm. It was found that a little amount of tritium was adsorbed on the inner surface of pipe of sweep gas line. And after 3h from the starting time of flowing the sweep gas, gaseous tritium concentration became the background level.

4.4 Results of Irradiation Test in the JMTR 122nd Cycle

4.4.1 Outline of the Second Irradiation Test

The second irradiation test of Li₂TiO₃ with JMTR was carried out from March 2 to 29, 1998 at the 50MW full power. The JMTR 122nd cycle was operated with a middle shut down and a reactor scram due to loss of commercial electric power. A reactor scram by the loss of commercial electric power will simulate the ITER pulse operation because the reactor power was quickly decreased. Outline of experimental conditions is shown in Fig.4-26. The second irradiation test was focused on the evaluation of the irradiation temperature. Flow rate of sweep gas was constant at 200cm³/min, and the hydrogen concentration in the sweep gas was

constant at 1,000ppm. Main experiments of the second irradiation test are shown in Fig.4-27. Unfortunately, the total tritium at the JMTR 122nd cycle could not be measured except at the start-up because of a trouble of the total tritium measurement line. The results concerning the effects of irradiation temperature and reactor shut down were obtained. These are described below in turn.

4.4.2 Tritium Release at Reactor Power-up

Figure 4-28 shows the release rate of gaseous tritium (HT), the moisture concentration at the capsule outlet and the center temperature measured by thermocouple #15 under reactor power-up. Released tritium was almost gaseous tritium because the moisture concentration at the reactor power-up was low level (~1ppm). Tritium release started from 10MW (the center temperature of thermocouple #15 was about 100°C), and the release rate of total tritium increased with increasing the irradiation temperature of the Li_2TiO_3 pebble region. When the reactor power became 30MW, the center temperature measured by thermocouple #15 was 194°C, and the moisture concentration of capsule outlet was about 0.5ppm. At this time, the ratio of HT/(HT+HTO) was about 87%. Furthermore, when the reactor power became 50MW, the ratio of HT/(HT+HTO) increased to 92%. The results of the JMTR 121st and 122nd cycles showed that the moisture concentration affected tritium release from Li_2TiO_3 pebbles. On the other hand, when the center temperature was 350°C and the moisture concentration of capsule outlet was about 0.5ppm, the ratio of HT/(HT+HTO) decreased from 92 to 86%. It seems that the desorption of moisture adsorbed at the Li_2TiO_3 surface increases with increasing the irradiation temperature.

4.4.3 Effect of Irradiation Temperature on Tritium Release

Effects of irradiation temperature on tritium release are shown in Figs.4-28, 4-29 and 4-30. The sweep gas flow rate and the hydrogen content in sweep gas were 200cm³/min and 1,000ppmH₂, respectively. Release rate of total tritium increased with increasing the irradiation temperature, and the moisture concentration increased at above 350°C. Tritium release rate increased to about 50 times by the temperature change from 280 to 350°C (see Fig.4-29), and to five times by the temperature change from 350 to 415°C (see Fig.4-30). On the other hand, moisture concentration at the capsule outlet increased with increasing the center temperature measured by thermocouple #15. It seems that the desorption of moisture adsorbed at the Li_2TiO_3 surface increases with increasing the irradiation temperature, as mentioned in 4.4.2.

4.4.4 Tritium Release at Reactor Shutdown

Tritium release at a reactor shutdown and a scram are shown in Figs.4-31 and 4-32, respectively. Decreasing behavior of tritium release at the reactor shutdown was similar to that at the reactor shutdown of the JMTR 121st cycle.

4.5 Results of Irradiation Test in the JMTR 123rd Cycle

4.5.1 Outline of the Third Irradiation Test

The third irradiation test of Li_2TiO_3 with JMTR was conducted from April 16 to May 11, 1998 at the 50MW full power. Outline of experimental conditions is shown in Fig.4-33. The third irradiation test was focused on evaluation of high temperature irradiation behavior of Li_2TiO_3 . The center temperature of the Li_2TiO_3 pebble region was set at 442°C (this temperature corresponds to the maximum power of the heater). The flow rate of sweep gas was constant at 200cm³/min mostly and changed to 500 and 950cm³/min partly. And the hydrogen content in the sweep gas was also constant at 1,000ppm mostly and changed to 100 and 10,000ppm partly. Main experiments of the third irradiation test are shown in Fig.4-34. Unfortunately, the total tritium in initial data at the JMTR 123rd cycle could not be measured because of trouble of the total tritium measurement line. Radial temperature distribution in the inner capsule at 50MW is shown in Fig.4-35. The center temperature of the Li_2TiO_3 pebble region was about 442°C, and the edge temperature of the Li_2TiO_3 container was about 280°C. The three-dimensional temperature distributions calculated by TRAMP code both for heater-on and for heater-off are shown in Figs.4-36 and 4-37, respectively. The effects of the sweep-gas flow rate and the hydrogen content in the sweep gas on tritium release from Li_2TiO_3 were obtained. These are described below in turn.

4.5.2 Tritium Release at Reactor Power-up

Figure 4-38 shows that the release rate of gaseous tritium (HT), the moisture concentration of capsule outlet and the center temperature measured by thermocouple #15 during the reactor power-up. Tritium release started from 10MW (the center temperature of thermocouple #15 was about 100°C). Then, the release rate of total tritium increased with increasing the irradiation temperature of the Li_2TiO_3 pebble region. The moisture concentration at the capsule outlet was low level (~5ppm) during the operation in the JMTR 123rd cycle.

4.5.3 Effect of Sweep-gas Flow Rate on Tritium Release

The effect of sweep-gas flow rate on tritium release was examined by changing the flow rate from 200 to 500cm³/min and from 200 to 950cm³/min. The results are shown in Figs.4-39 and 4-40, respectively. Tritium release rate was basically similar to that for the low temperature irradiation (see 4.3.5). In the transient, the increase of tritium release rate depended on the increase of sweep-gas flow rate (the tritium release rate became about twice for the change from 200 to 500cm³/min, and about five times for the change from 200 to 950cm³/min). However, the tritium release rate did not change in the steady state.

4.5.4 Effect of Hydrogen Content on Tritium Release

The effect of hydrogen content on tritium release was examined by changing the content from 1,000 to 100ppm. The result is shown in Fig.4-41. The tritium release rate became about half by the change from 1,000 to 100ppm. From the former results (see 4.3.4, tritium release rate became about twice by the change from 1,000 to 10,000ppm), it seems that the tritium release rate depends on the hydrogen content in the sweep gas.

4.5.5 Tritium Release at Reactor Shutdown

The data were obtained at a reactor shutdown. This experiment is for evaluating the effect of neutron flux on tritium release from Li₂TiO₃. The sweep-gas flow rate was 200cm³/min, and the hydrogen content in the sweep gas was 1,000ppm. The heater was turned off before 60min of reactor shutdown. Therefore, the center temperature measured by thermocouple #15 changed from about 445 to 300°C. The experimental results are shown in Fig.4-42. The ratio of HT/(HT+HTO) increased with decreasing the neutron flux and irradiation temperature and the decreasing behavior of tritium release at the reactor shutdown was similar to that at the reactor shutdown of the 121st and 122nd cycles.

5. Discussion

Vented capsule tests permit continuous on-line monitoring of the tritium release from the ceramic breeders during the irradiation, by passing the sweep gas around or through the ceramic and into an analysis train. Summary of irradiation tests so far by other researchers is shown in Table 5-1 [14-21]. These tests allow one to measure important fundamental parameters (diffusion, desorption, and tritium residence time) so that the behavior of other blanket assemblies can be inferred.

The sweep gas flowing through the test material collects the tritium released from the lithium ceramic and passed through a tritium analysis system to determine the tritium release rate and the chemical form of the tritium. For a chosen material with specific characteristics, the ceramic temperature and the sweep gas composition can be varied to determine their effect on the release rate and form of tritium recovered. Other variables include flow rate and neutron flux.

CRITIC-III (Canada) [16], BEATRIX-II, Phase-II (US/Japan/Canada) [22] and EXOTIC-8 (Netherlands/EU) [18] were performed as recent in-situ irradiation tests. Comparison of results of in-situ irradiation tests is shown in Table 5-2. CRITIC-III The experiment was very similar to CRITIC-II and lithium titanate (Li_2TiO_3) pebbles were used as the ceramic breeder. The data of CRITIC-III experiment have not been published.

BEATRIX-II experimental program was an International Energy Agency sponsored collaborative effort between Japan, Canada and the United States to evaluate the performance of ceramic solid breeder materials in a fast-neutron environment at high burnup levels. The results of the BEATRIX-II, Phase-II irradiation experiment provided an extensive database on the in-situ tritium release characteristics of Li_2O and Li_2ZrO_3 . Ratio of recovered/generated tritium and average temperature for the temperature change canister in Phase-IIB is shown in Fig.5-1. In this test, increasing the amount of hydrogen in sweep gas resulted in a transient tritium recovery peak indicative of a decrease in tritium inventory in the specimen. And recovered tritium during sweep gas composition changes is shown in Fig.5-2. Decreasing hydrogen concentration from the reference sweep gas (0.1% H_2) resulted in an increase in the tritium inventory.

An obvious question is whether increasing the hydrogen concentration above 0.1% H_2 would result in a lower tritium inventory in the specimen. Compared to peaks recovered during transitions from helium and 0.01 to 0.1% H_2 , the peaks for the transition from 0.1% H_2 to 1.0% H_2 are small. The recovery rate in 1.0% H_2 appears larger than the steady-state recovery rate in 0.1% H_2 . This larger recovery rate in 1.0% H_2 more likely results from the uncertainty of the ion-chamber correction factor used for 1.0% H_2 . In the JMTR irradiation tests, transients were followed by positive tritium recovery peaks for hydrogen concentration increases and negative recovery peaks for hydrogen concentration decreases. Obtained data will be tried to estimate the effect of hydrogen concentration on tritium inventory in the Li_2TiO_3 pebbles. Typical tritium recovery peaks for a temperature change series of 640-530-640°C in reference sweep gas of 0.1% H_2 is shown in Fig.5-3. Temperature transients in Phase-II were followed by positive tritium recovery peaks for temperature increases and negative recovery peaks for

temperature decreases. In the JMTR irradiation tests, tritium release rate increased rate with increasing the temperature of Li_2TiO_3 pebble region. Inner temperature and sweep-gas moisture for first 550h in Phase-IIA is shown in Fig.5-4. A large peaks in the sweep gas moisture flowing out of the temperature-change canister at 110h suggests that the sintering could have occurred concurrently with the decomposition of residual LiOH . On the other hand, moisture concentration peak with Li_2ZrO_3 pebble bed was maximum 2,000ppm at 600°C. In the JMTR irradiation tests, the sweep-gas flow rate was 200cm³/min and the moisture concentration peaks was about 1,000ppm.

On the other hand, the EXOTIC-8 experiments are performed in the High Flux Reactor (HFR) and provide an extensive data base on the in-situ tritium release characteristics of Li_2TiO_3 pebbles ($\phi 0.7\text{-}0.85\text{mm}$) and pellets. During the irradiations a number of temperature transients were performed and the tritium residence times were determined from the tritium release history measured during temperature transients. Additionally, isothermal annealing tests for the irradiated Li_2TiO_3 pebbles at temperatures in the range 250-400°C were carried out before the EXOTIC-8 experiments and the peak of tritium release was located at about 335°C at 1°C/min [23].

6. Conclusions

In-situ irradiation tests with capsule packed Li_2TiO_3 pebbles were started using JMTR, and tritium release properties were evaluated at the reactor power-up. Particular implications of the results are:

- 1) When the reactor power was 50MW (thermal power), temperature at the center of the Li_2TiO_3 pebble region was about 267°C and temperature at the edge of the Li_2TiO_3 pebble region was between 215 and 263°C. These temperatures were almost constant at the full reactor power of 50MW for each JMTR cycle.
- 2) Tritium release from Li_2TiO_3 pebbles occurred between 100 and 140°C. Release rate of total tritium increased with increasing the temperature at the center of the Li_2TiO_3 pebble region. When the reactor power reached 50MW, release rate of the total and the gaseous tritium was about 1.7×10^6 and $1.1 \times 10^6 \text{Bq/min}$, respectively.
- 3) When the reactor power reached 50 MW in the first irradiation test, the ratio of $\text{HT}/(\text{HT}+\text{HTO})$ was about 30%. The ratio increased with decreased the moisture concentration. The amount of HT increased to >92% of the total tritium. It seems that the moisture concentration also influenced the release rate of both the total and the gaseous

tritium.

- 4) In the effect of hydrogen content on tritium release, transients were followed by positive tritium recovery peaks for hydrogen content increases and by negative recovery peaks for hydrogen content decreases.
- 5) In the effect of irradiation temperature on tritium release, the tritium release rate increased with increasing the temperature of the Li_2TiO_3 pebble region.
- 6) In the effect of sweep-gas flow rate on tritium release, transients were followed by positive tritium recovery peaks for sweep-gas flow rate increases and by negative recovery peaks for sweep-gas flow rate decreases.

Acknowledgments

The authors wish to thank Dr. Y. Gohar (former ITER Joint Central Team Task Officer) and Dr. Y. Kawamura (JAERI, Department of Fusion Engineering Research) for many helpful discussions, and also Dr. K. Hayashi (JAERI, Department of Fusion Engineering Research) for his helpful advice on the manuscript of this report.

We would like to thank Mr. Y. Ikeshima and Mr. I. Hisa (former members in Blanket Irradiation and Analysis Laboratory, JMTR) for a lot of supports. We would like to acknowledge Mr. Y. Nagao (Project Engineering Division, JMTR) for the nuclear calculations, Mr. T. Saito (Irradiation Division I, JMTR) and Mr. T. Kikuchi (Division of Engineering Services) for the design and fabrication of the irradiation capsule, Mr. T. Kitajima, Mr. K. Tomita and Mr. H. Magome (Irradiation Division II, JMTR) for maintenance and uncountable of the irradiation facility.

Finally, specialists in Japanese companies such as Mitsubishi Heavy Industries, Ltd. (fabrication of the Li_2TiO_3 pebbles and the pebble-pac assembly), NGK Insulators, Ltd. (construction of the irradiation facility), Sukegawa Electric Co., Ltd. (fabrication of the irradiation capsule and instruments) have cooperated in this achievement of this study.

References

- [1] C.E. Johnson, K.R. Kummerer and E. Roth, J. Nucl. Mater., 155-157 (1988) 188.
- [2] C.E. Johnson, G.W. Hollenberg, N. Roux, and H. Watanabe, Fusion Eng. Des., 8 (1989) 145.
- [3] K. Kurasawa, S. Nasu, K. Noda, T. Takahashi, H. Takeshita, T. Tanifuji and H. Watanabe, Proc. IEEE 9th Symp. on Engineering Problems of Fusion Research, Vol.II, (1981) 1200.

- [4] J.M. Miller, H.B. Hamilton and J.D. Sullivan, J. Nucl. Mater., 212-215 (1994) 877.
- [5] P. Gierszewski, CFFTP G-9703(1997).
- [6] T. Suzuki, O. Murata and S. Hirata, Ceram. Trans., 27 (1991) 37.
- [7] N. Asami, K. Nagashima, et al., Ceram. Trans., 27 (1991) 17.
- [8] P. Gierszewski, M.D. Donne, H. Kawamura and M. Tillack, Fusion Eng. Des., 27 (1995) 167.
- [9] K. Tsuchiya, H. Kawamura, M. Nakamichi, H. Imaizumi, M. Saito, T. Kanzawa and M. Nagakura, J. Nucl. Mater., 219 (1995) 240.
- [10] H. Kawamura, K. Tsuchiya, M. Nakamichi, J. Fujita, H. Sagawa, et. al., Fusion Technology, (1998) 1289.
- [11] K. Tsuchiya, M. Nakamichi, Y. Nagao, S. Tanaka, H. Kawamura, et. al., Fusion Eng. Des., 51-52 (2000) 887.
- [12] K. Tsuchiya, A. Kikukawa, D. Yamaki, M. Nakamichi, M. Enoeda, H. Kawamura, Fusion Eng. Des., 58-59 (2001) 679.
- [13] K. Tsuchiya, M. Nakamichi, Y. Nagao, M. Enoeda, T. Osaki, S. Tanaka, H. Kawamura, Journal of Nuclear Science and Technology, 38, (2001) 996.
- [14] J.M.Miller, International School of Plasma physics, ISPP-5, "Tritium and Advanced Fuels in Fusion Reactors", Varenna, 6-15, Sept. 1989.
- [15] R.A.Verrall, J.M.Miller and L.K.Jones, AECL-11768 (CFFTP G-9637), 1997.
- [16] R.A. Verrall et al., AECL, private communication, May 1997.
- [17] H.Kwast, M.Stijkel, R.Muis and R.Conrad, ECN-C-95-123, 1995.
- [18] J.G. van der Laan, M.P.Stijkel, K.Bakker and R.Conrad, HCPB WP 8 Progress Meeting, Paris, 23 Jan. 1998.
- [19] O.D.Slagle and G.W.Hollenberg, PNL-7477, Oct. 1990.
- [20] O.D.Slagle and G.W.Hollenberg, PNL-7858, Oct. 1991.
- [21] O.D.Slagle and G.W.Hollenberg, PNL-8423, Dec. 1992.
- [22] O.D.Slagle and G.W.Hollenberg, PNL-7477, Jan. 1995.
- [23] J.G. van der Laan, paper submitted to IVFRM-8, Sendai, 26-31, Oct. 1997.

Table 3-1 Chemical analysis of Li_2TiO_3 and TiO_2 powders.

	Li_2CO_3 Powder	TiO_2 Powder
Purity	99.99 %	99.98 %
Moisture Content	0.01 %	0.049 %
Impurity Element	(in ppm)	(in ppm)
Al	ND	ND
Si	1.0	ND
Fe	1.0	7.0
Ca	1.0	-
Na	1.0	-
K	1.0	-
Mg	ND	-
Cr	47.2	14.0
Pb	0.2	ND
Cu	< 0.5	ND

ND : not detected.

Table 3-2 Impurity contents of Li_2TiO_3 powder and Li_2TiO_3 pebbles.

Element	(in ppm)	
	Li_2TiO_3 Powder	Li_2TiO_3 Pebbles
Al	49.2	ND
Si	11.5	61.5
Fe	ND	75.3
Co	83.4	ND
Ca	20.8	41.4
Na	ND	50.0
K	6.6	ND
B	ND	ND
Mg	47.2	ND
Cr	ND	45.2
Zr	ND	ND
Ni	ND	ND
Mo	ND	ND
Cu	ND	ND
C	-	20
U	ND	ND
Li	12.1wt%	13.0wt%
Ti	40.8wt%	45.2wt%

ND : not detected.

Table 3-3 Characterization of Li_2TiO_3 pebbles.

Properties	Measuring Methods	Measuring Values
Density	Liquid Immersion Method (Hg)	80.1 %T.D.
Sphericity	Photographic Analysis	1.11 (av.)
Pebble Diameter	Sieve Classification	0.85 - 1.18 mm
Grain Size	SEM Observation	3 μm (av.)
Crystal Structure	XD Analysis	XD Pattern
Impurity Content	ICP Analysis	Content (see Table 3-2)
Collapse Load	Autograph	22~30 N

Table 4-1 Detail specifications of Li_2TiO_3 pebble region and Be pebble region in the mockup.

	Li_2TiO_3 pebble region	Be pebble region
Packing fraction	62.0%	61.2%
Loaded weight	133.54 g	288.95 g
Length of packing region	261.1mm	261.9 mm

Table 4-2 Main design conditions.

Items	Design condition
Operation method	Once through
Bulk sweep gas	Helium
Hydrogen content	10 - 10,000 ppm
Oxygen content	10 - 1,000 ppm
Moisture concentration	10 - 1,000 ppm
Flow rate of sweep gas	1×10^{-5} - 1×10^{-3} m ³ /min
Oxidation method	Pd-catalyst
Reducing method	Ceramic electrolytic cell
Total leak rate	5×10^{-7} Pa·m ³ /s
Exhaustion of tritium	$< 1 \times 10^{10}$ Bq/y

Table 5-1 Summary of irradiation tests.

Test Designation	Materials	Particulars
TRIO (U.S.)	LiAlO ₂	42g of 9mm annular pellets, He and He-0.1%H ₂ sweep gas, temperature step change tests over range 400-700°C, 1.48 TBq of tritium collected.
LISA-1, -2 (Germany)	Li ₂ SiO ₃ Li ₄ SiO ₄ Li ₂ O	Material comparison, He-0.1%H ₂ sweep gas, temperature step change tests over range 350-650°C.
VOM (Japan)	Li ₂ O LiAlO ₂ (-22), LiAlO ₂ Li ₄ SiO ₄ (-23)	Material comparison, VOM-22H had 5mm spheres with 10µm grain size, temperature range from 300-900°C, sweep gas composition, varied from He to He-1%D ₂ . In VOM-23, fine-grained (0.40µm) LiAlO ₂ , and 14µm grain size Li ₄ SiO ₄ were compared, He-1%D ₂ sweep gas, temperature step change tests over range 500-800°C. Similar release results obtained for the two.
LILA 1-3 (France)	LiAlO ₂	Effect of different textures-grain size and density, temperature step change tests over range 400-600°C, sweep gas composition tested-He, He-0.1%CO and He-0.1%H ₂ .
EXOTIC1-8 (Netherlands/ UK/Belgium)	Li ₂ SiO ₃ LiAlO ₂ (-1), Li ₂ SiO ₃ Li ₂ O (-2), Li ₂ SiO ₃ Li ₂ Si ₂ O ₅ Li ₄ SiO ₄ Li ₂ ZrO ₃ (-3)	Material comparison-different density, grain size, ⁶ Li content, single temperature step-change tests over range from 400 to 600°C, He-0.1%H ₂ sweep gas, vary irradiation time.
CRITIC I-III (Canada)	Li ₂ O (-I), Li ₂ ZrO ₃ (-II), Li ₂ TiO ₃ (-III)	Long-term irradiation, ~100g pellets or 1.2mm pebbles, temperature step-change tests over range from 390 to 650°C higher (850 to 1050°C), vary sweep gas composition from He to He-1% H ₂ , achieved 1% burnup.
MOZART (France/US/ Japan)	LiAlO ₂ Li ₂ ZrO ₃ Li ₂ O	Material comparison, investigate performance at low temperature, temperature step-change tests, pure He and He-0.1%H ₂ sweep gas.
BEATRIX-II (US/Canada/ Japan)	Li ₂ ZrO ₃ Li ₂ O	Material comparison, 10~30g pellet or pebbles, ⁶ Li content : 95at% or 85at%, temperature step-change tests over range from 440 to 1100°C (Li ₂ ZrO ₃), pure He and He-1%H ₂ sweep gas, PIE (compatibility of lithium ceramics and beryllium under irradiation)

Table 5-2 Comparison of results of in-situ irradiation tests

Test Designation	JMTR Irradiation Test	BEATRIX-II, Phase 2		EXOTIC-8
Materials	Li ₂ TiO ₃ (pebbles) ~134g, 80%T.D., 3μm, ⁶ Li : natural	Li ₂ O (ring) 8.1g, 87.3%T.D., 22μm, ⁶ Li : 95at%	Li ₂ ZrO ₃ (pebbles) 29.5g, 80%T.D., 10μm, ⁶ Li : 85at%	Li ₂ TiO ₃ (pellet&pebbles) 8.7g&13.6g, 83%T.D., 48% (smear density), ?μm, ⁶ Li : natural
Irradiation Conditions	Neutron Flux $\phi_{th} \sim 2.0 \times 10^{13}$ n/cm ² /s Tritium generation ~5.6X10 ⁷ Bq/min	Neutron Flux $\phi_{th} = ?$ Tritium generation ~8.1X10 ⁷ Bq/min	Neutron Flux $\phi_{th} = ?$ Tritium generation ~2.0X10 ⁷ Bq/min	Neutron Flux $\phi_{th} = ?$ Tritium generation ~2.2X10 ⁷ Bq/min
Recovery Conditions	Sweep gas flow Rate 200~950 cm ³ /min Hydrogen Concentration 100~10000ppm Irradiation Temperature 260~450 °C (center)	Sweep gas flow Rate 100 cm ³ /min Hydrogen Concentration 0~10000ppm Irradiation Temperature ~1000 °C (center)	Sweep gas flow Rate 100 cm ³ /min Hydrogen Concentration 0~10000ppm Irradiation Temperature ~1100 °C (center)	Sweep gas flow Rate ? cm ³ /min Hydrogen Concentration 1000ppm Irradiation Temperature 380~640 °C (center)
Results	Effect of Irradiation Temperature	Temperature transients were followed by positive tritium recovery peaks for temperature increases and negative recovery peaks for temperature decreases.	Temperature transients were followed by positive tritium recovery peaks for temperature increases and negative recovery peaks for temperature decreases.	Tritium release rate increased with increasing the irradiation temperature. Tritium residence time was estimated.
	Effect of Sweep Gas Flow Rate	Transients were followed by positive tritium recovery peaks for sweep gas flow rate increases and negative recovery peaks for sweep gas flow rate decreases.	Transients were followed by positive tritium recovery peaks for sweep gas flow rate increases and negative recovery peaks for sweep gas flow rate decreases.	_____
	Effect of Hydrogen Concentration	Transients were followed by positive tritium recovery peaks for hydrogen concentration increases and negative recovery peaks for hydrogen concentration decreases.	Transients were followed by positive tritium recovery peaks for hydrogen concentration increases and negative recovery peaks for hydrogen concentration decreases.	_____
	Effect of Moisture Concentration	Moisture was released at reactor start-up. (concentration : max. 1000ppm)	Moisture was released at reactor start-up. (concentration : max. 6000ppm)	_____

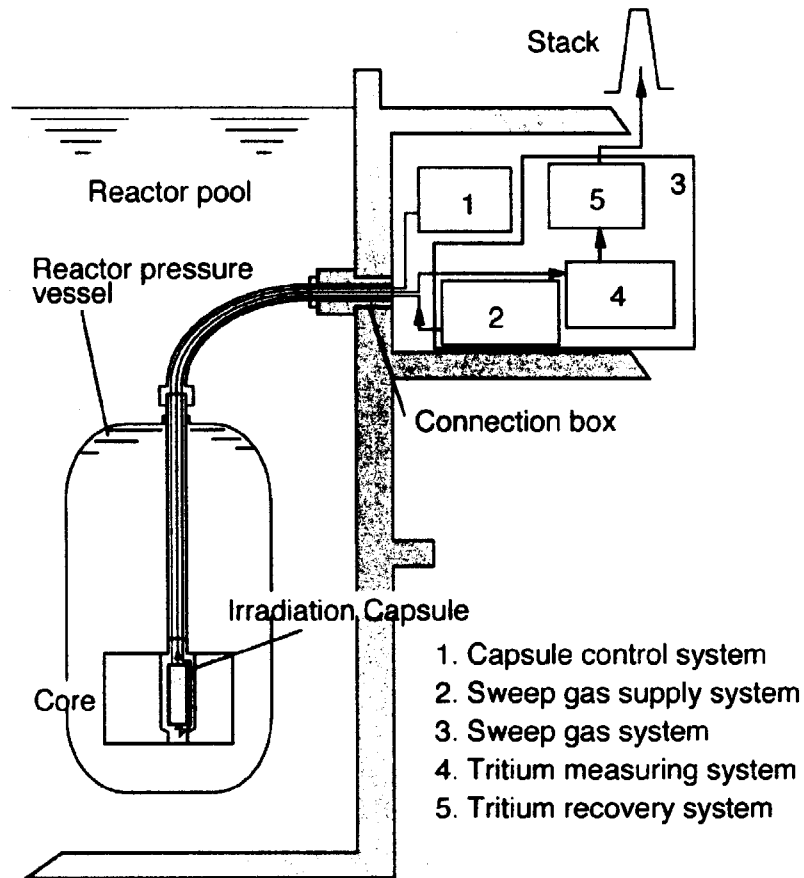


Fig.2-1 JMTR irradiation facility for in-situ irradiation test.

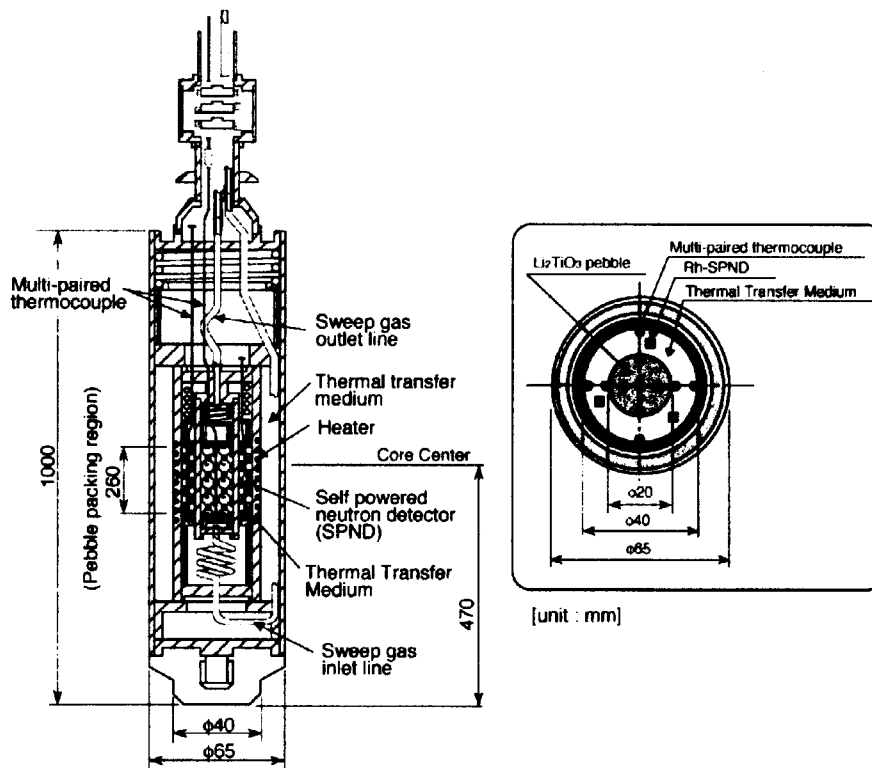


Fig. 2-2 Structure of irradiation capsule.

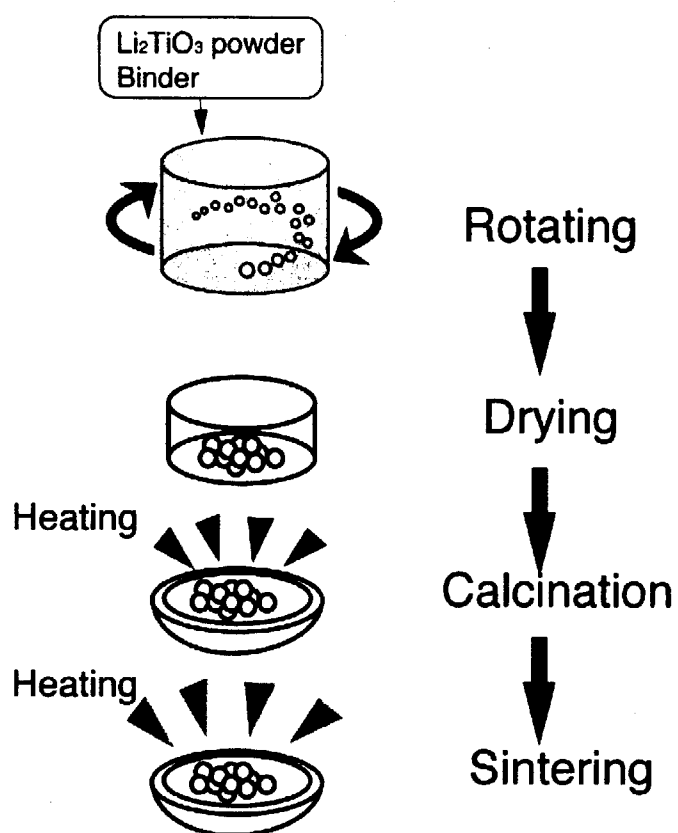


Fig.3-1 Fabrication flow of Li_2TiO_3 pebbles for the rotating-granulation/sintering method.

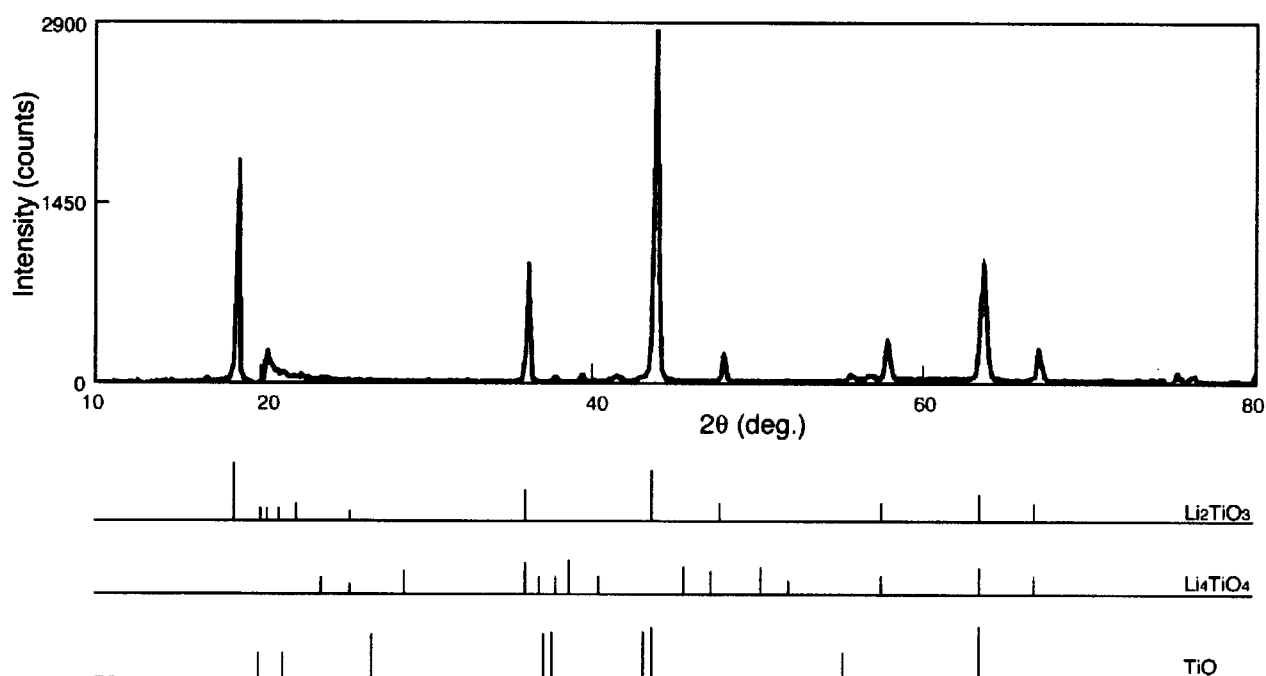
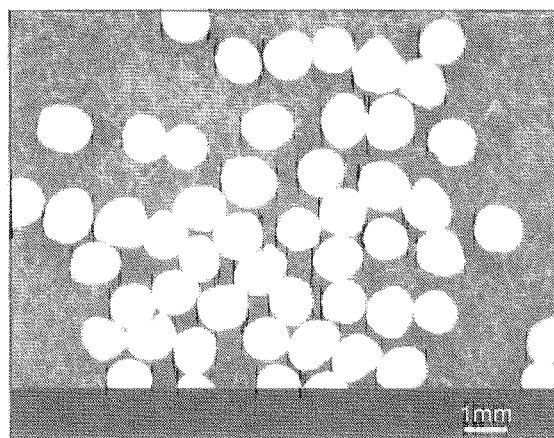
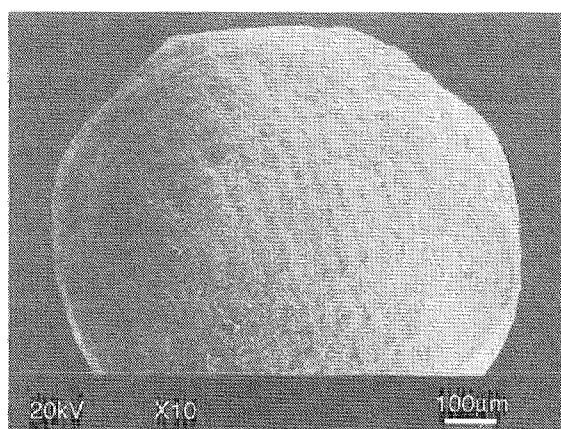


Fig.3-2 X-ray diffraction patterns of Li_2TiO_3 powder.



a) Visual photograph



b) SEM photograph

Fig.3-3 Photographs of Li_2TiO_3 pebbles.

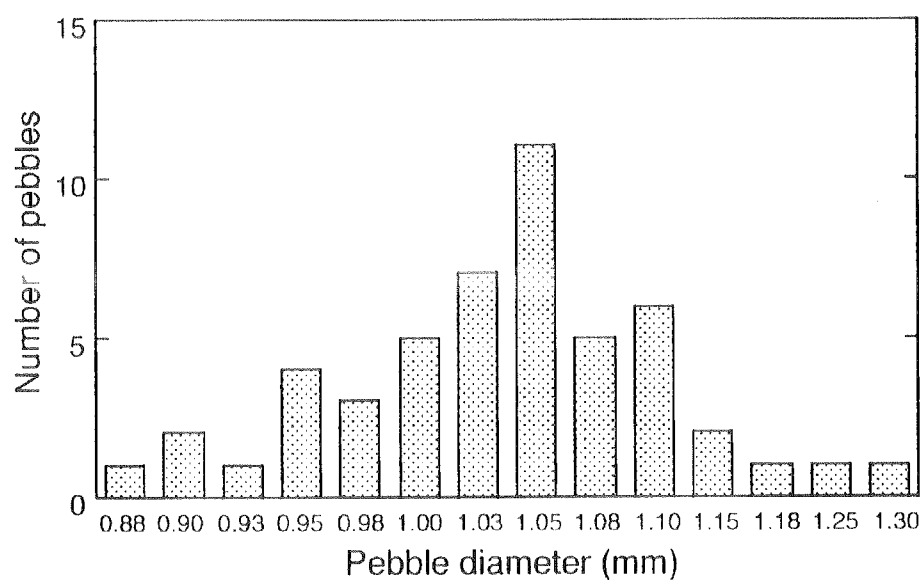
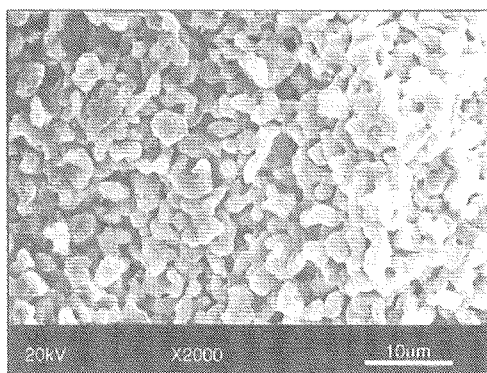
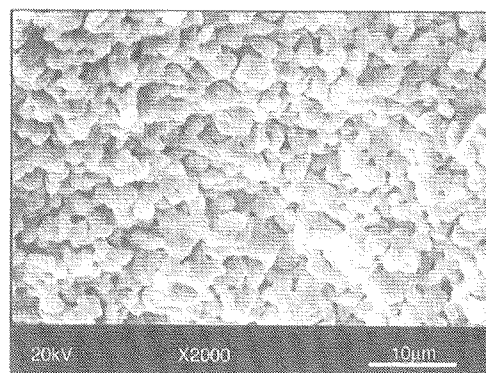


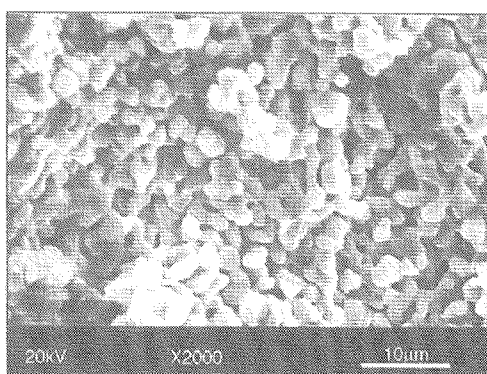
Fig.3-4 Distribution on diameter of Li_2TiO_3 pebbles fabricated by rotating granulation method.



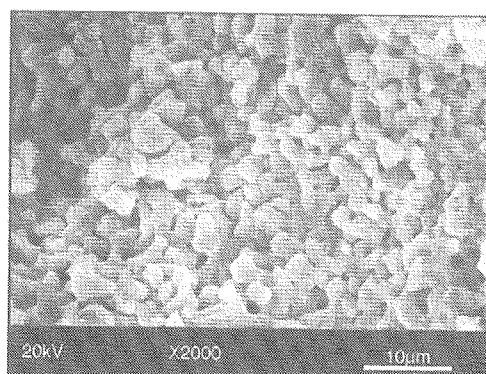
a) Pebble No.1



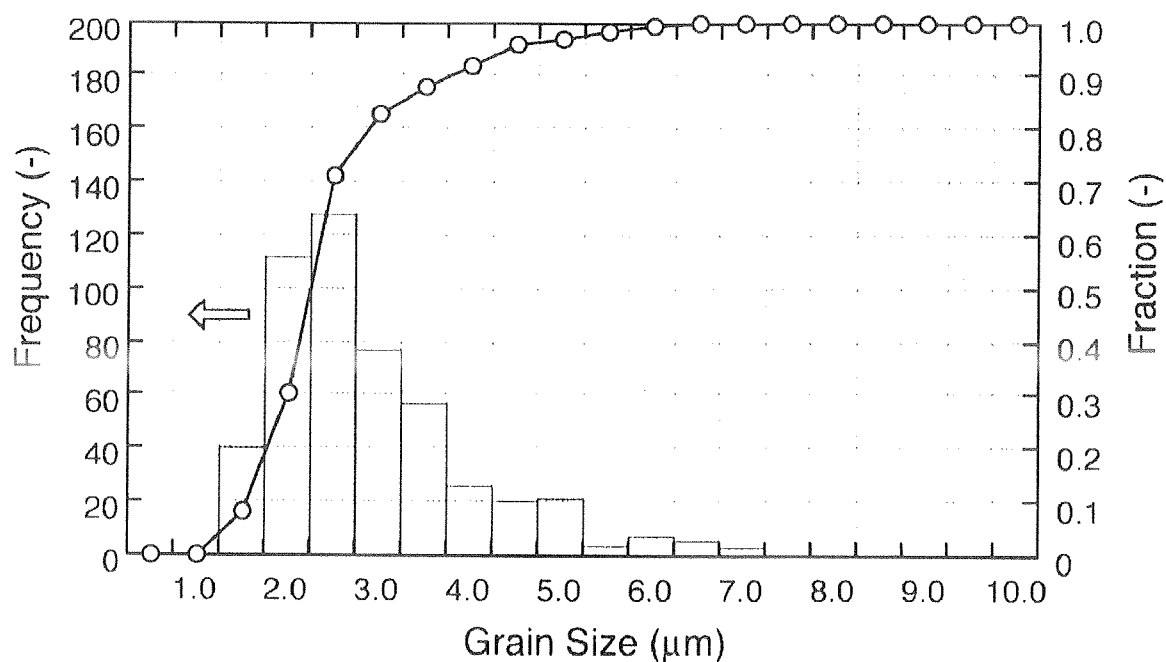
b) Pebble No.2



c) Pebble No.3



d) Pebble No.4

Fig.3-5 SEM photographs of cross sections of Li_2TiO_3 pebbles.Fig.3-6 Distribution of grain size of Li_2TiO_3 pebbles.

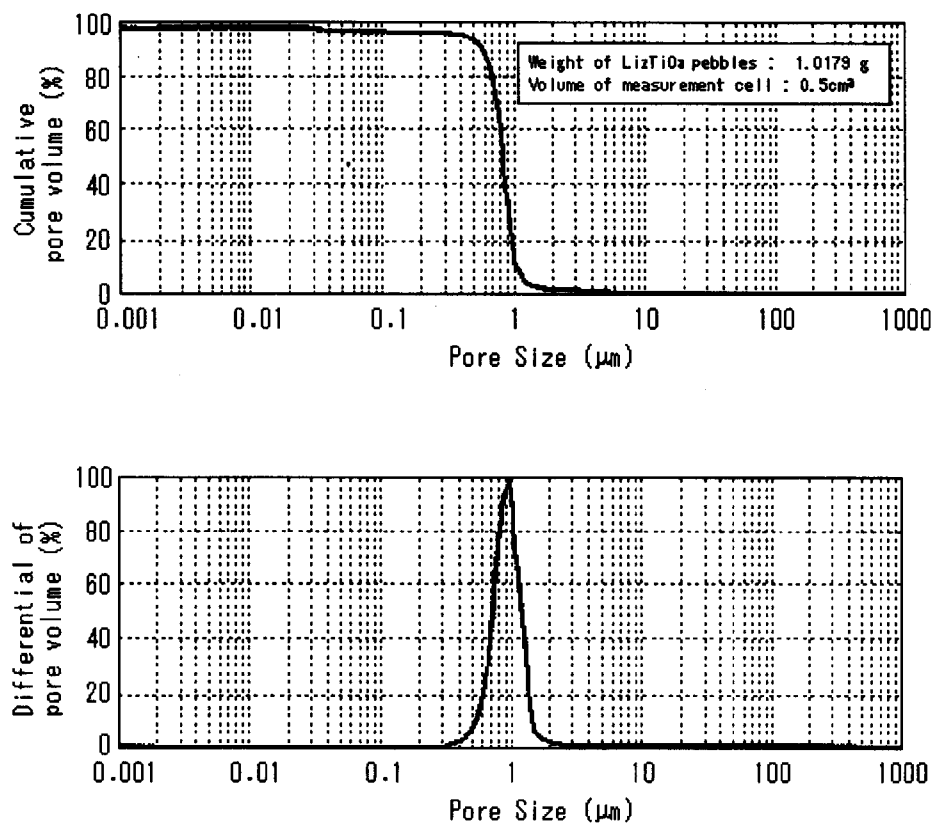


Fig.3-7 Distribution of pore size of Li_2TiO_3 pebbles measured by mercury porosimetry.

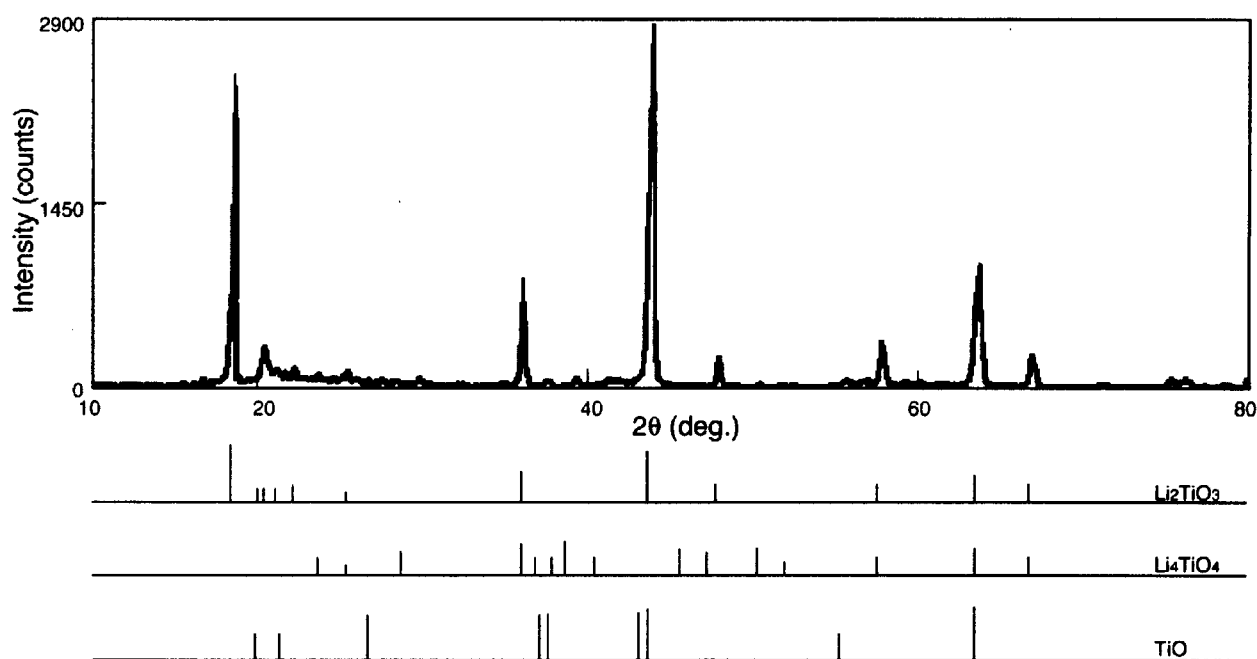


Fig.3-8 X-ray diffraction patterns of Li_2TiO_3 pebbles.

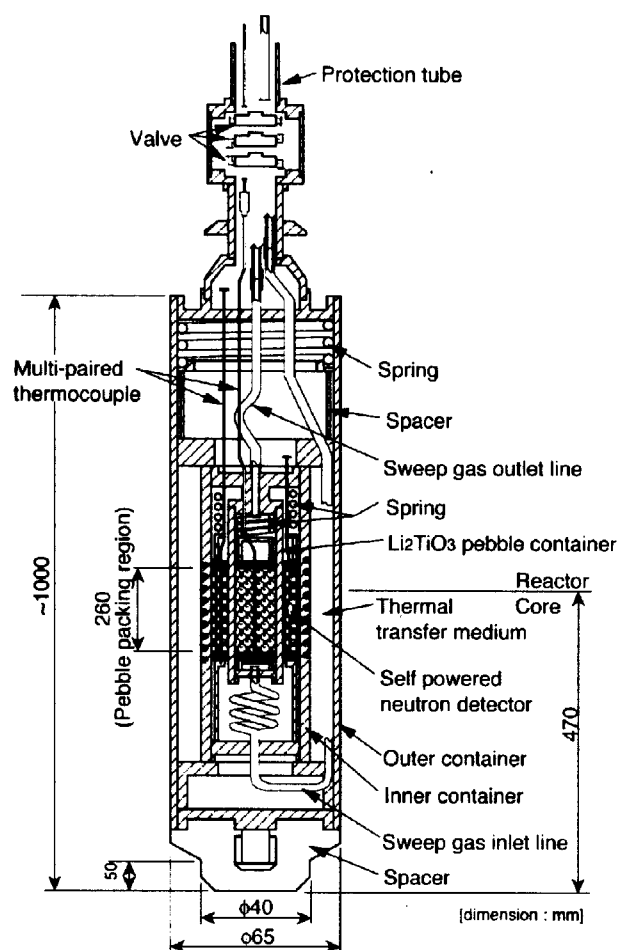


Fig.4-1 Vertical cross section of irradiation capsule.

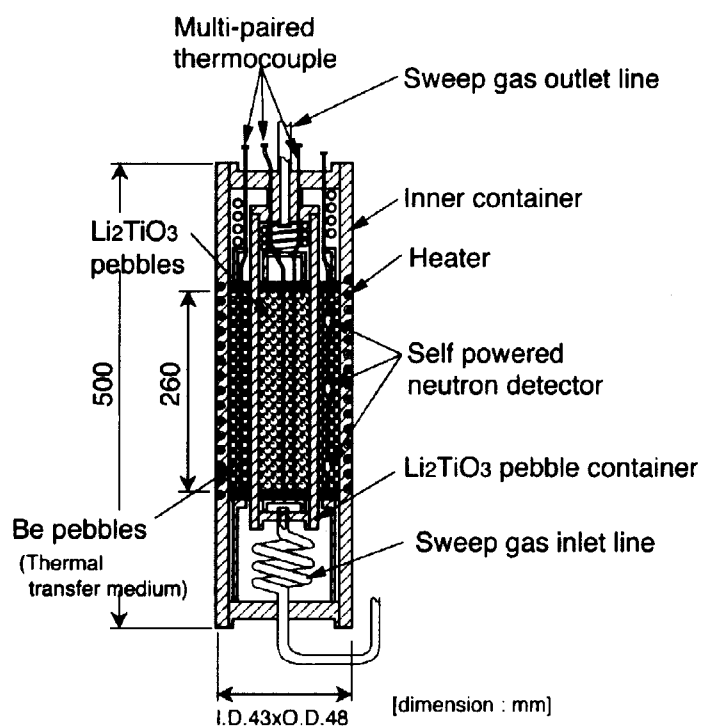


Fig.4-2 Vertical cross section of inner capsule.

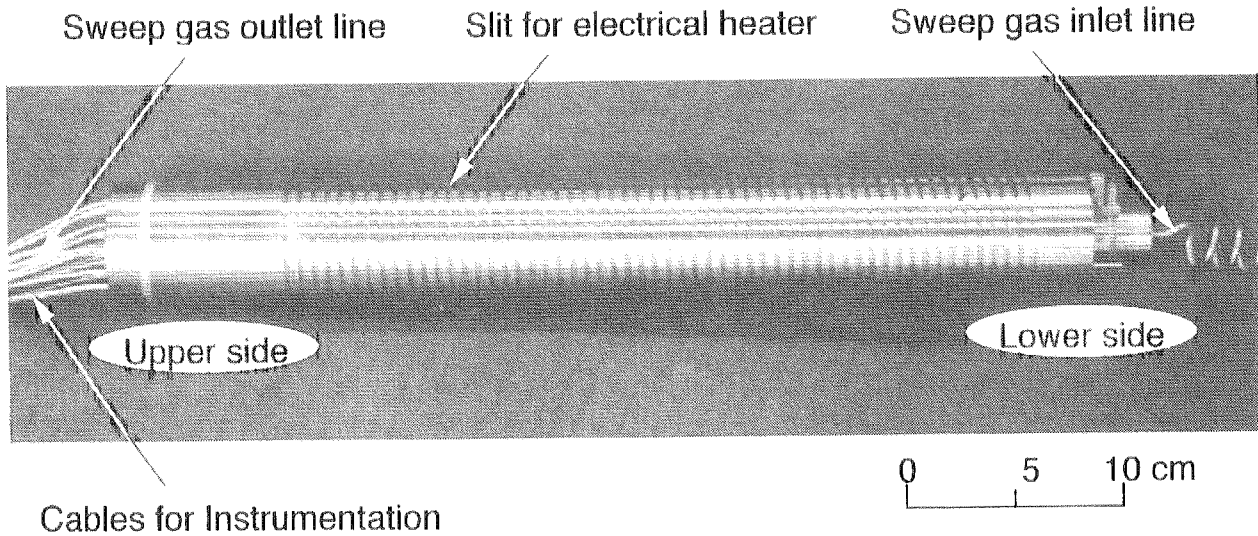


Fig.4-3 Photograph of inner capsule.

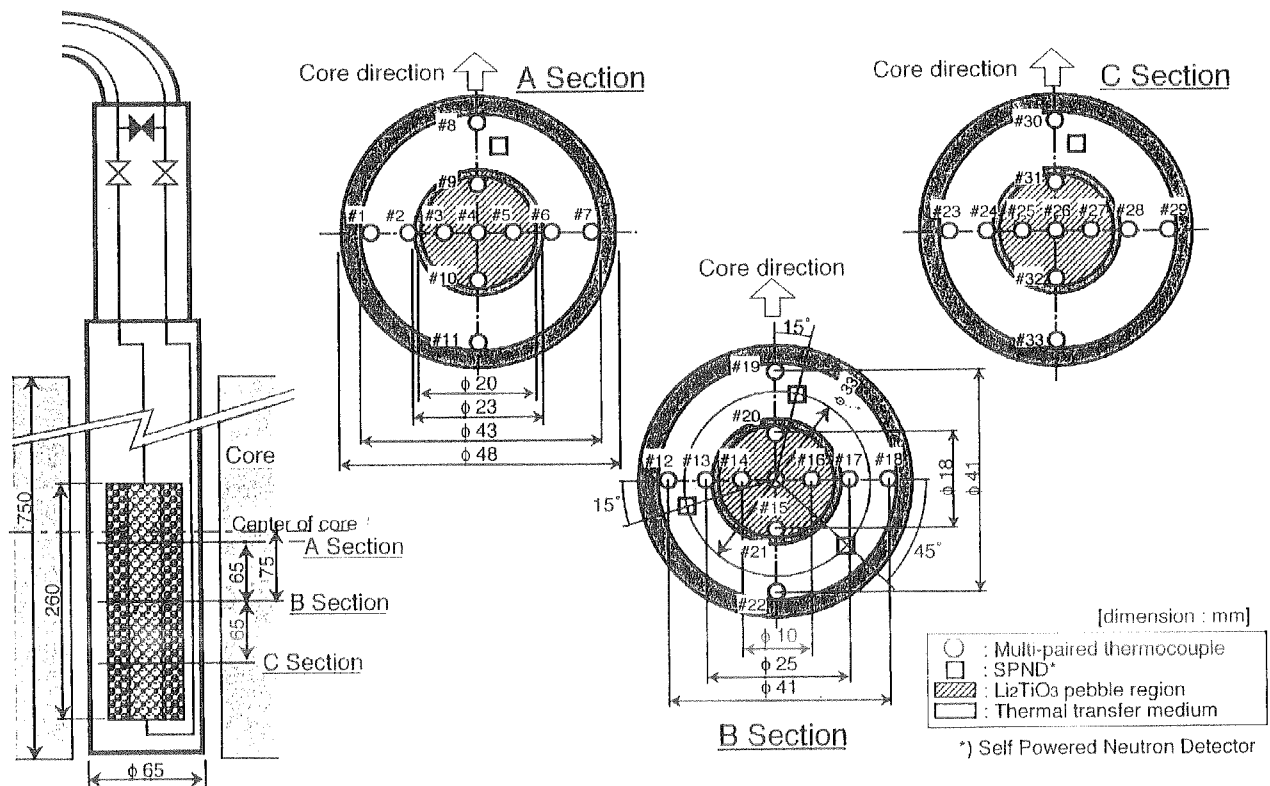


Fig.4-4 Arrangement of thermocouples (T/Cs) and self-powered neutron detectors (SPNDs).

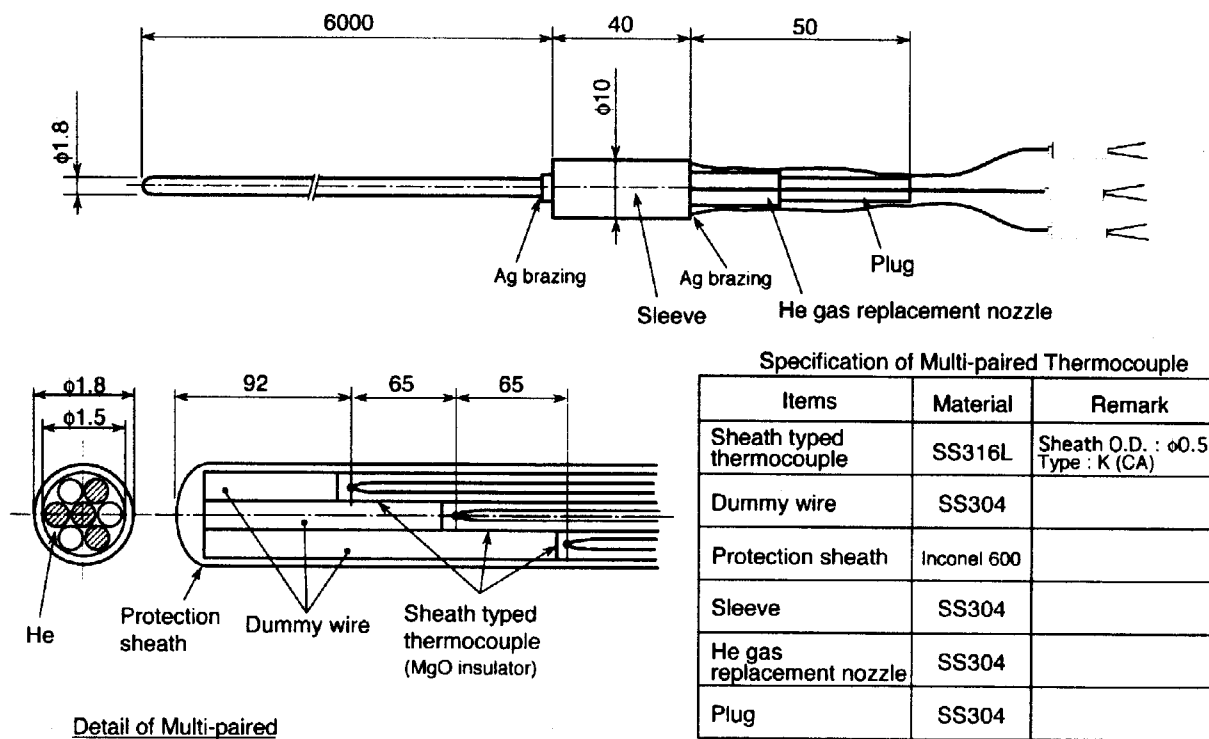
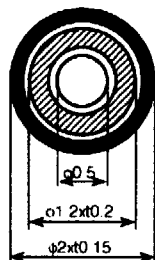
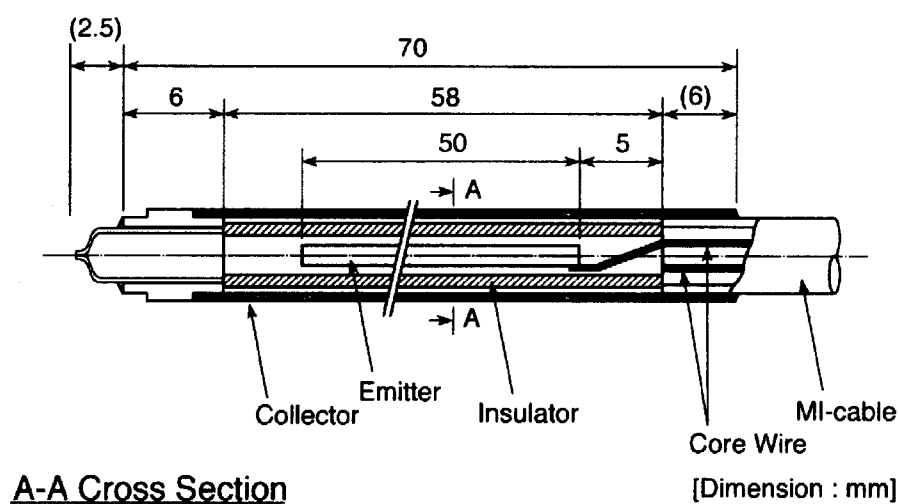


Fig.4-5 Conceptual structure and specification of multi-paired thermocouple (T/Cs).

**Specification of SPND**

Part of measurement			MI-cable		
Emitter	Collector	Insulator	Core wire (twin)	Insulator	Sheath
Rh	Inconel 600	Al ₂ O ₃ (99.5wt%)	Inconel 600	Al ₂ O ₃ (99.6wt%)	Inconel 600 ($\phi 1.5$ mm)

Fig.4-6 Conceptual structure and specification of self-powered neutron detectors (SPNDs).

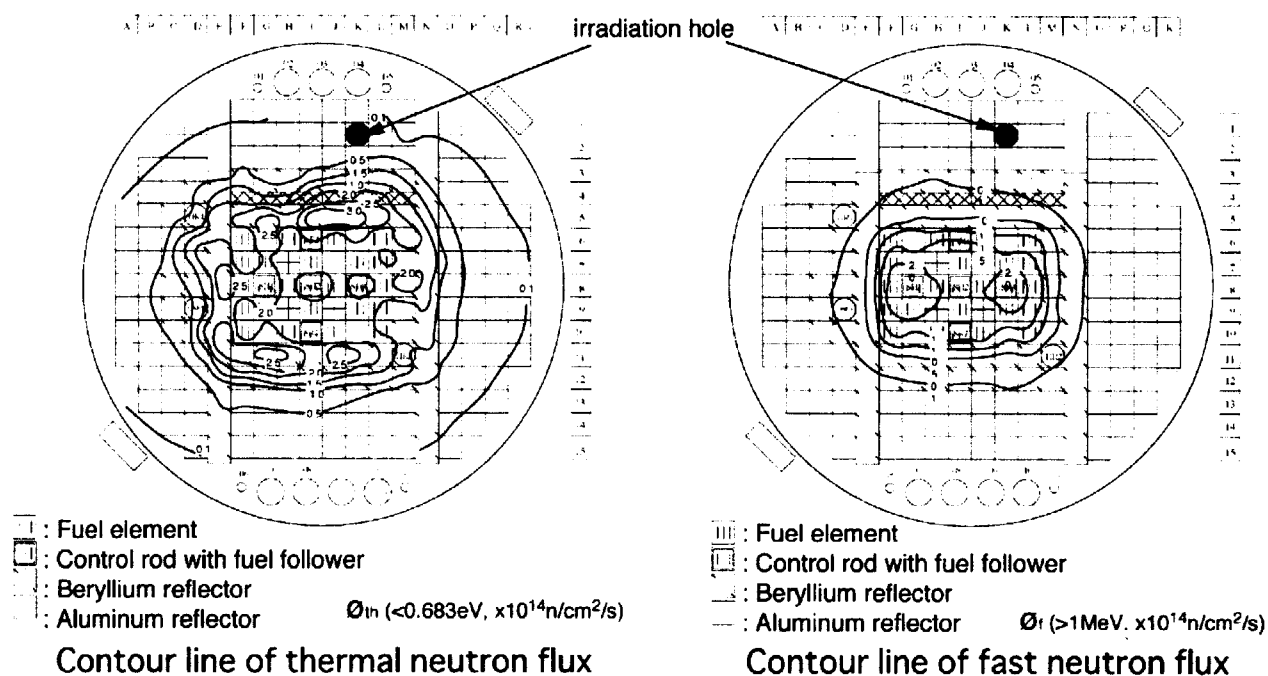


Fig.4-7 Irradiation hole for irradiation capsule.

Conditions

Nuclear calculation code : ANISN
 Thermal calculation code : GENGTC
 Packing fraction of pebble
 Li_2TiO_3 : 62%P.F.
 Pebble density
 Li_2TiO_3 : 80.1%T.D.
 ^6Li enrichment : 7.5at%
 Candidate irradiation hole : K-2

Results of nuclear calculation

Heating value : 12.1W/cm
 Tritium production : $\sim 1.7\text{Ci/d}$
 (Breeder region : $\phi 20 \times 1260\text{mm}$)

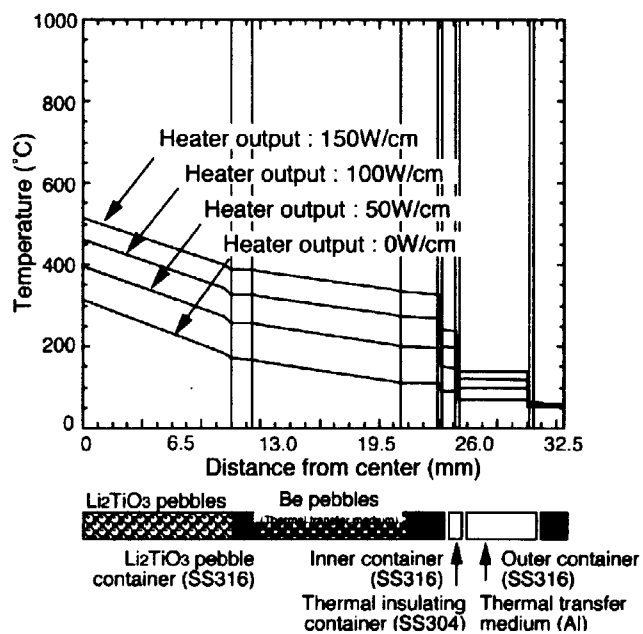


Fig.4-8 Result of nuclear and thermal calculation of irradiation capsule.

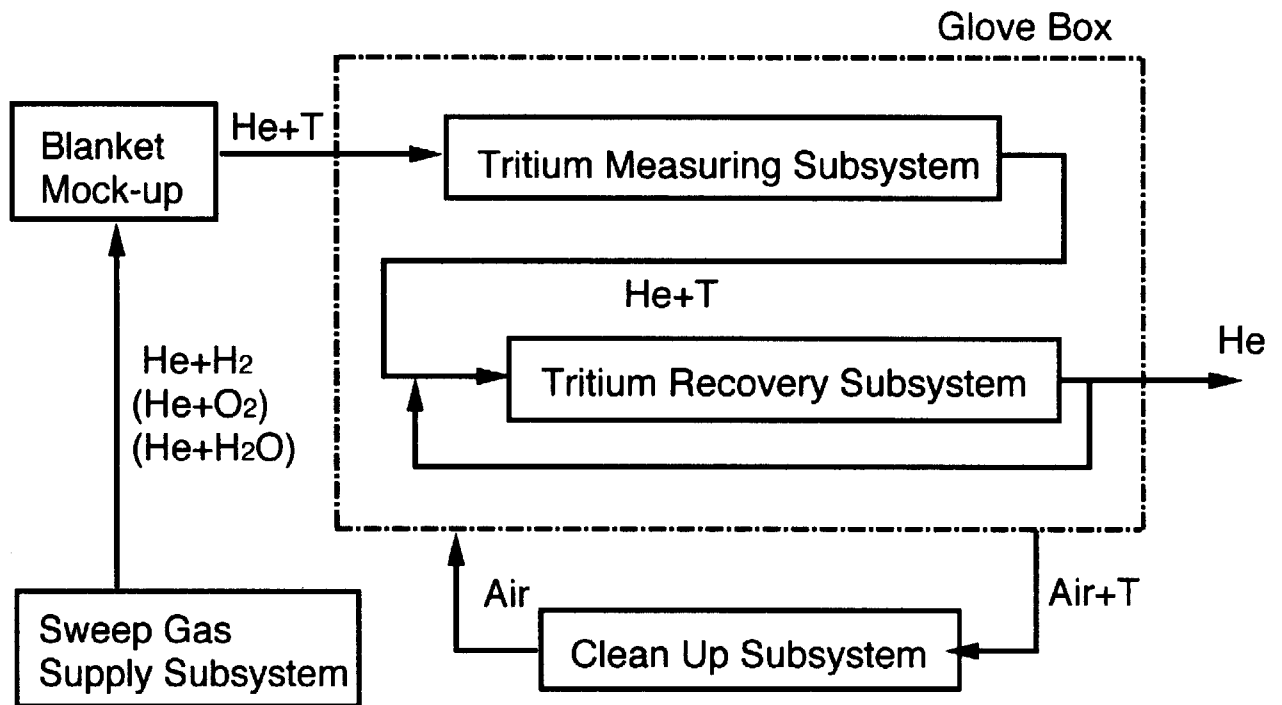


Fig.4-9 Block diagram of the sweep gas system.

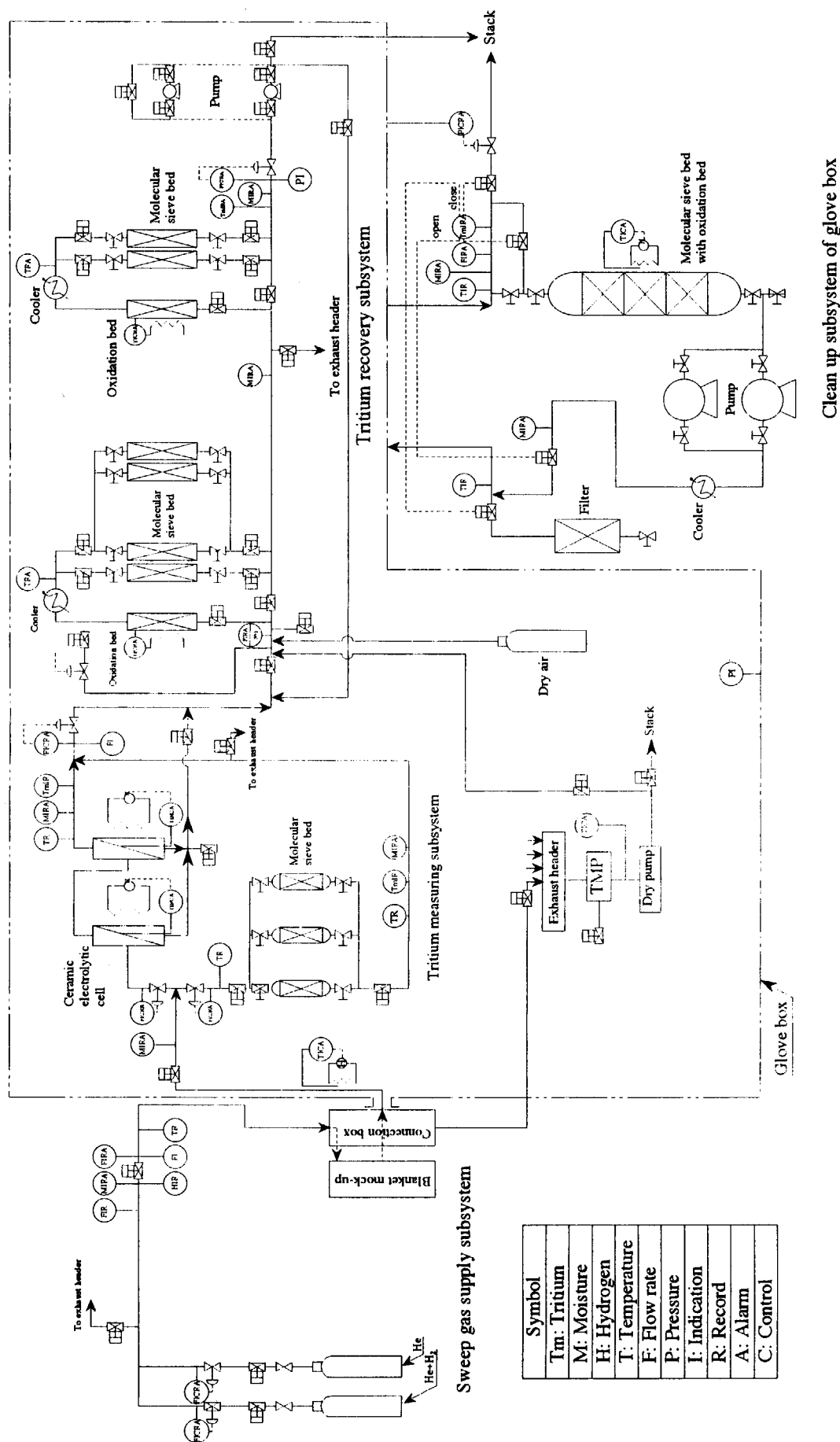


Fig.4-10 Schematic flow diagram of the sweep gas system.

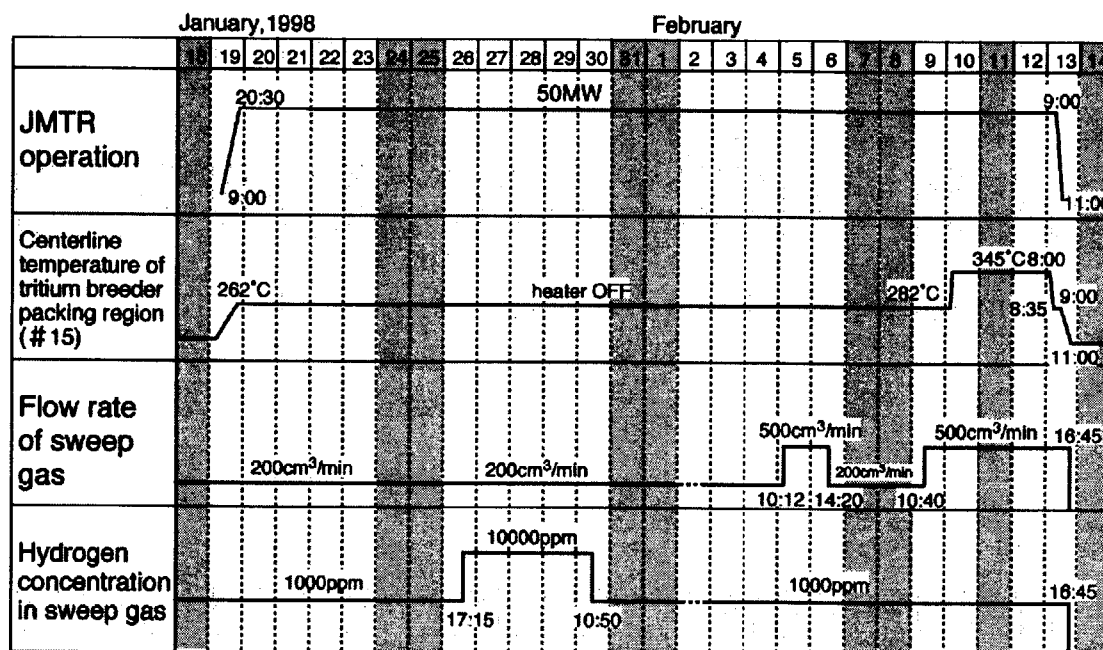


Fig.4-11 Outline of experimental conditions on the first irradiation test.

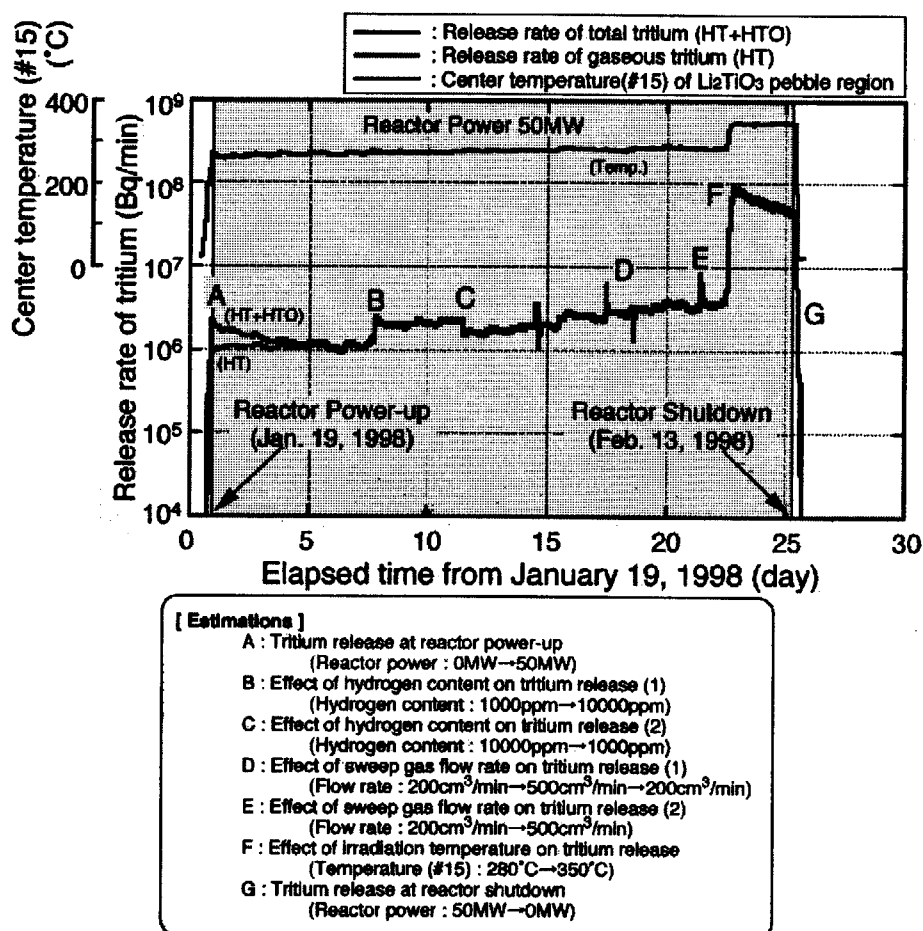


Fig.4-12 Result of the first irradiation test in the 121st cycle.

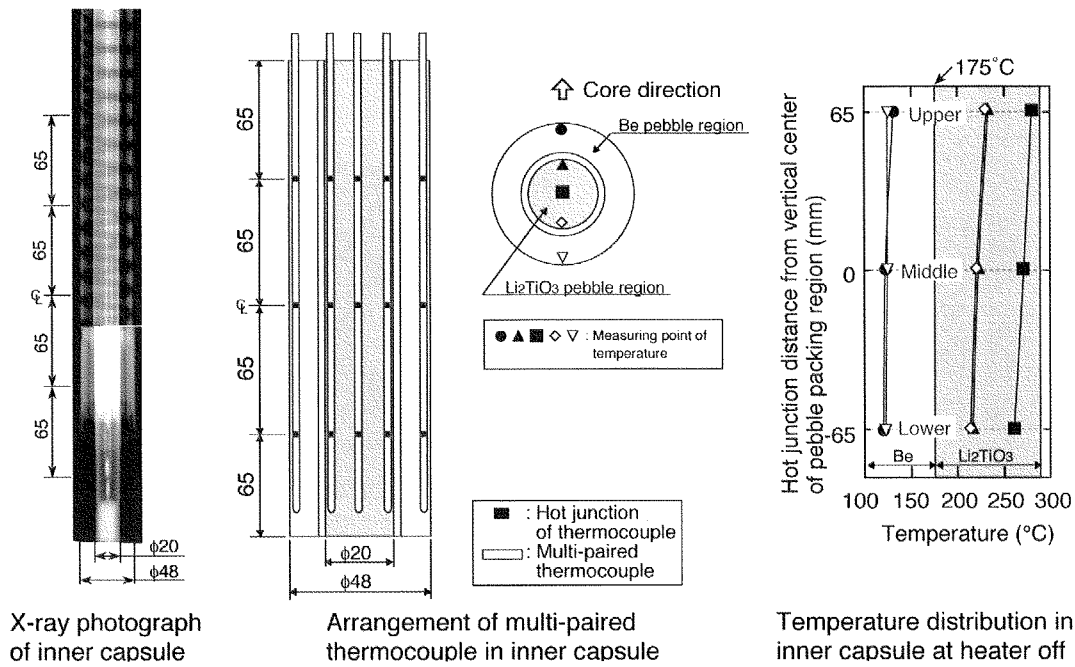


Fig.4-13 Axial temperature distribution in the 121st cycle.

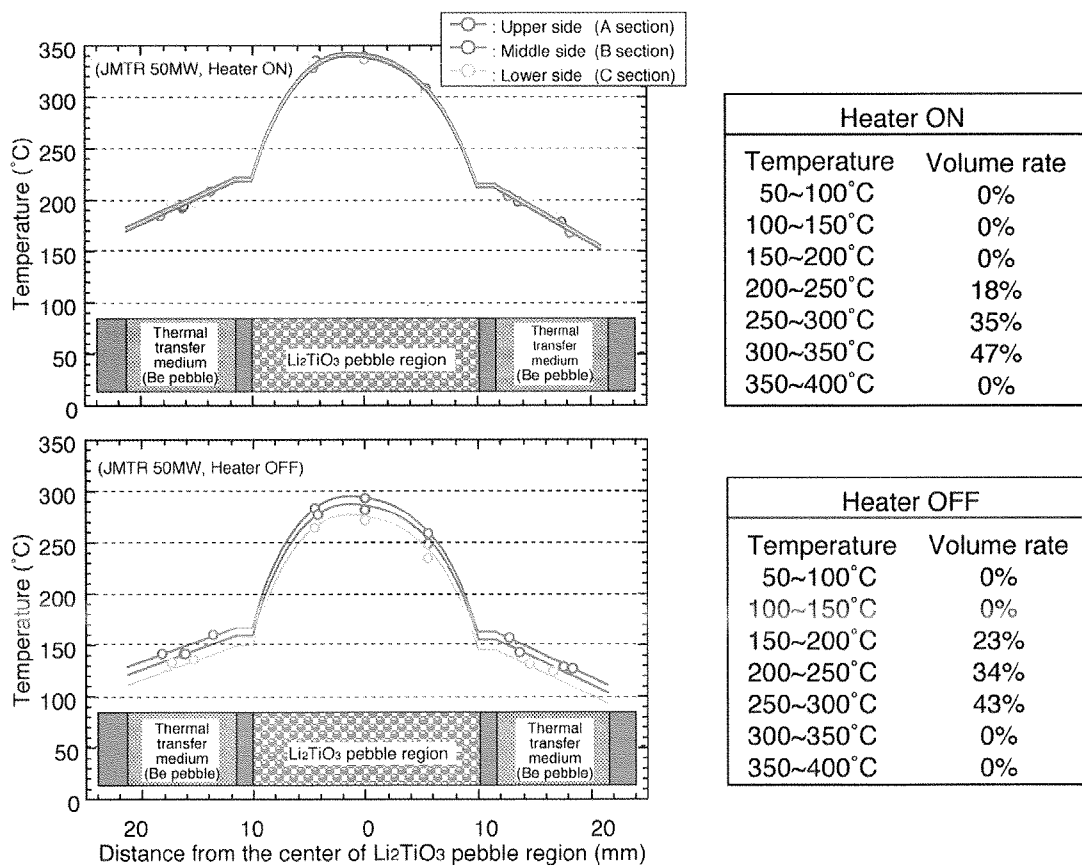


Fig.4-14 Radial temperature distribution in the 121st cycle.

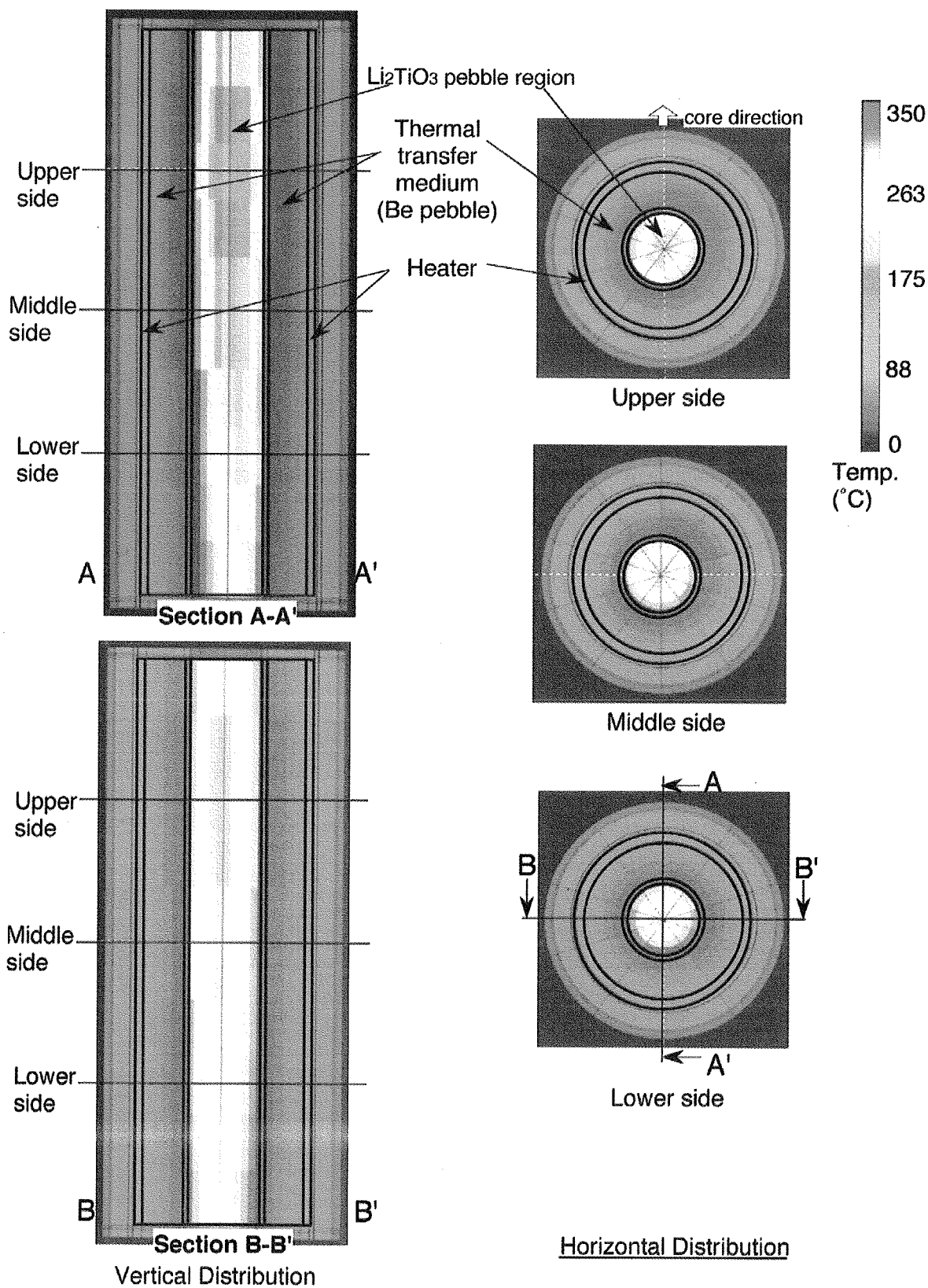


Fig.4-15 Result of 3-dimensional temperature distributions calculated by TRAMP.
(the 121st cy, 50MW, Heater-OFF).

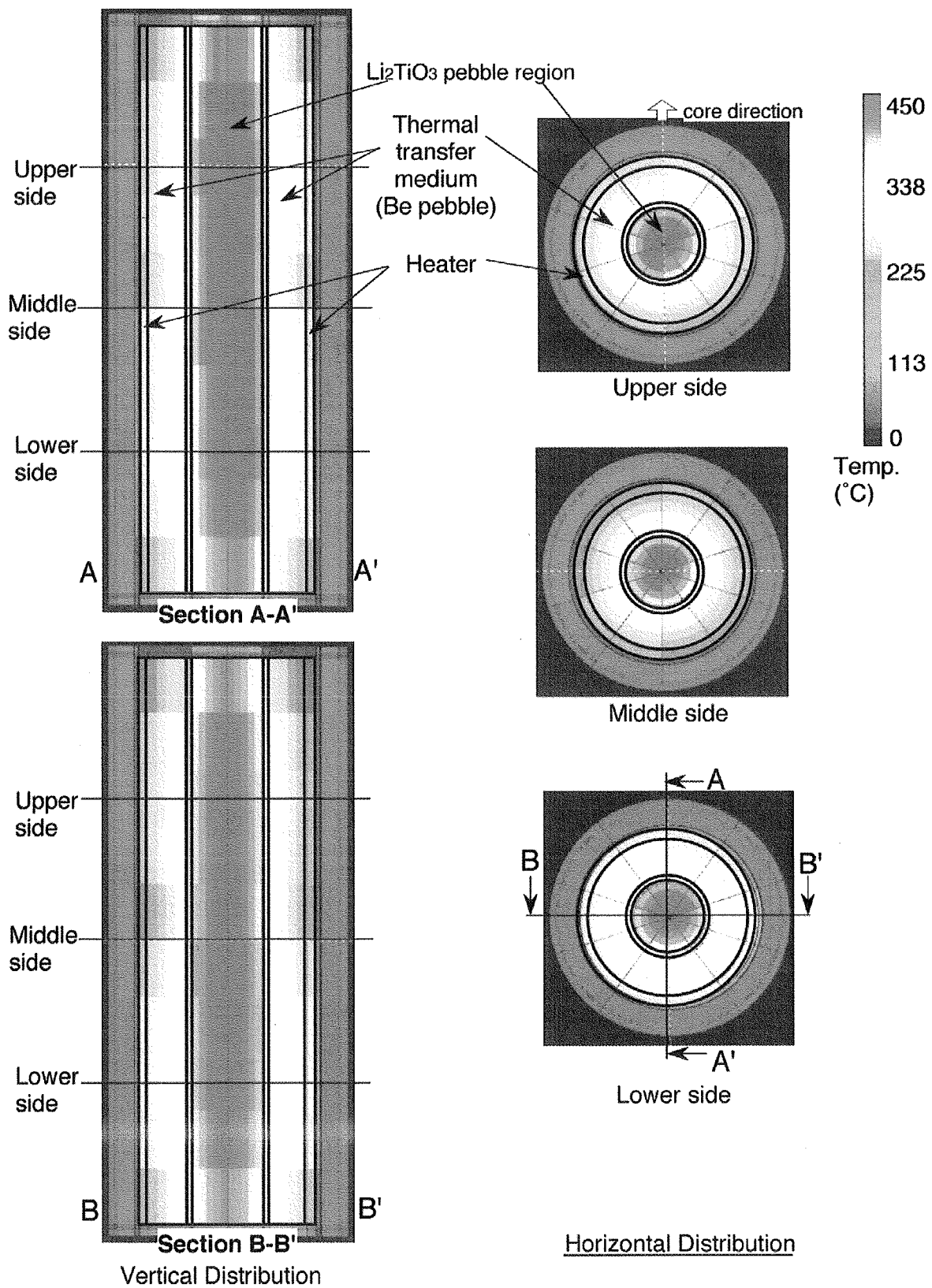


Fig.4-37 Result of 3-dimensional temperature distributions calculated by TRAMP.
(the 123rd cy, 50MW, Heater-ON).

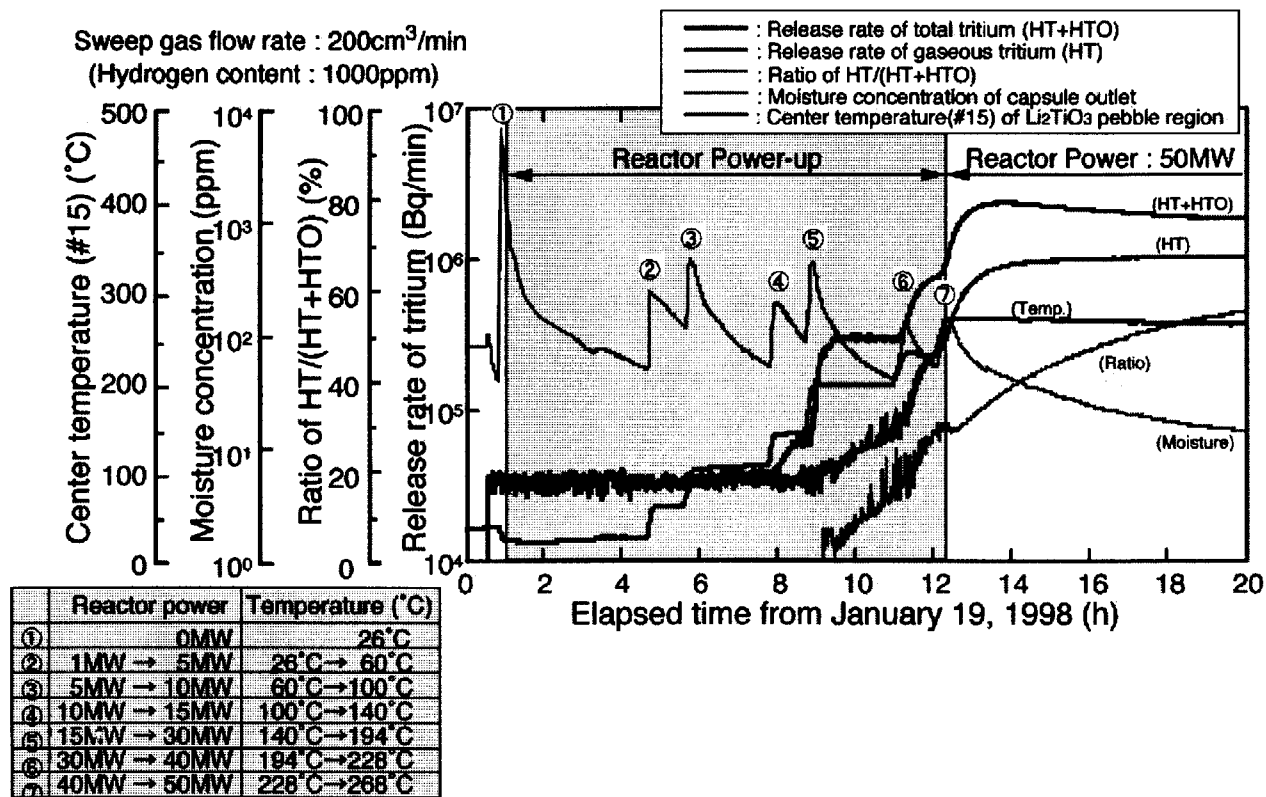


Fig.4-17 Tritium release at the reactor power-up in the 121st cycle.

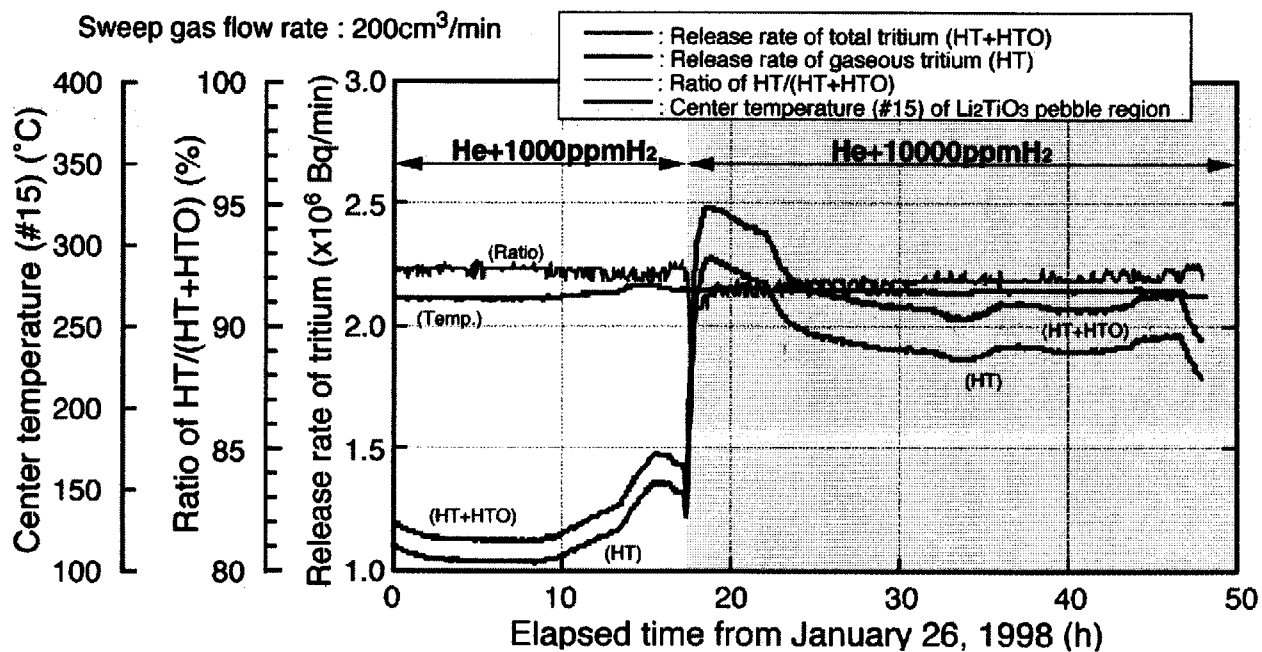


Fig.4-18 Result of hydrogen content change test in the 121st cycle (1).

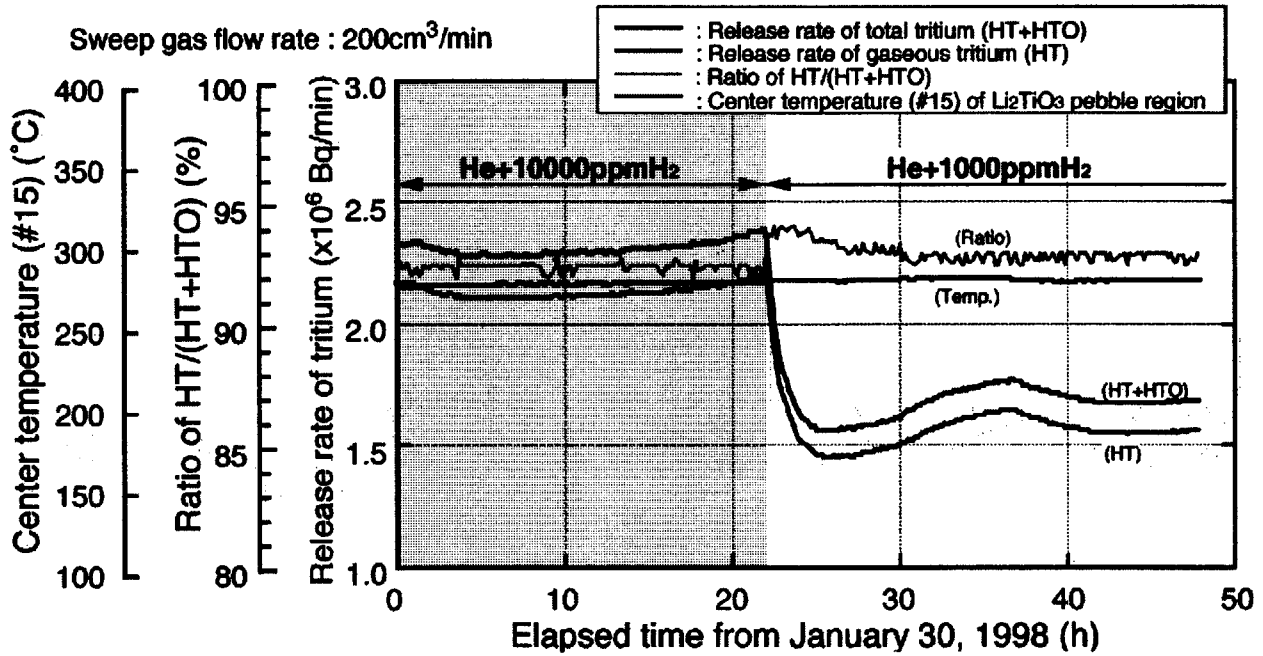


Fig.4-19 Result of hydrogen content change test in the 121st cycle (2).

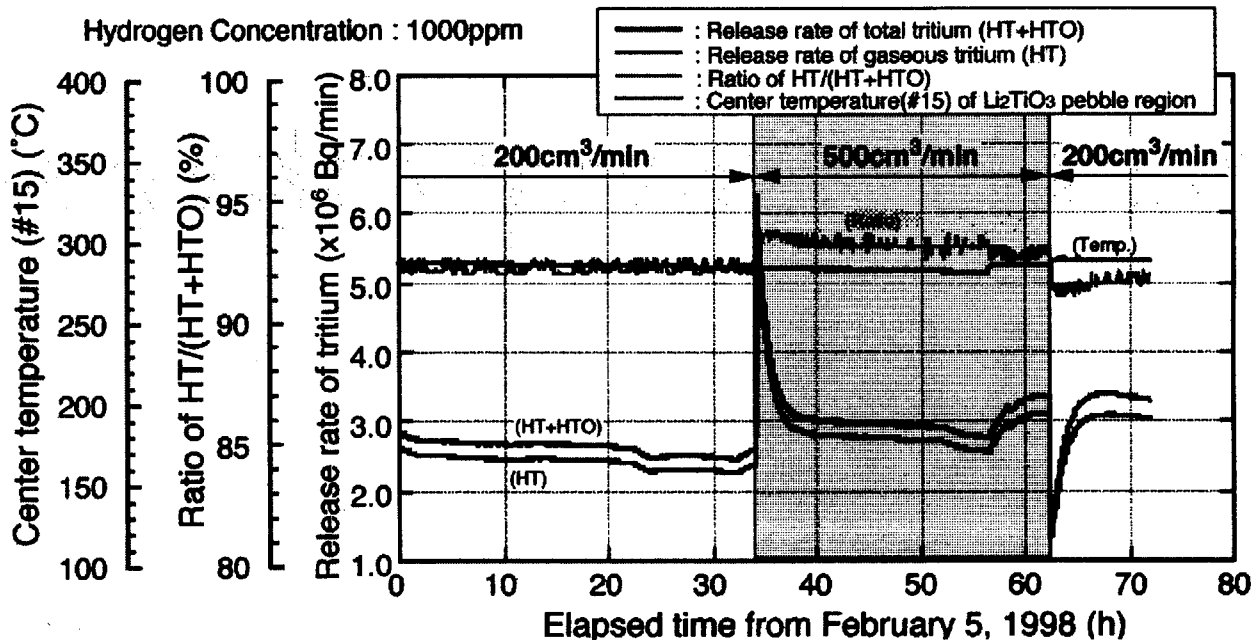


Fig.4-20 Result of sweep-gas flow rate change test in the 121st cycle (1).

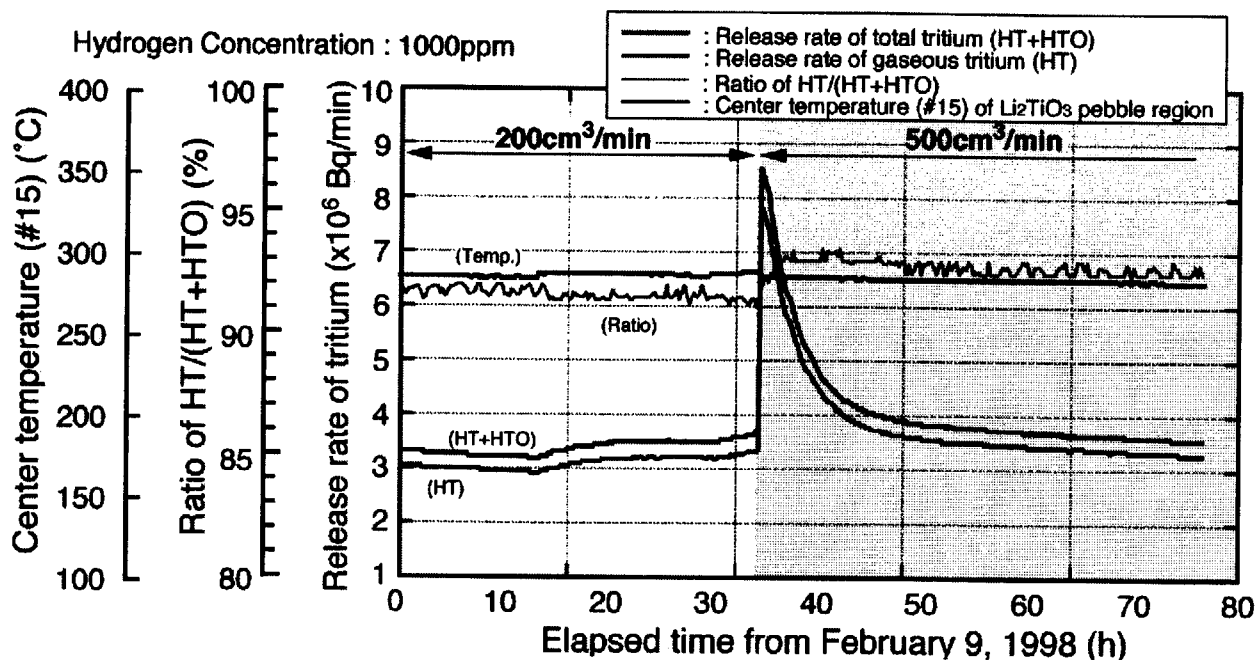


Fig.4-21 Result of sweep-gas flow rate change test in the 121st cycle (2).

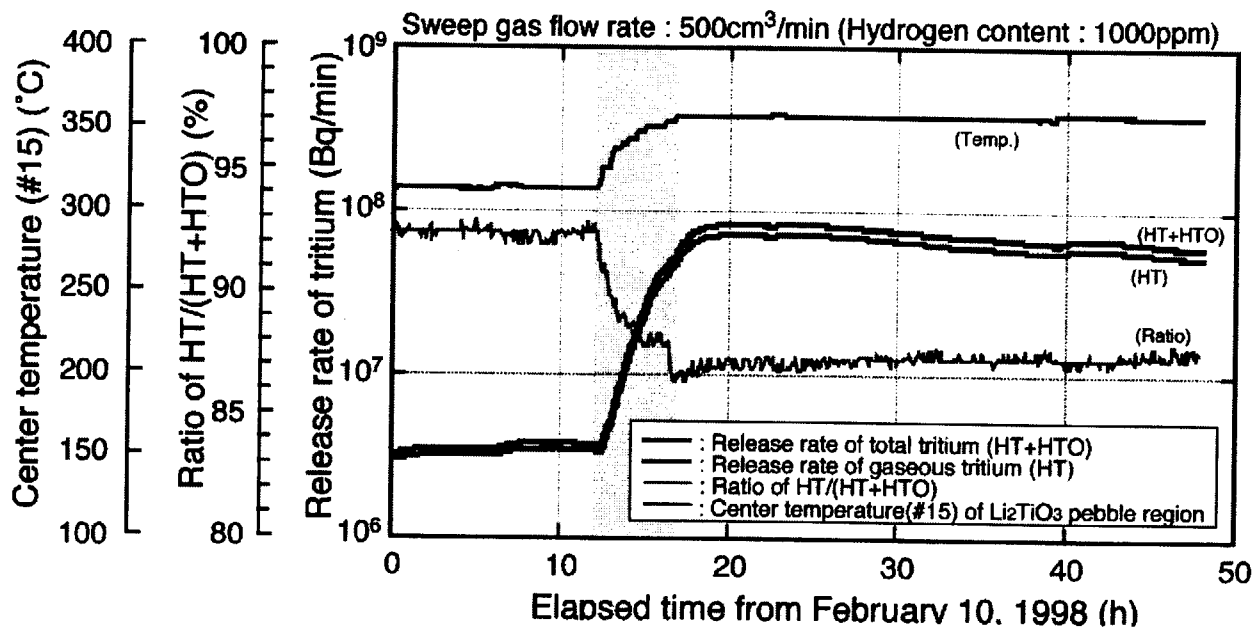


Fig.4-22 Result of temperature step-change test in the 121st cycle.

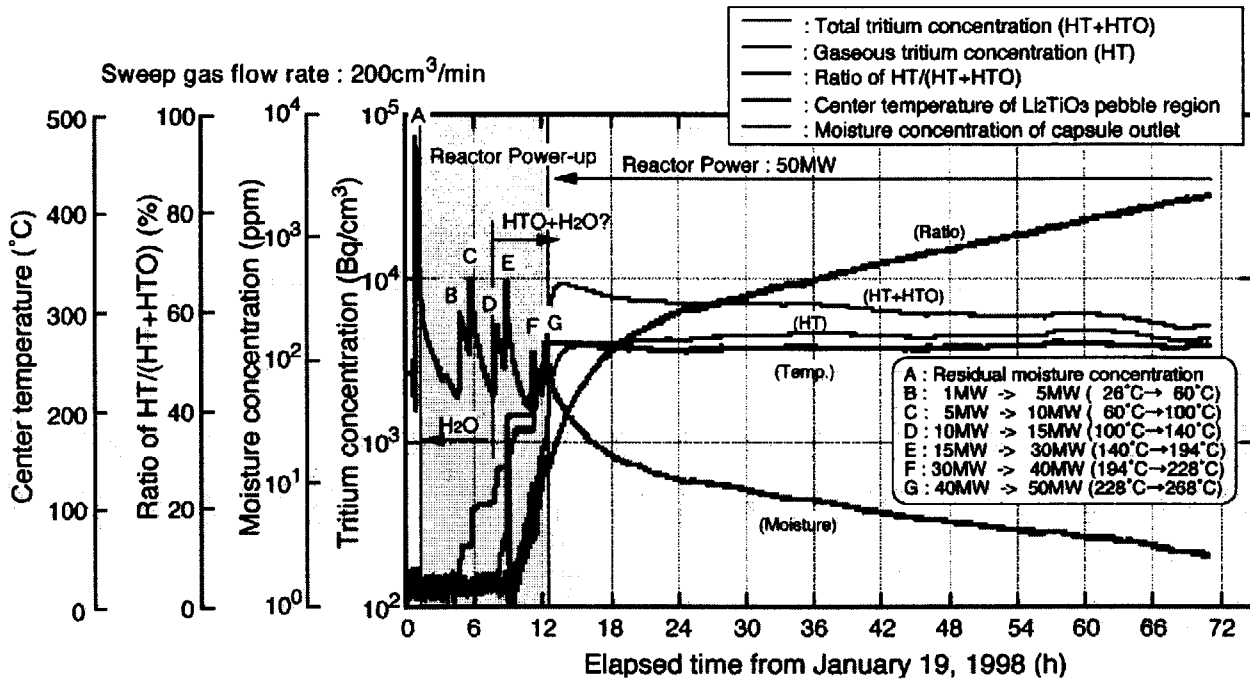


Fig.4-23 Dependence on moisture concentration of capsule outlet and ratio of HT/(HT+HTO).

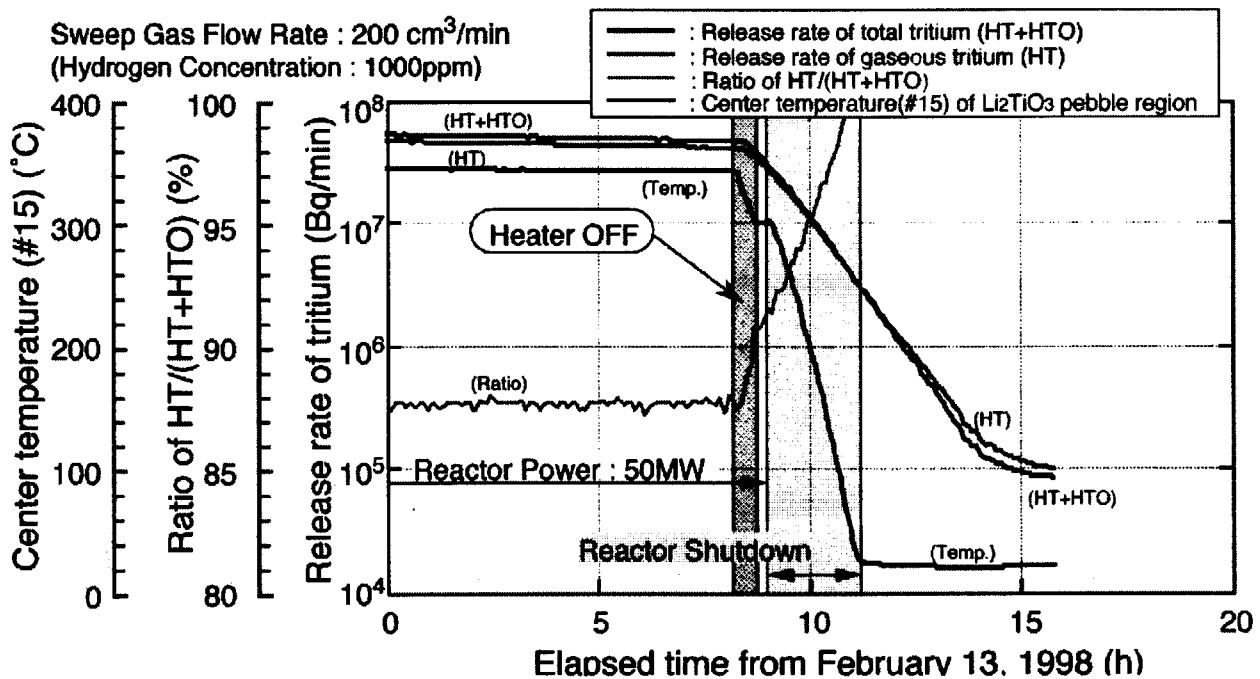


Fig.4-24 Tritium release at the reactor shutdown in the 121st cycle.

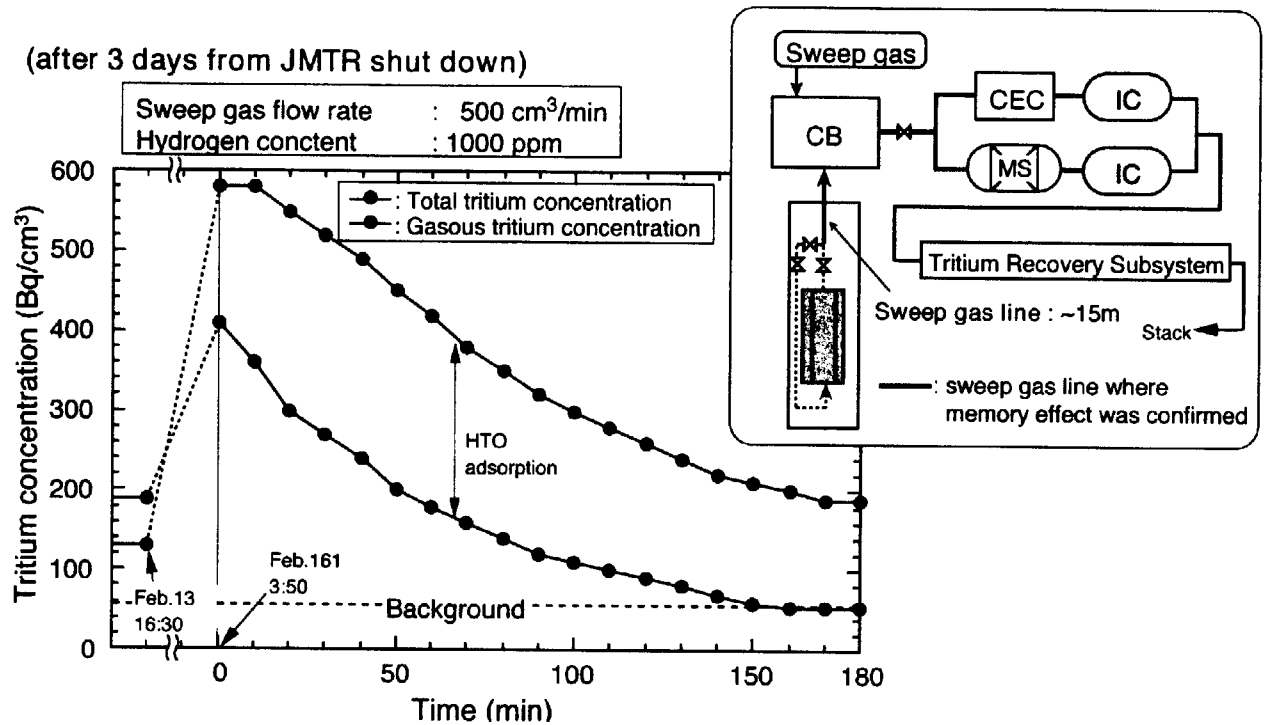


Fig.4-25 Memory effect of tritium in sweep gas line after the 121st cycle.

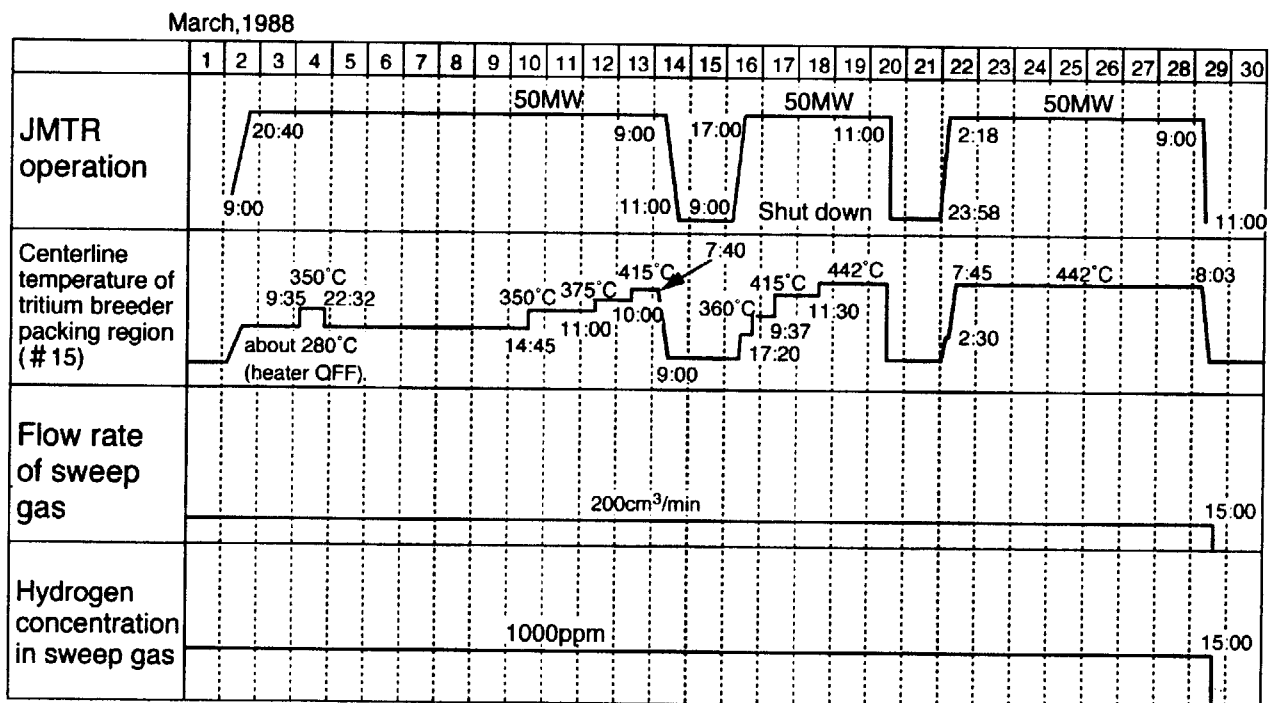
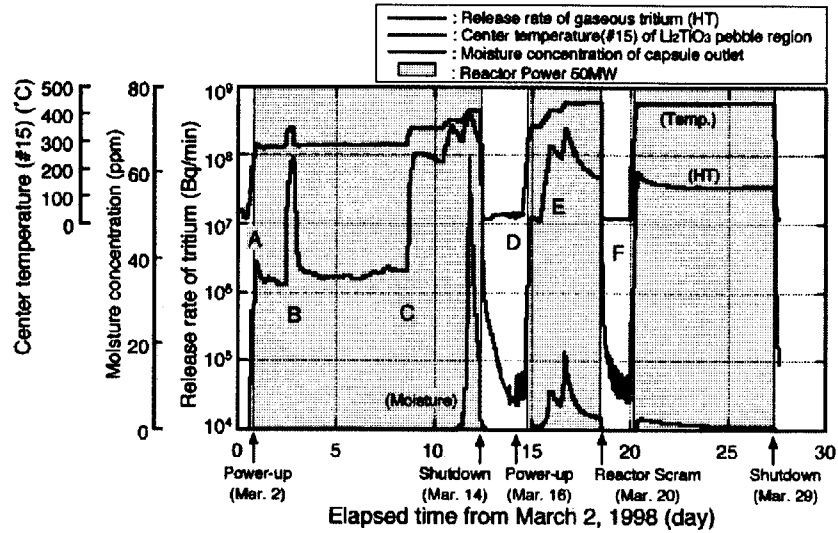


Fig.4-26 Outline of experimental conditions on the second irradiation test.



[Estimations]

- A : Tritium release at reactor power-up
(Reactor power : 0MW → 50MW)
- B : Effect of irradiation temperature on tritium release (1)
(Temperature (#15) : 280°C → 350°C)
- C : Effect of irradiation temperature on tritium release (2)
(Temperature (#15) : 280°C → 420°C)
- D : Tritium release at reactor shut-down and power-up (1)
(Reactor power : 50MW → 0MW → 50MW)
- E : Effect of irradiation temperature on tritium release (3)
(Temperature (#15) : 280°C → 450°C)
- F : Tritium release at reactor shut-down and power-up (2)
(Reactor power : 50MW → 0MW → 50MW)
(Temperature (#15) : 450°C → ~30°C → 450°C)

Fig.4-27 Result of the second irradiation test in the 122nd cycle.

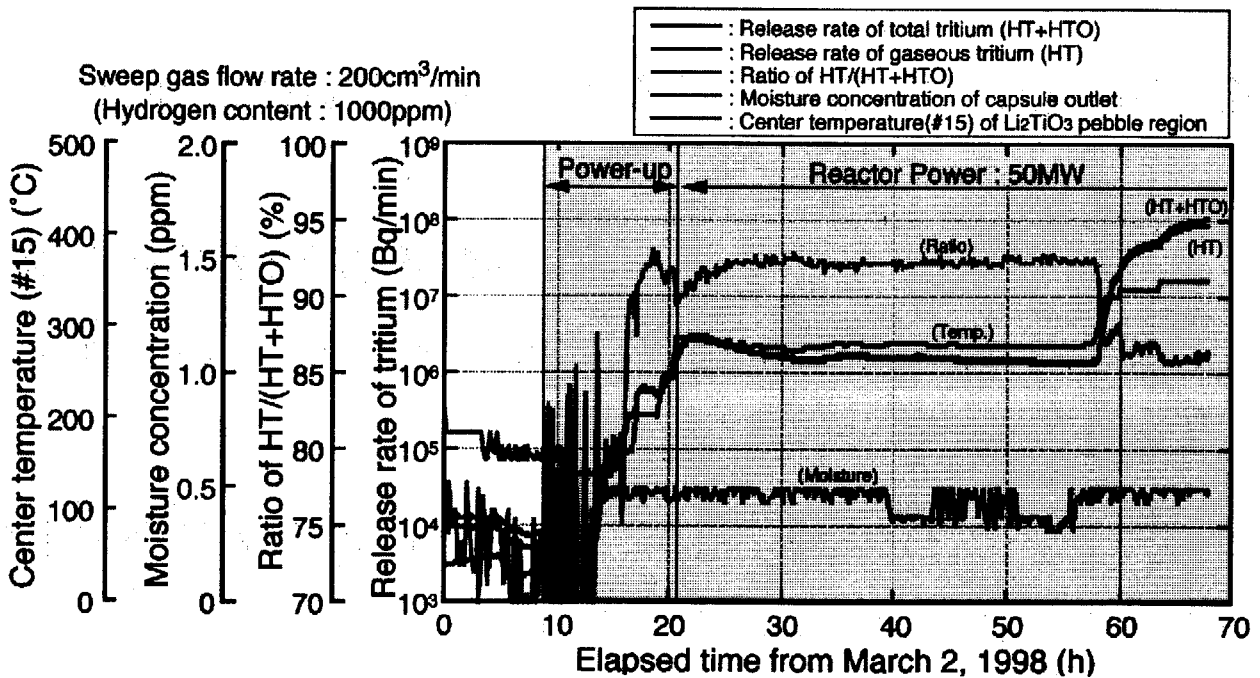


Fig.4-28 Tritium release at the reactor power-up in the 122nd cycle.

Sweep gas flow rate : 200cm³/min (Hydrogen content : 1000ppm)

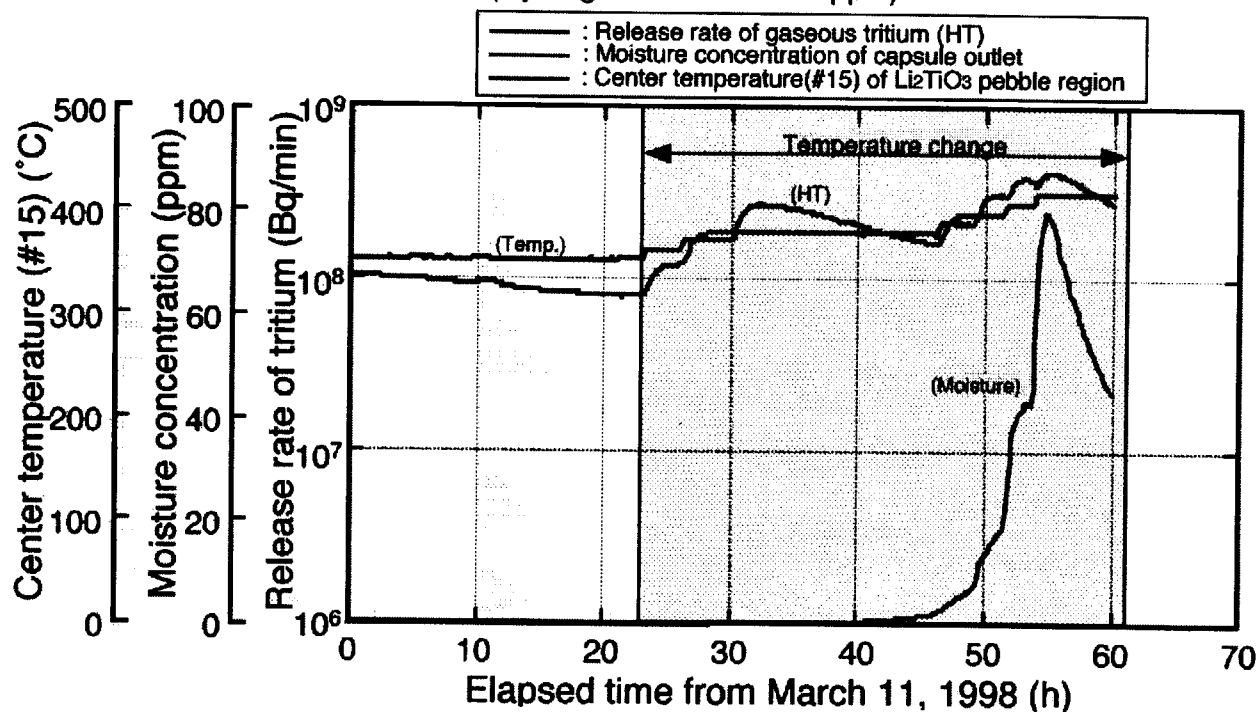


Fig.4-29 Result of temperature change test in the 122nd cycle. (1).

Sweep gas flow rate : 200cm³/min (Hydrogen content : 1000ppm)

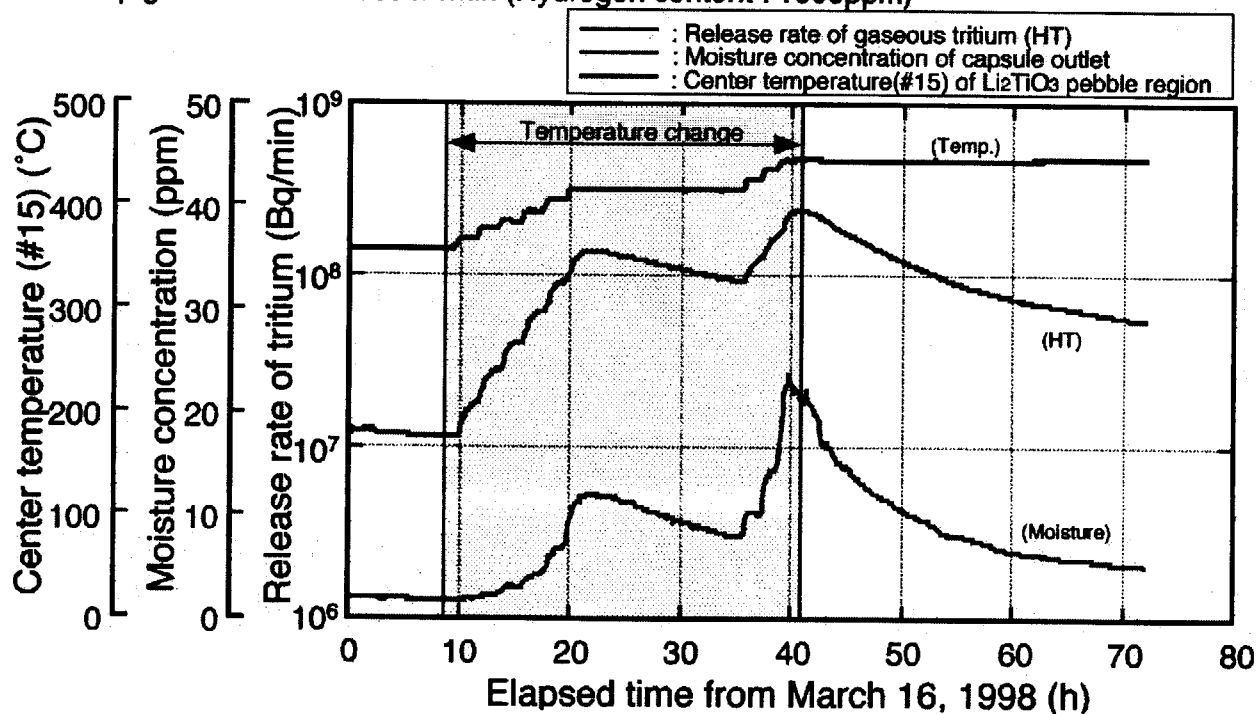


Fig.4-30 Result of temperature change test in the 122nd cycle. (2).

Sweep gas flow rate : 200cm³/min (Hydrogen content : 1000ppm)

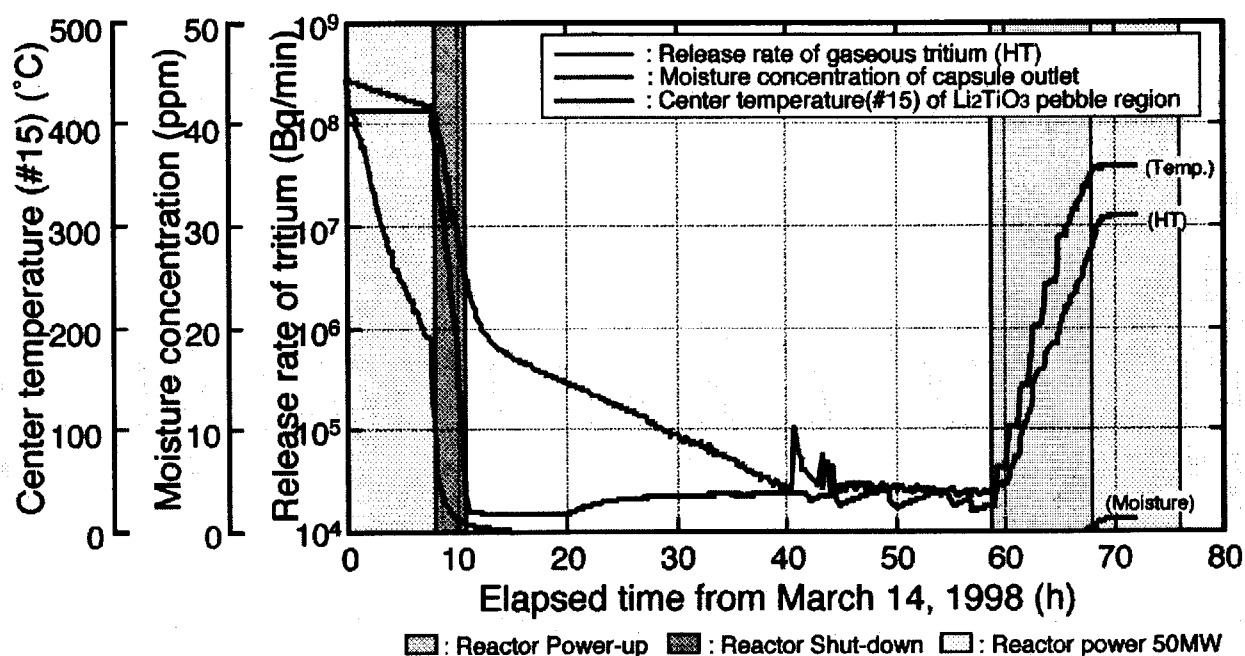


Fig.4-31 Tritium release at the reactor shutdown in the 122nd cycle.

Sweep gas flow rate : 200cm³/min (Hydrogen content : 1000ppm)

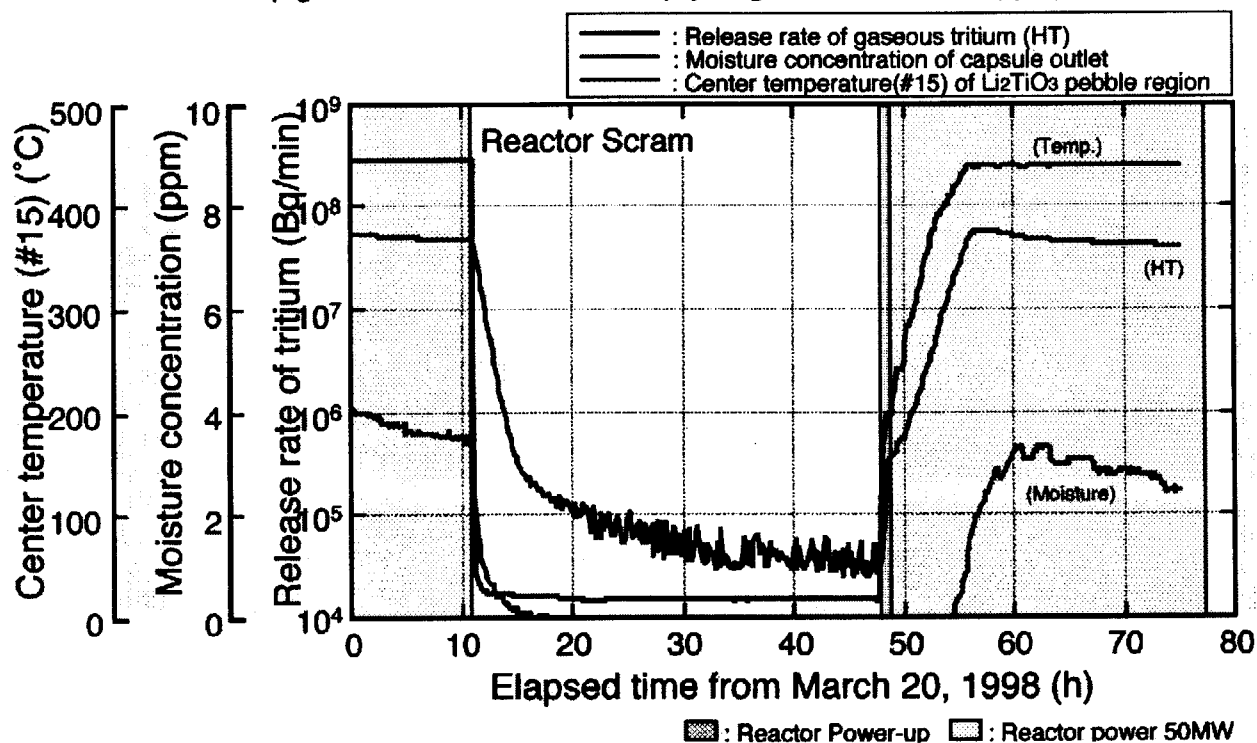


Fig.4-32 Tritium release at the reactor scram in the 122nd cycle.

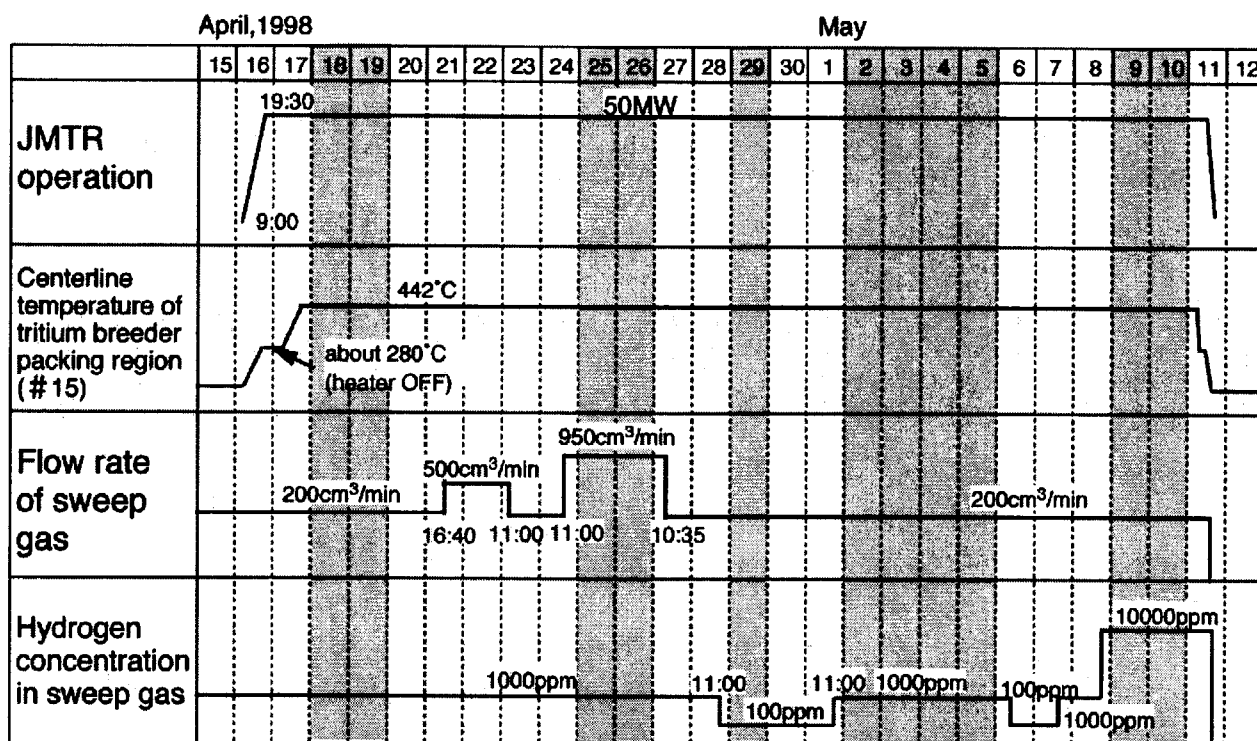


Fig.4-33 Outline of experimental conditions on the third irradiation test.

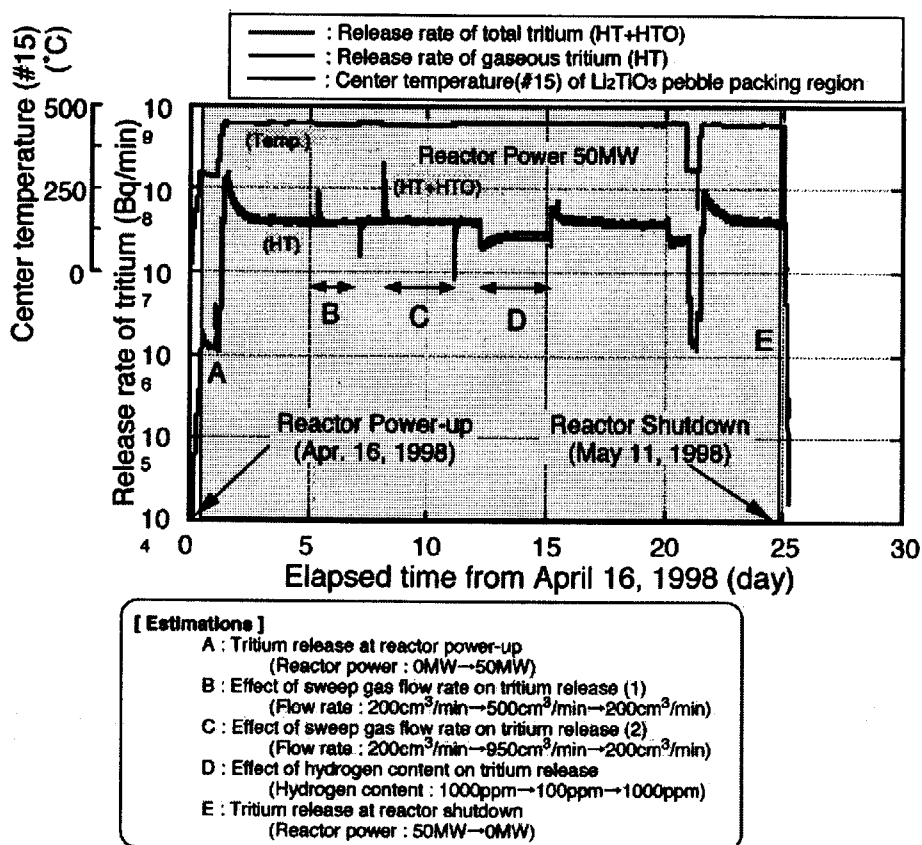
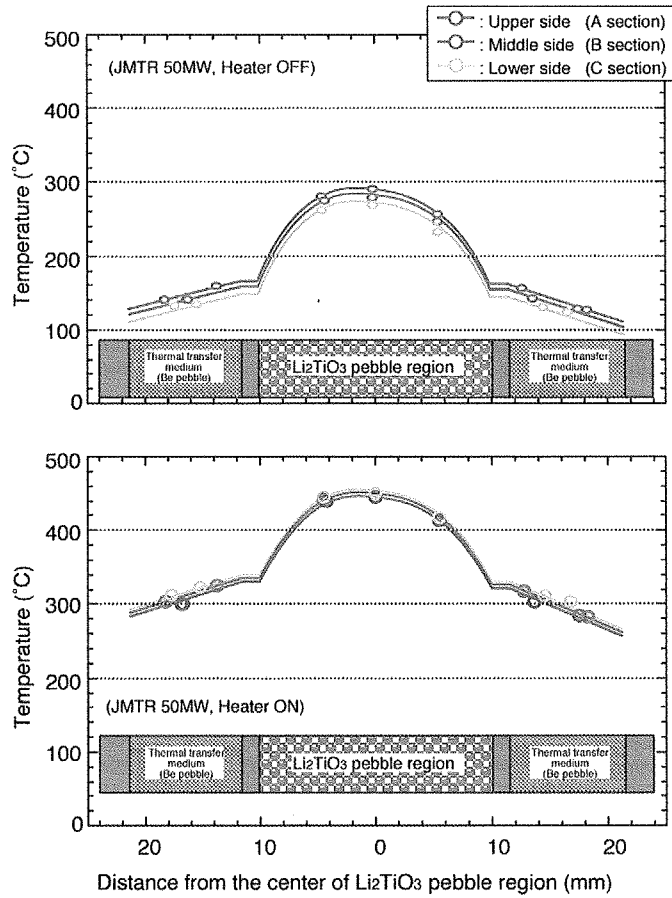


Fig.4-34 Result of the third irradiation test in the 123rd cycle.



Heater OFF	
Temperature	Volume rate
100~150°C	0%
150~200°C	23%
200~250°C	34%
250~300°C	43%
300~350°C	0%
350~400°C	0%
400~450°C	0%

Heater ON	
Temperature	Volume rate
100~150°C	0%
150~200°C	0%
200~250°C	0%
250~300°C	0%
300~350°C	1%
350~400°C	13%
400~450°C	86%

Fig.4-35 Radial temperature distribution in the 123rd cycle.

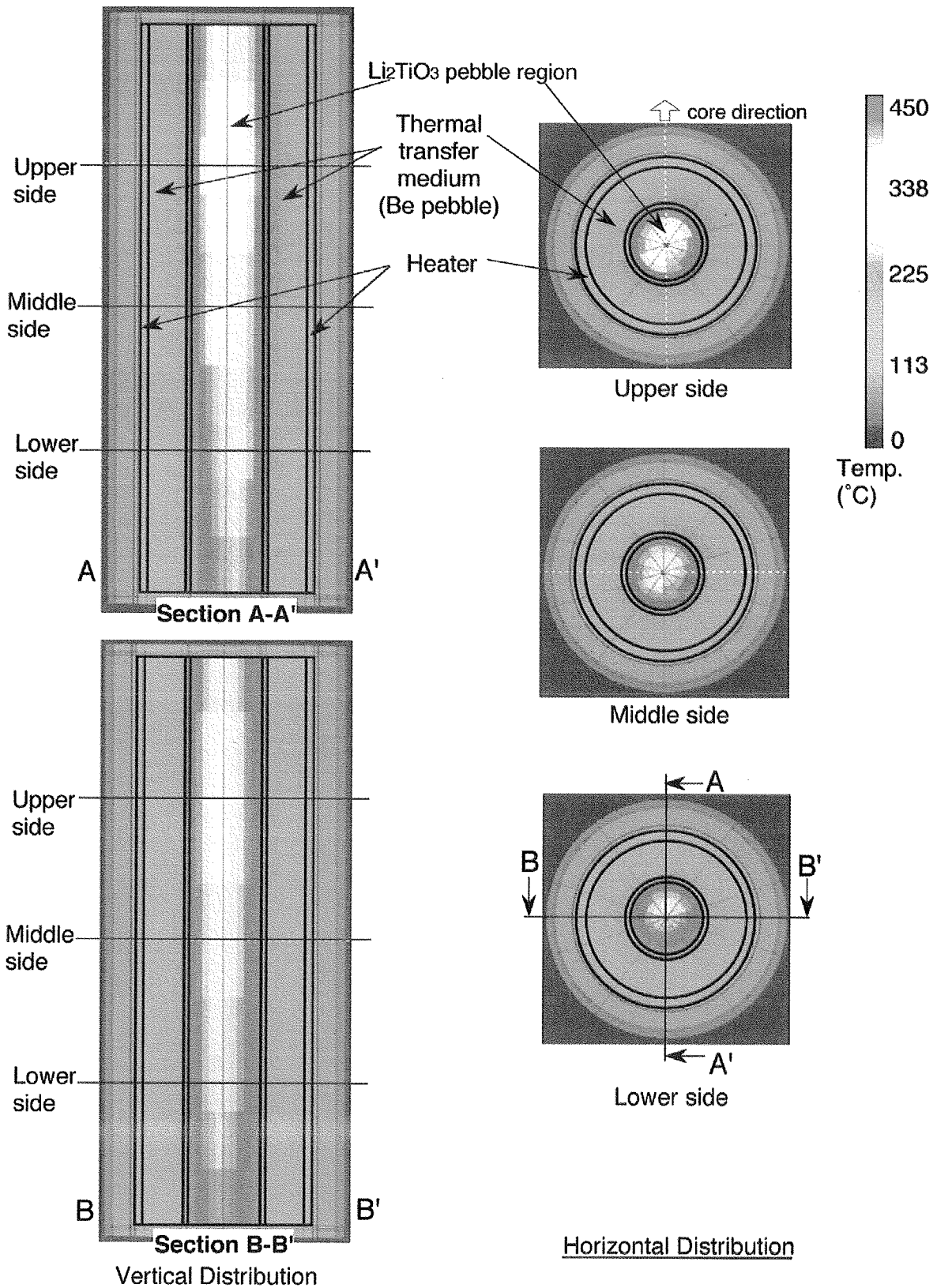


Fig.4-36 Result of 3-dimensional temperature distributions calculated by TRAMP.
(the 123rd cy, 50MW, Heater-OFF).

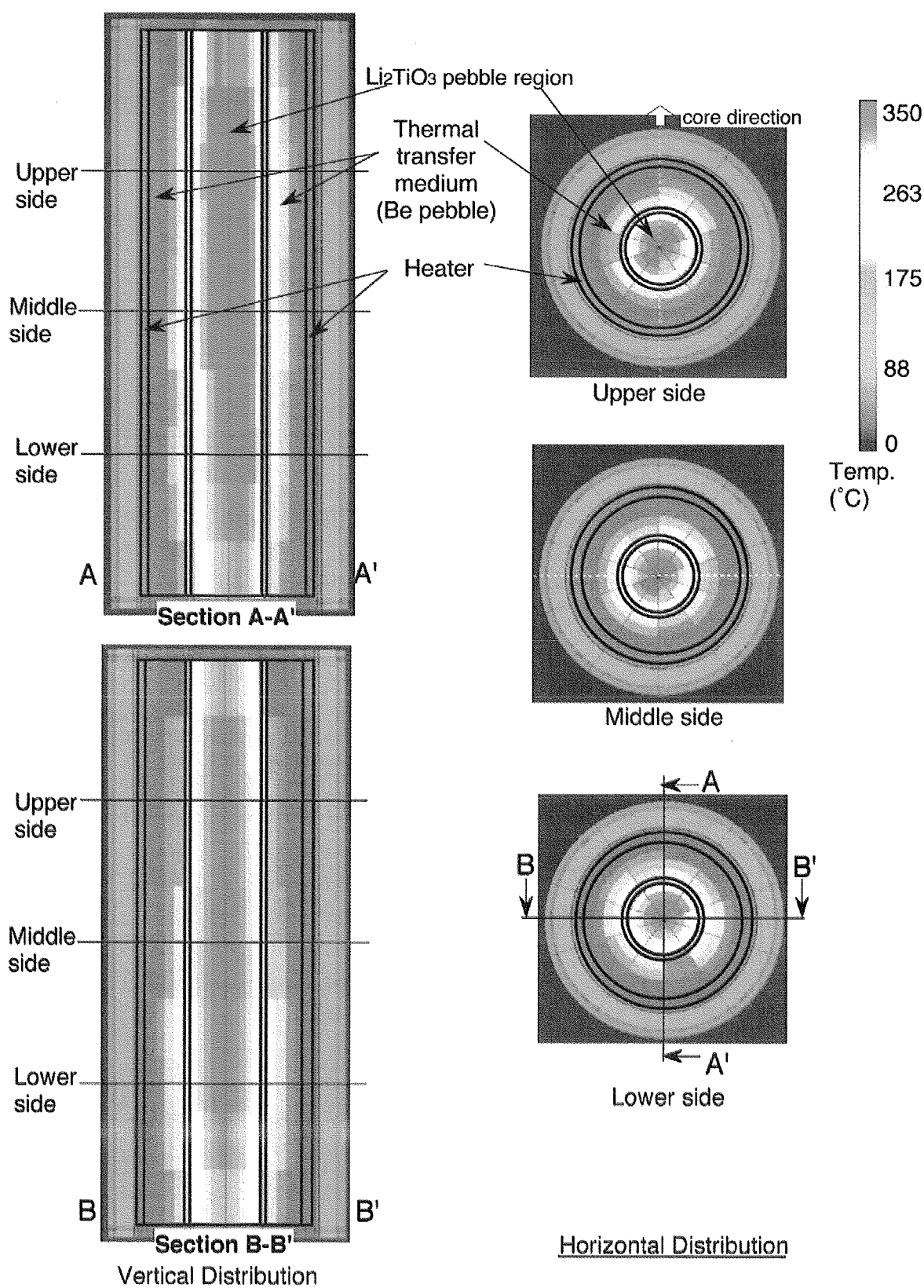


Fig.4-16 Result of 3-dimensional temperature distributions calculated by TRAMP.
(the 121st cy, 50MW, Heater-ON).

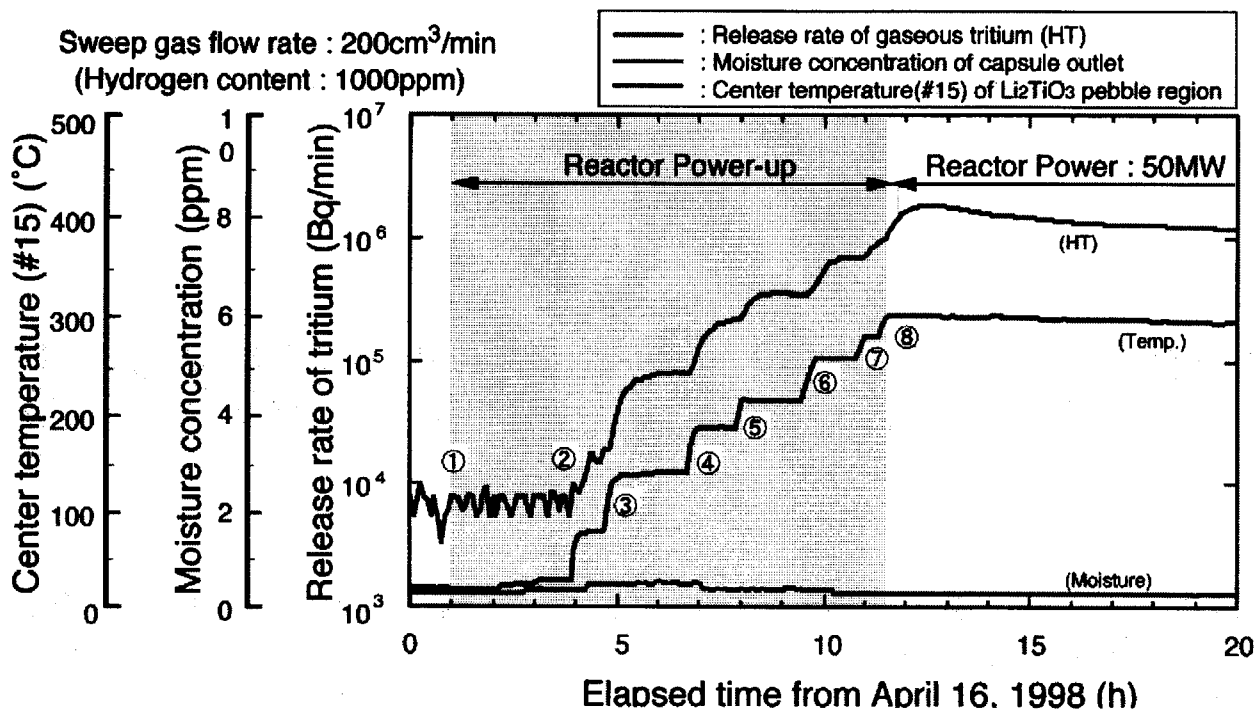


Fig.4-38 Tritium release at the reactor power-up (the 123rd cycle).

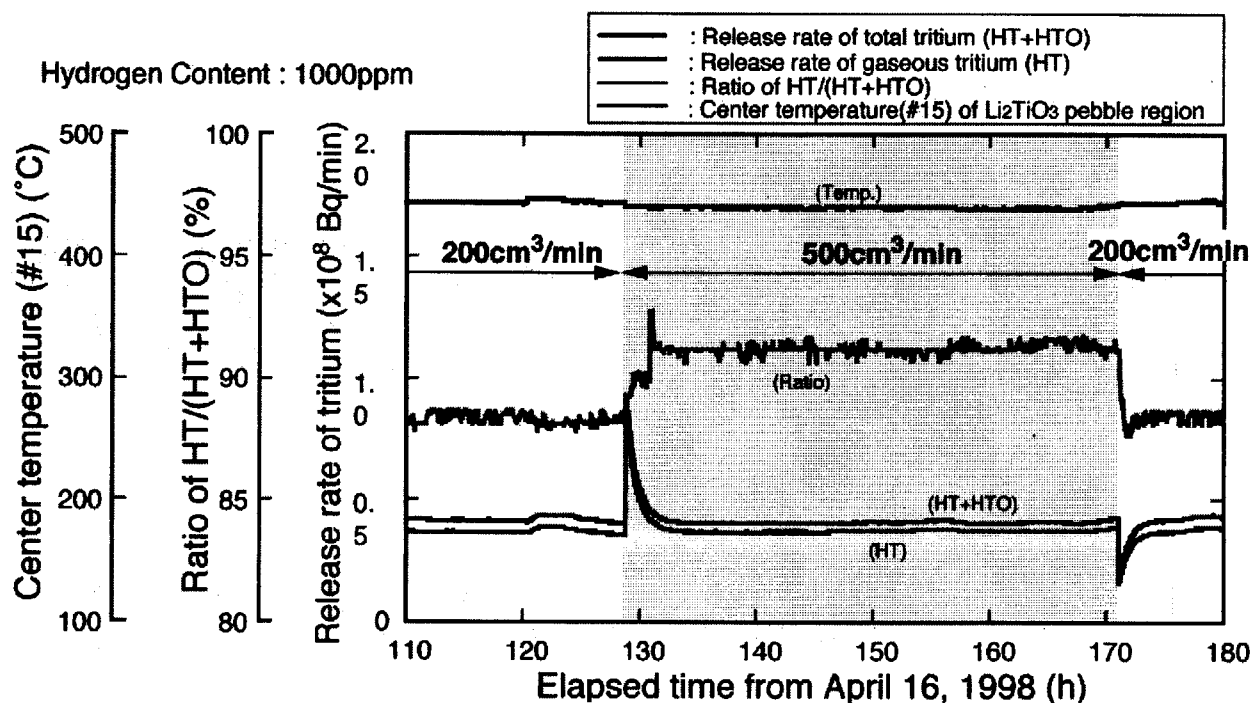


Fig.4-39 Result of sweep-gas flow rate change test in the 123rd cycle (1).

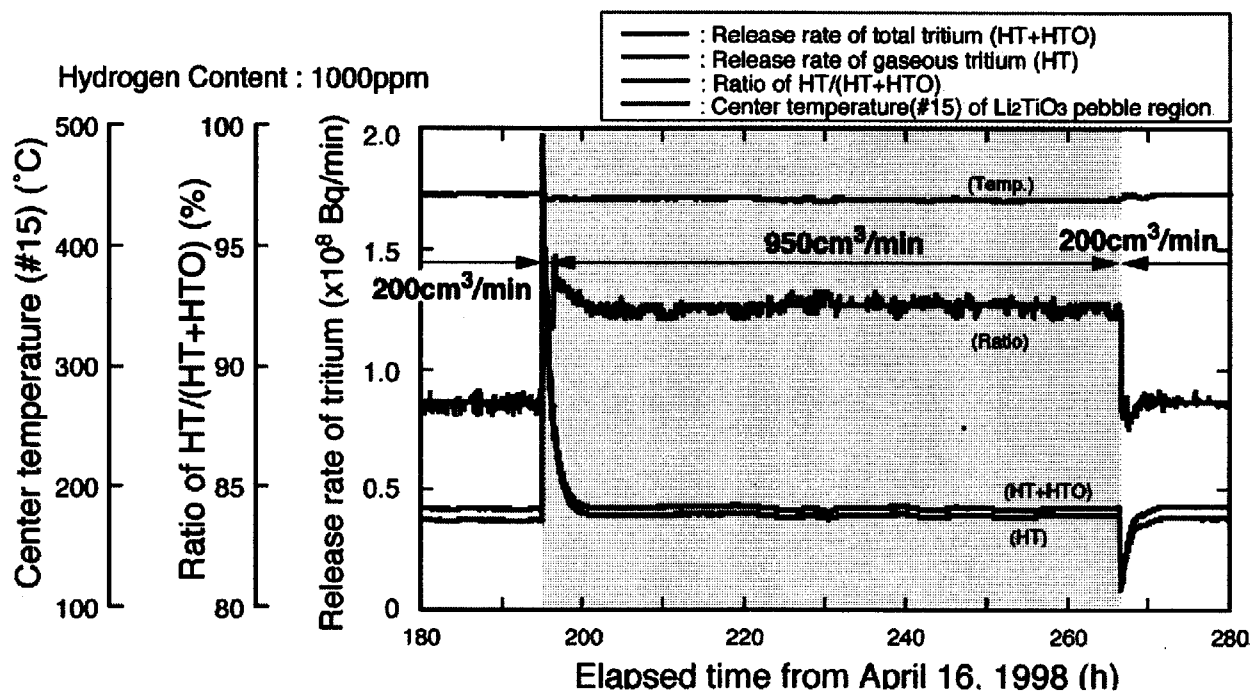


Fig.4-40 Result of sweep-gas flow rate change test in the 123rd cycle (2).

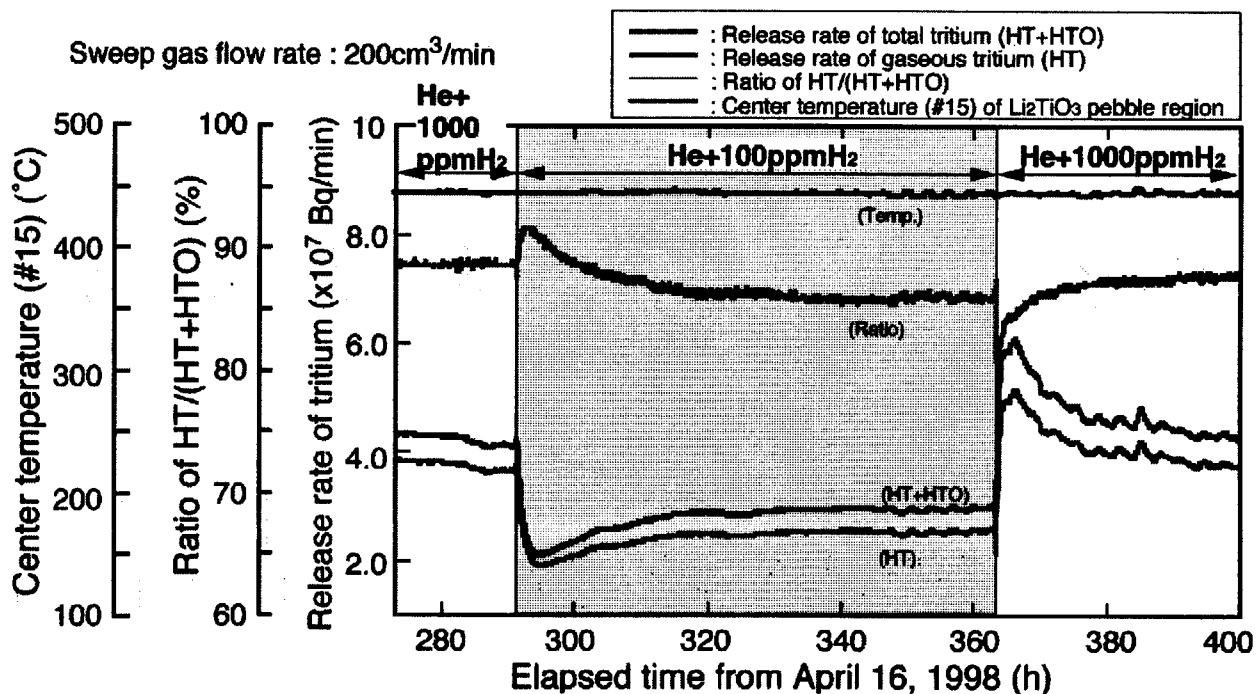


Fig.4-41 Result of hydrogen content change test in the 123rd cycle (1).

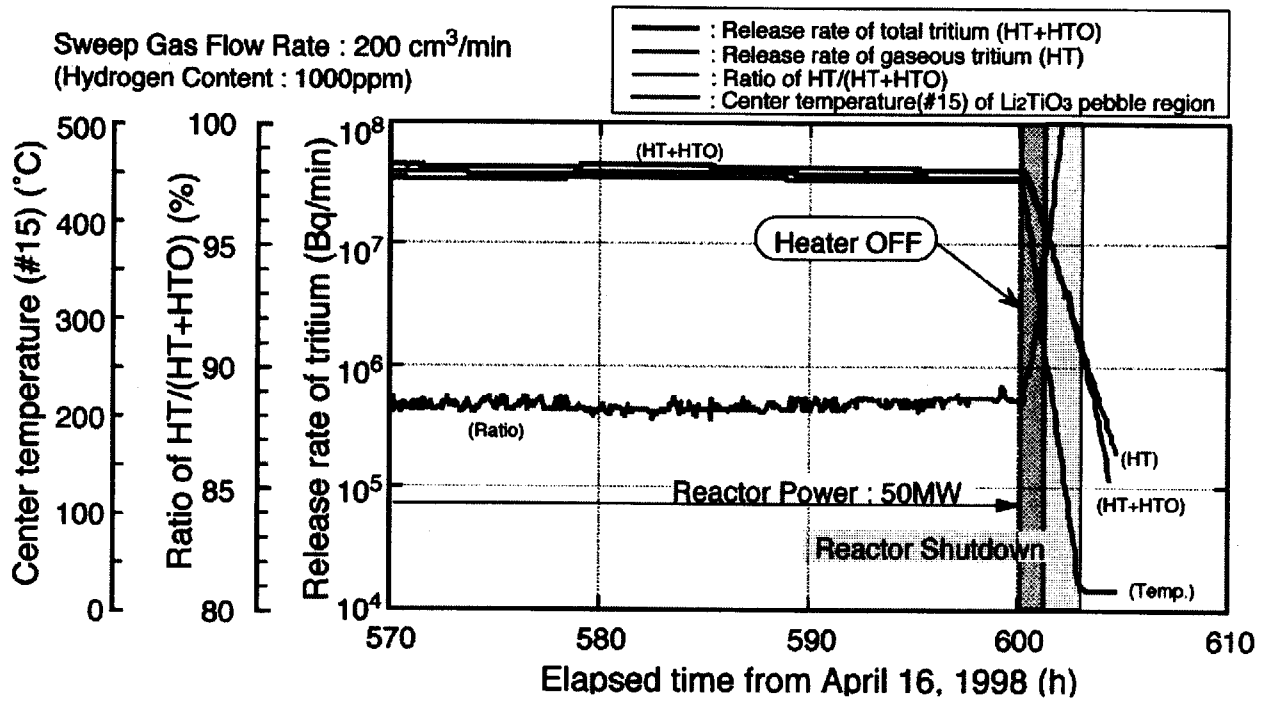


Fig.4-42 Tritium release at the reactor shutdown in the 123rd cycle.

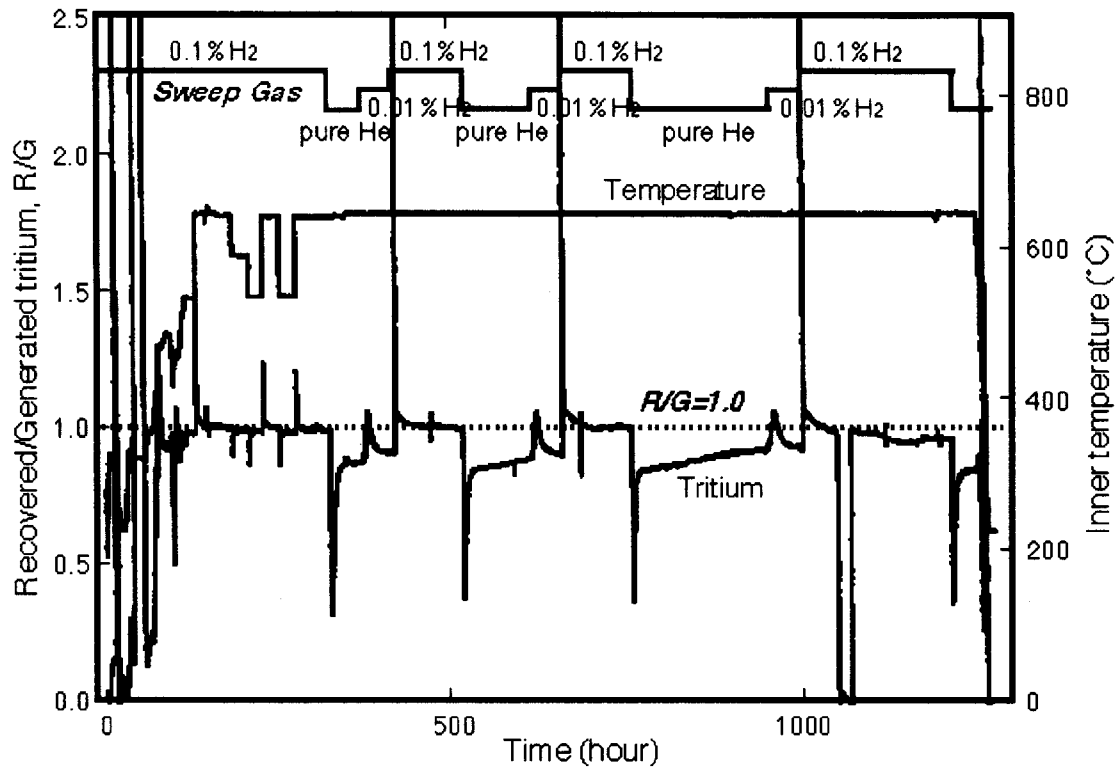


Fig.5-1 Ratio of recovered/generated tritium and average temperature for the temperature change canister in Phase-IIB.

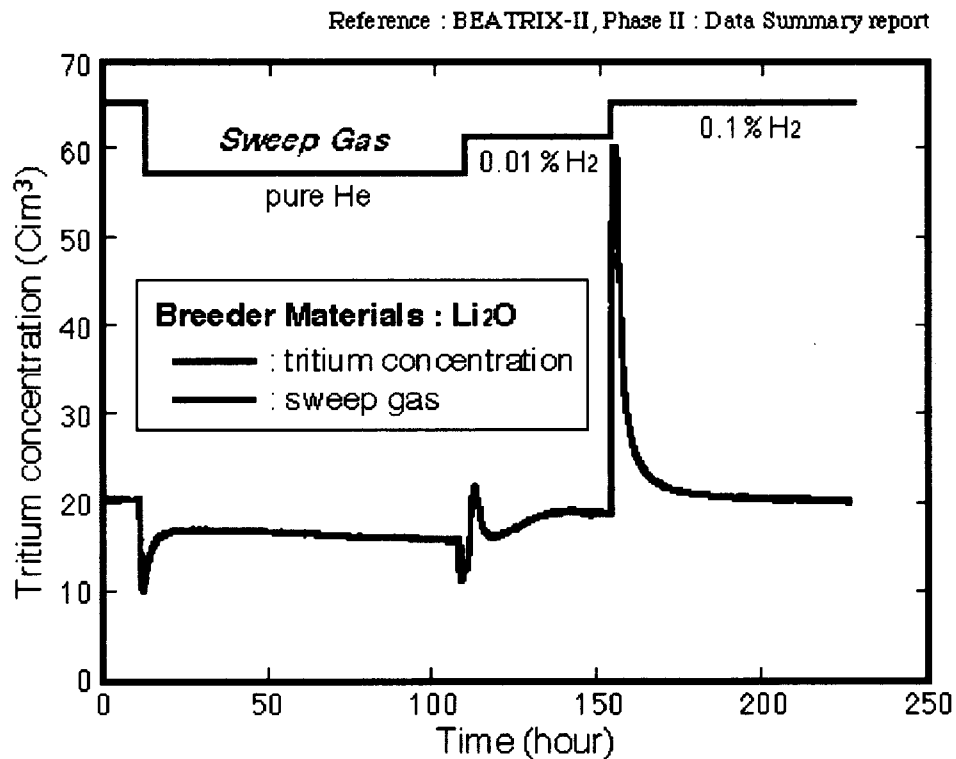


Fig.5-2 Recovered tritium during sweep-gas composition changes.

reference : BEATRIX-II, Phase II : Data Summary report

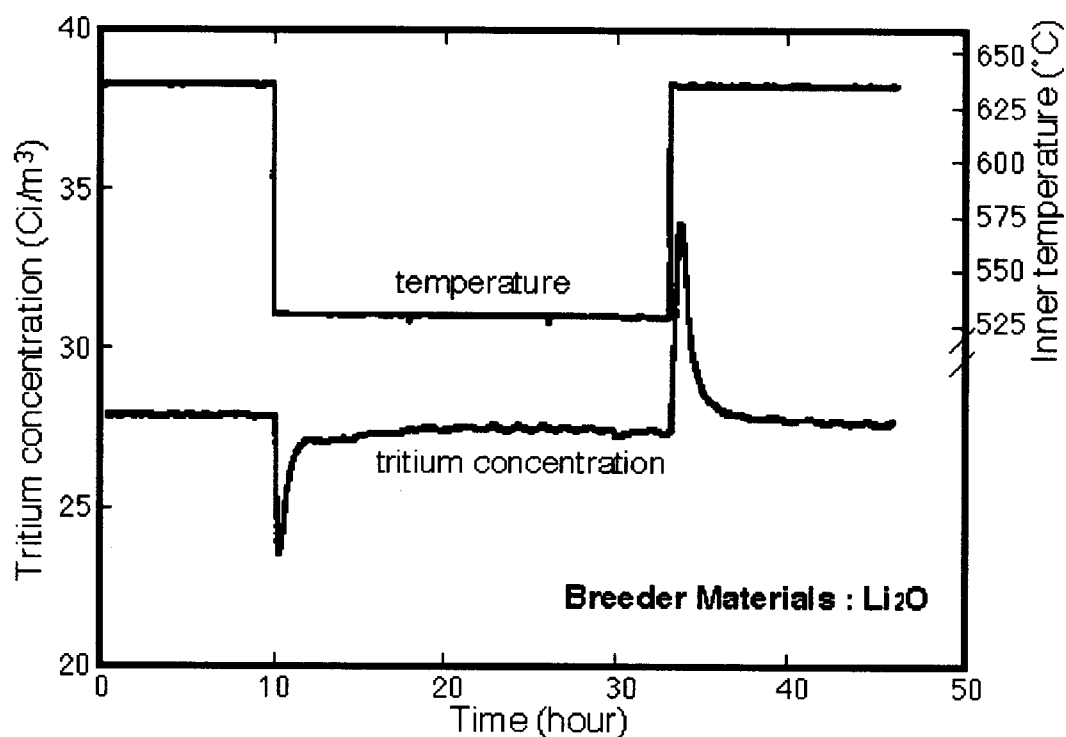


Fig.5-3 Typical tritium recovery peaks for a temperature change series of 640-530-640°C in reference sweep gas of 0.1%H₂.

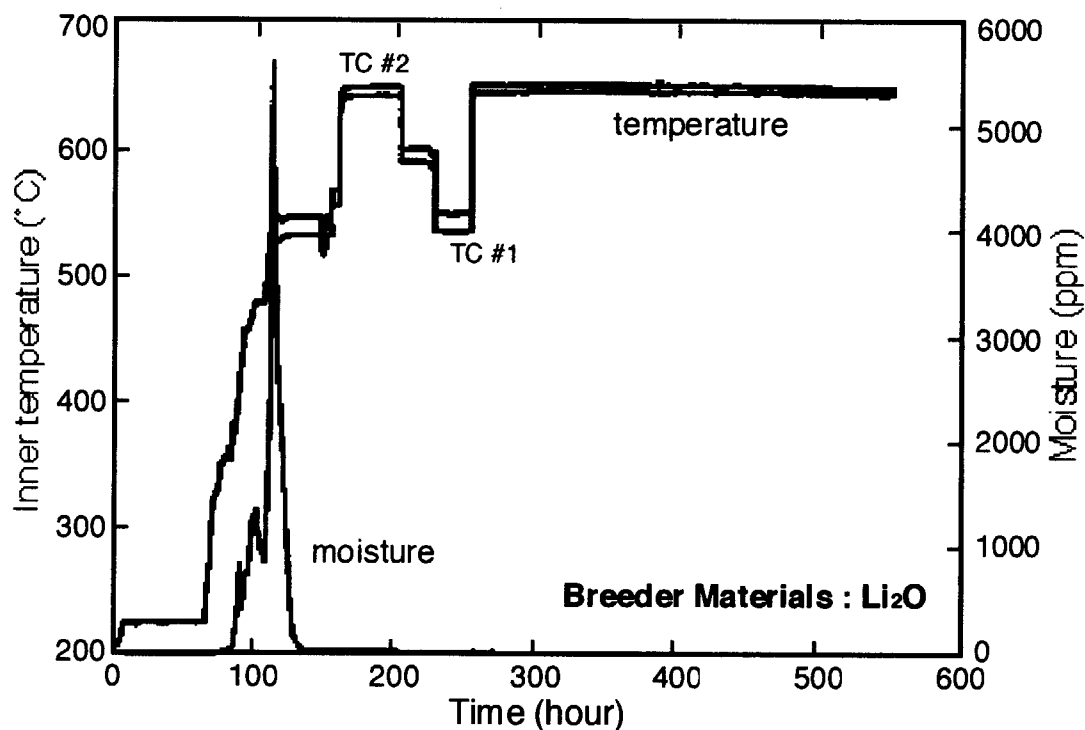


Fig.5-4 Inner temperature and sweep-gas moisture for first 550 h in Phase-IIA.

国際単位系 (SI) と換算表

表 1 SI 基本単位および補助単位

量	名 称	記 号
長 度	メ ー ト ル	m
質 量	キ ロ グ ラ ム	kg
時 間	秒	s
電 流	ア ン ペ ア	A
熱力学温度	ケ ル ビ ン	K
物 質 量	モ ル	mol
光 度	カ ン デ ラ	cd
平 面 角	ラ ジ ア ン	rad
立 体 角	ステラジアン	sr

表 3 固有の名称をもつ SI 組立単位

量	名 称	記号	他の SI 単位 による表現
周 波 数	ヘル ツ	Hz	s ⁻¹
力	ニュートン	N	m·kg/s ²
圧 力 , 応 力	パスカル	Pa	N/m ²
エネルギー, 仕事, 熱量	ジュール	J	N·m
工 率 , 放 射 束	ワ ッ ト	W	J/s
電 気 量 , 電 荷	クーロン	C	A·s
電位, 電圧, 起電力	ボ ル ト	V	W/A
静 電 容 量	ファラド	F	C/V
電 気 抵 抗	オーム	Ω	V/A
コンダクタンス	ジーメンズ	S	A/V
磁 束	ウェーバ	Wb	V·s
磁 束 密 度	テスラ	T	Wb/m ²
インダクタンス	ヘンリー	H	Wb/A
セルシウス温度	セルシウス度	°C	
光 束 度	ルーメン	lm	cd·sr
照 度	ルクス	lx	lm/m ²
放 射 能	ベクレル	Bq	s ⁻¹
吸 収 線 量	グレイ	Gy	J/kg
線 量 当 量	シーベルト	Sv	J/kg

表 2 SI と併用される単位

名 称	記 号
分, 時, 日	min, h, d
度, 分, 秒	°, ', "
リットル	l, L
トン	t
電子ボルト	eV
原子質量単位	u

$$1 \text{ eV} = 1.60218 \times 10^{-19} \text{ J}$$

$$1 \text{ u} = 1.66054 \times 10^{-27} \text{ kg}$$

表 4 SI と共に暫定的に維持される単位

名 称	記 号
オングストローム	Å
バ ー ン	b
バ ー ル	bar
ガ ル	Gal
キ ュ リ ー	Ci
レン ト ゲ ン	R
ラ ッ ド	rad
レ ム	rem

$$1 \text{ Å} = 0.1 \text{ nm} = 10^{-10} \text{ m}$$

$$1 \text{ b} = 100 \text{ fm}^2 = 10^{-28} \text{ m}^2$$

$$1 \text{ bar} = 0.1 \text{ MPa} = 10^5 \text{ Pa}$$

$$1 \text{ Gal} = 1 \text{ cm/s}^2 = 10^{-2} \text{ m/s}^2$$

$$1 \text{ Ci} = 3.7 \times 10^{10} \text{ Bq}$$

$$1 \text{ R} = 2.58 \times 10^{-4} \text{ C/kg}$$

$$1 \text{ rad} = 1 \text{ cGy} = 10^{-2} \text{ Gy}$$

$$1 \text{ rem} = 1 \text{ cSv} = 10^{-2} \text{ Sv}$$

表 5 SI 接頭語

倍数	接頭語	記 号
10 ¹⁸	エクサ	E
10 ¹⁵	ペタ	P
10 ¹²	テラ	T
10 ⁹	ギガ	G
10 ⁶	メガ	M
10 ³	キロ	k
10 ²	ヘクト	h
10 ¹	デカ	da
10 ⁻¹	デシ	d
10 ⁻²	センチ	c
10 ⁻³	ミリ	m
10 ⁻⁶	マイクロ	μ
10 ⁻⁹	ナノ	n
10 ⁻¹²	ピコ	p
10 ⁻¹⁵	フェムト	f
10 ⁻¹⁸	アト	a

(注)

- 表 1-5 は「国際単位系」第 5 版, 国際度量衡局 1985 年刊行による。ただし, 1 eV および 1 u の値は CODATA の 1986 年推奨値によった。
- 表 4 には海里, ノット, アール, ヘクトールも含まれているが日常の単位なのでここでは省略した。
- bar は, JIS では流体の圧力を表わす場合に限り表 2 のカテゴリーに分類されている。
- EC 閣僚理事会指令では bar, barn および「血圧の単位」mmHg を表 2 のカテゴリーに入れている。

換 算 表

力	N (=10 ⁵ dyn)	kgf	lbf
	1	0.101972	0.224809
	9.80665	1	2.20462
	4.44822	0.453592	1

$$\text{粘 度 } 1 \text{ Pa} \cdot \text{s} (= \text{N} \cdot \text{s} / \text{m}^2) = 10 \text{ P (ポアズ)} (\text{g} / (\text{cm} \cdot \text{s}))$$

$$\text{動粘度 } 1 \text{ m}^2 / \text{s} = 10^4 \text{ St (ストークス)} (\text{cm}^2 / \text{s})$$

圧	MPa (=10 bar)	kgf/cm ²	atm	mmHg (Torr)	lbf/in ² (psi)
	1	10.1972	9.86923	7.50062 × 10 ³	145.038
力	0.0980665	1	0.967841	735.559	14.2233
	0.101325	1.03323	1	760	14.6959
	1.33322 × 10 ⁻⁴	1.35951 × 10 ⁻³	1.31579 × 10 ⁻³	1	1.93368 × 10 ⁻²
	6.89476 × 10 ⁻³	7.03070 × 10 ⁻²	6.80460 × 10 ⁻²	51.7149	1

エネルギー・仕事・熱量	J (=10 ⁷ erg)	kgf·m	kW·h	cal (計量法)	Btu	ft·lbf	eV
	1	0.101972	2.77778 × 10 ⁻⁷	0.238889	9.47813 × 10 ⁻⁴	0.737562	6.24150 × 10 ¹⁸
	9.80665	1	2.72407 × 10 ⁻⁶	2.34270	9.29487 × 10 ⁻³	7.23301	6.12082 × 10 ¹⁹
	3.6 × 10 ⁶	3.67098 × 10 ⁵	1	8.59999 × 10 ⁵	3412.13	2.65522 × 10 ⁶	2.24694 × 10 ²⁵
	4.18605	0.426858	1.16279 × 10 ⁻⁶	1	3.96759 × 10 ⁻³	3.08747	2.61272 × 10 ¹⁹
	1055.06	107.586	2.93072 × 10 ⁻⁴	252.042	1	778.172	6.58515 × 10 ²¹
	1.35582	0.138255	3.76616 × 10 ⁻⁷	0.323890	1.28506 × 10 ⁻³	1	8.46233 × 10 ¹⁸
	1.60218 × 10 ⁻¹⁹	1.63377 × 10 ⁻²⁰	4.45050 × 10 ⁻²⁶	3.82743 × 10 ⁻²⁰	1.51857 × 10 ⁻²²	1.18171 × 10 ⁻¹⁹	1

$$1 \text{ cal} = 4.18605 \text{ J (計量法)}$$

$$= 4.184 \text{ J (熱化学)}$$

$$= 4.1855 \text{ J (15 °C)}$$

$$= 4.1868 \text{ J (国際蒸気表)}$$

$$\text{仕事率 } 1 \text{ PS (仏馬力)}$$

$$= 75 \text{ kgf} \cdot \text{m/s}$$

$$= 735.499 \text{ W}$$

放射能	Bq	Ci
	1	2.70270 × 10 ⁻¹¹
	3.7 × 10 ¹⁰	1

吸収線量	Gy	rad
	1	100
	0.01	1

照射線量	C/kg	R
	1	3876
	2.58 × 10 ⁻⁴	1

線量当量	Sv	rem
	1	100
	0.01	1

R100

古紙配合率100%
白度度70%再生紙を使用しています。